PERFORMANCE INVESTIGATIONS ON LOW VOLTAGE HIGH CURRENT RECTIFIER WITH LOW HARMONIC DISTORTION

A DISSERTATION

Submitted in partial fulfilment of the requirements for the award of the degree of

MASTER OF TECHNOLOGY

in

ELECTRICAL ENGINEERING

(With Specialization in Power Apparatus and Electric Drives)

By

PRASHANT SHARMA

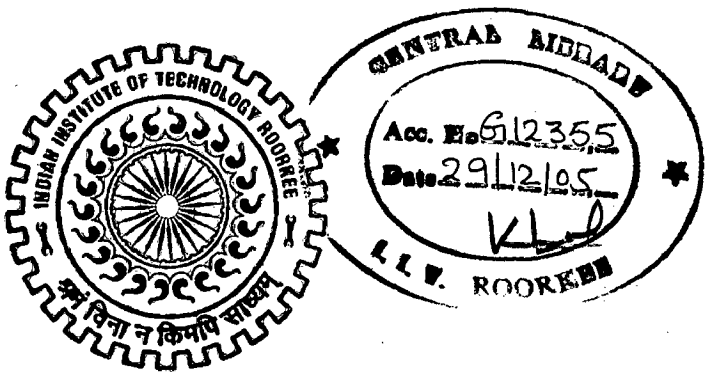

DEPARTMENT OF ELECTRICAL ENGINEERING
INDIAN INSTITUTE TECHNOLOGY ROORKEE
ROORKEE-247 667 (INDIA)

JUNE, 2005

CANDIDATE'S DECLARATION

I hereby declare that the work that is being presented in this dissertation report entitled **"PERFORMANCE INVESTIGATIONS ON LOW VOLTAGE HIGH CURRENT RECTIFIER WITH LOW HARMONIC DISTORTION"** submitted in partial fulfillment of the requirements for the award of the degree of **MASTER OF TECHNOLOGY** in **ELECTRICAL ENGINEERING** with specialization in **POWER APPARATUS AND ELECTRIC DRIVE**, submitted in the Department of Electrical Engineering, Indian Institute of Technology, Roorkee, is an authentic record of my own work carried out, under the guidance of Dr. Pramod Agrawal, Professor, Department of Electrical Engineering.

The matter embodied in this dissertation report has not been submitted by me for the award of any other degree or diploma.

Date: 31/05/2005

Place: Roorkee

Prashant Sharma

(PRASHANT SHARMA)

This is to certify that the above statement made by the candidate is correct to the best of my knowledge.

(DR. PRAMOD AGRAWAL)

Professor,
Department of Electrical Engineering,
Indian Institute of Technology,
ROORKEE – 247 667,
INDIA.

ACKNOWLEDGEMENT

I avail this opportunity to express my deep sense of gratitude and sincere thanks to Dr.Pramod Agrawal, Professor, Electrical Engineering Department, Indian Institute of Technology, Roorkee for the invaluable guidance he rendered me during the course of my work. The patience with which he dealt with the various problems encountered during the course of this dissertation is also quite inspiring. His constant encouragement and painstaking efforts have been the sole endeavors to bring this dissertation report in its present form.

I would also like to extend my sincere thanks to Shri.B.K.Nashine, Head, ESS, STD, EDG, IGCAR (Indira Gandhi Centre for Atomic Research) for his support and for providing me the opportunity to work on this dissertation topic. I am also grateful to the persons in the electrical engineering department workshop and store for their help and corporation. The support extended by Drives Lab assistants Shri. Gautum Singh and Shri Rakesh Saini has also been appreciable.

I am also grateful to Shri.D.C.Pandey, my physics teacher, who first guided me on this path for quest of knowledge. I gratefully acknowledge my sincere thanks to all my friends and family members for their inspirational impetus and moralsupport during the course of this work.

Date: 31/05/2005

Place: Roorkee

Prashant Sharma

(PRASHANT SHARMA)

ABSTRACT

Low voltage high current rectifiers are required for many industrial applications. Traditionally, these rectifiers have been manufactured by using simple diode bridge rectifiers fed through auto-transformer and transformer combination where the auto-transformer controls the input voltage to the three phase uncontrolled rectifiers to obtain the required voltage level conversion. The disadvantage with such systems is that they are quite bulky. The power factor and the response of the system are also poor. In this dissertation, a switch mode type of low voltage high current rectifier is designed and fabricated. This rectifier is operated at high frequency to reduce the size and weight of the transformer. The mathematical model of the system is developed. Both the simulation and experimental results are presented and compared. The performance of the system is investigated and it is found that both response and input power factor are improved.

Contents

CHAPTER-1

INTRODUCTION

Low voltage high current rectifiers are finding applications in industries. There are many situations when we want high power output from the power supply but cannot apply high voltage due to the environment in which the system works or due to the system itself. With the advances in semiconductor technology the number of transistors per chip are increasing quite rapidly and in order to accommodate large number of transistor in smaller area the voltage levels are getting reduced to 3V and 2.5V instead of traditional 5V system but since the number of transistors are increasing the current requirement is also increasing making the use of a low voltage high current power supply necessary. Stepper motor drives such as in electrochemical machine also require high current low voltage power supply.

Conventionally such rectifiers have been being made using a diode bridge rectifier the input to which is given through a three phase autotransfomer which in turn is controlled by a stepper or a servomotor to get a controlled output. Such systems are simple in configuration but they have many drawbacks. They are quite bulky especially due to the transformers used in them. For high power output generally two 3-phase transformers, one is star and the other in delta, are used which makes the system still bulkier. The power factor of the system is poor and the total harmonic distortion (THD) is also high. The system is slow in response due to the mechanical movement of the motor used to control the applied input voltage. This mechanical movement also requires regular maintenance due to wear and tear.

The switch mode power supply offers a better solution in this case. Though it is somewhat complex but its performance is much better than the conventional solutions. It had got high power factor, low harmonic distortion and excellent closed loop operation and no mechanical wear and tear. The weight of the overall system also reduces since the size of the transformer reduces due to the high frequency of operation.

One typical application of such a low voltage high current source is in the nuclear reactors for feeding the D.C. Conduction Pump which is used for pumping out the liquid sodium (which is being used as coolant in the new reactors).

1.1: DC Conduction Pump

Liquid Sodium is a good electrical conductor and this property is effectively used in the design of Electro Magnetic (EM) pump for pumping sodium. These pumps find wide applications in experimental facilities and auxiliary systems of fast reactors, where their operational simplicity, less maintenance and advantage of hermetically sealed construction, outweighs their poor efficiency, compared to centrifugal mechanical pump. One of the biggest advantages of these pumps is that they are non-intrusive. There are many types of EM pumps and one type called the DC conduction pump is good for low flow and high head. The DC Conduction Pump, even though less efficient than the other electromagnetic pumps, was chosen, because of its low voltage operation. At this lower voltage, argon/ air/ alumina ceramic can provide required electrical insulation even at operating temperature of 560 deg. C. without much complication on manufacturing front. One such pump is used in Failed Fuel Location Module (FFLM) for sampling sodium from different core sub-assemblies for detecting delayed neutrons released into sodium as a consequence of fuel failure.

The pump is immersed in sodium in the reactor. It pumps the sodium from the top of the fuel sub-assembly area to a sodium holdup capacity which is monitored for presence of neutrons, indicative of failure of fuel pin cladding. The D.C. Conduction Pump is an integral part of FFLM and is housed in control plug.

The D.C. Conduction Pump works on the principle that a current carrying conductor placed in the magnetic field, experiences a force. In D.C. Conduction Pump, current is forced through sodium kept in the pump duct placed in magnetic field. Hence force is developed in the sodium, which pumps the sodium away from the pump duct of the circuit. Current, which is passed through sodium, is also passed to electromagnetic coil for producing magnetic field in the pump. The current path is from one coil to SS duct filled with sodium through compensating bar back to the other coil through the other compensating bar. Figure-1.1 shows the internals of the D.C. conduction pump.

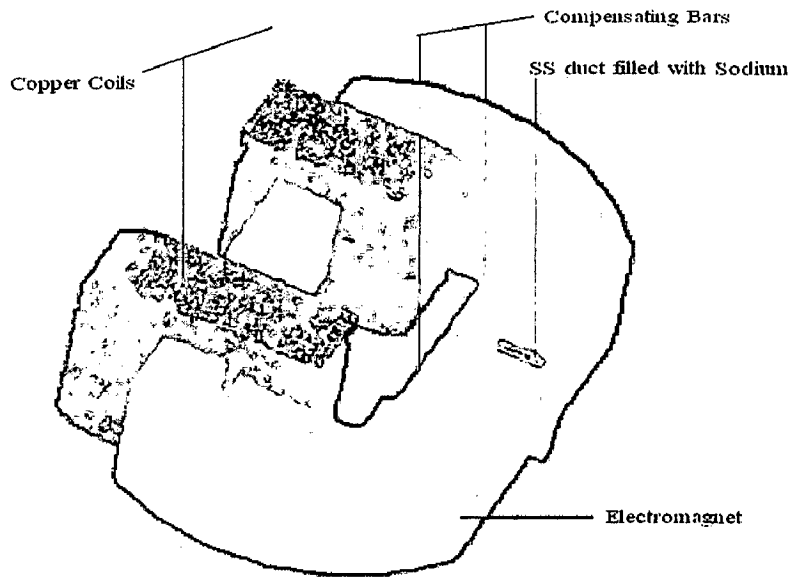

Figure-1.1: Internals of D.C. Conduction Pump

Figure -1.2 shows the complete assembly of D.C. Conduction Pump

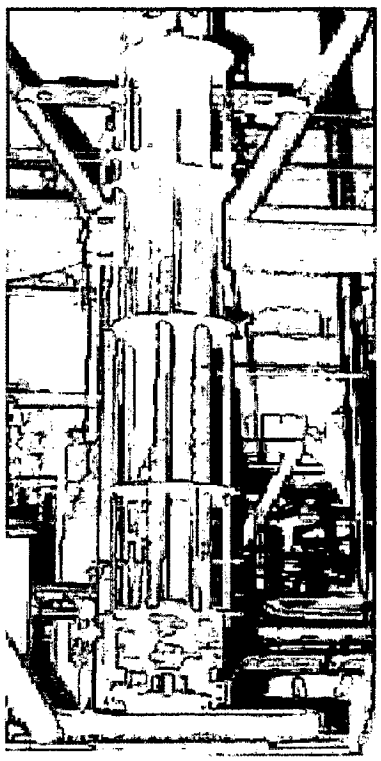

Figure-1.2: D.C. Conduction Pump Full Assembly

1.2 Power Supply Requirements:

The D.C. conduction pump requires a low voltage high current power source for its operation. The power source should be able to provide low voltage of 2 volts and a minimum current up to 3000Amps. The power supply is required to operate from 3-

CHAPTER -2

Low Voltage High Current Rectifiers

Low voltage high current rectifiers are used many a times in various industries such as electrochemical industry, cathodic protection power supplies, etc. A number of topologies are used to make such power supplies. Each power supply topology has got its own advantages and disadvantages and the real choice depends on the application. In this chapter, a brief overview of the various topologies used for low voltage high current rectifiers is presented.

Some of the topologies that are used in industry are given below.

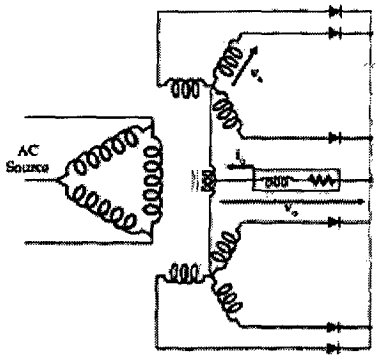

Figure-2.1: Delta –Star Topology

Delta-Star topology consists of delta-star transformer which rectifies the input voltage. The secondary side consists of two star connected windings the neutral of which in connected via an inter-phase reactor to prevent circulating currents between the two windings. The two star secondaries are paralleled to provide high output current. But he design of the transformer becomes complex and may lead to circulating currents.

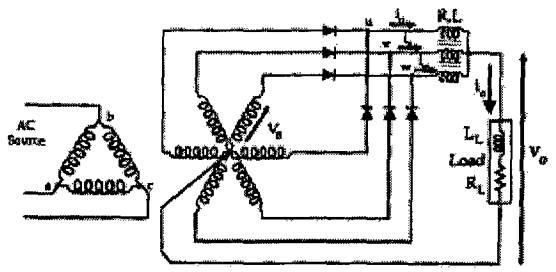

Figure-2.2 (a): 3-single phase center-tapped topology

Topology shown in figure-2.2 (a) can be considered as three single-phase center-tap rectifiers that are connected in parallel through a three phase output filter inductor. Each rectifier is supplied by one of the three separately center-tapped secondary windings of the transformer. Because of the 120° phase among the transformer secondary voltages, the full-wave output voltage of each rectifier will be displaced 60° among others. Theoretical output voltages of the rectifier are shown in figure-2.2 (b).

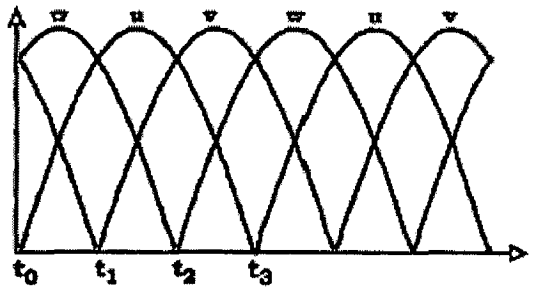

Figure-2.2 (b): Theoretical Output Voltages of rectifier shown in figure-2.2 (a)

The figure-2.2(b) shows that the output voltage has ripple six times the fundamental input frequency as in the case of conventional rectifier. The average value of the output voltage is given by

$$Vo = \frac{2\sqrt{2}}{\pi} Vs$$

Where Vs is the rms value of secondary phase-to-center-tap voltage of the transformer.

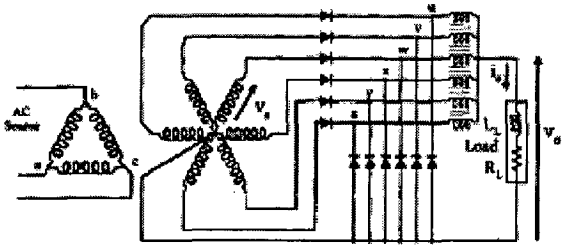

Figure-2.3: 6 Single Phase Half-Wave Rectifier Topology

Topology shown in figure-2.3 can be considered as six single-phase half-wave rectifiers that are connected in parallel through a 6-phase output inductor. Each single phase rectifier is supplied by each phase of the secondary winding of the three phase transformer that is connected as a three-phase-to-six-phase converter. The total output

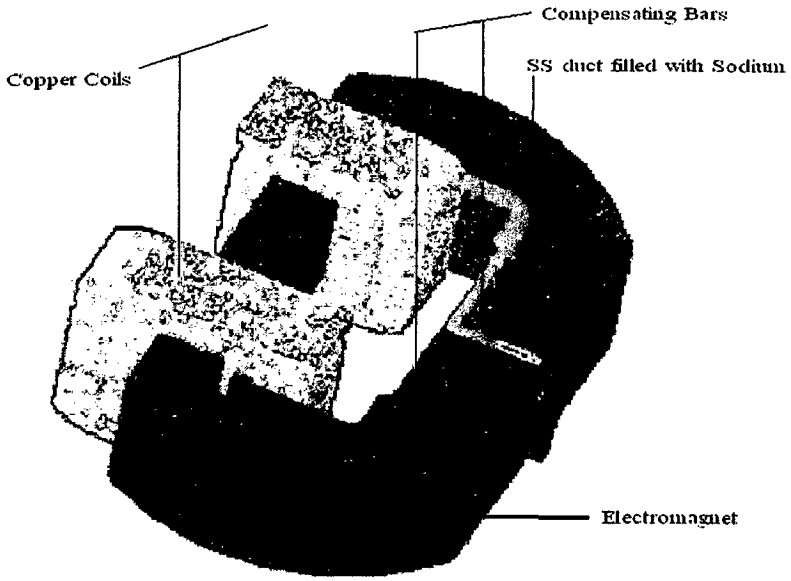

Figure-1.1: Internals of D.C. Conduction Pump

Figure -1.2 shows the complete assembly of D.C. Conduction Pump

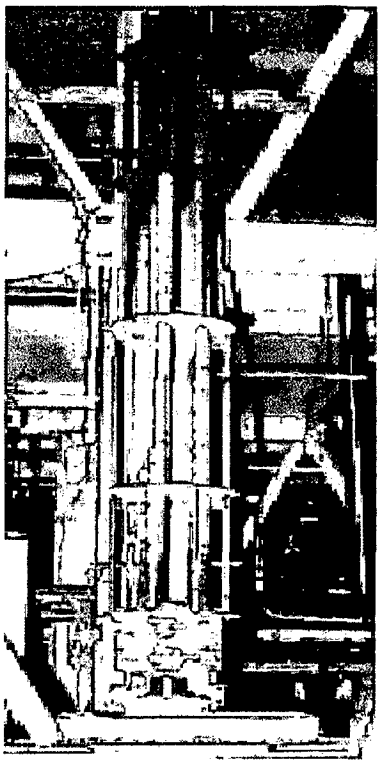

Figure-1.2: D.C. Conduction Pump Full Assembly

1.2 Power Supply Requirements:

The D.C. conduction pump requires a low voltage high current power source for its operation. The power source should be able to provide low voltage of 2 volts and a minimum current up to 3000Amps. The power supply is required to operate from 3-

phase 415V ± 10%, 50Hz supply. The power factor should not be less than 0.85 lag by P.F. meter. The ripple should be less than ±1% and should be designed for continuous duty with natural cooling.

Indira Gandhi Centre for Atomic Research (IGCAR), Kalpakkam (T.N.), India is currently having one power supply for supplying the D.C. conduction pump. The present power supply source uses auto transformers and diodes which makes it of higher size and more weight. The present size and weight is given below:

Height: 2215mm

Width: 1730mm

Depth: 1030mm

Weight: 1325Kgs

The task is to have a constant current source using more components of power electronics and solid state devices with emphasis on to reduce the size and weight of the power supply.

In this chapter, the need for a low voltage high current rectifier has been emphasized. The various industrial requirements for low voltage high current rectifier, in particular its application as power source for the DC Conduction pump has been discussed. Some detail regarding the DC conduction pump working has also been furnished. The details of the existing power supply have been provided, with stress upon reducing the size and weight of power supply.

CHAPTER -2

Low Voltage High Current Rectifiers

Low voltage high current rectifiers are used many a times in various industries such as electrochemical industry, cathodic protection power supplies, etc. A number of topologies are used to make such power supplies. Each power supply topology has got its own advantages and disadvantages and the real choice depends on the application. In this chapter, a brief overview of the various topologies used for low voltage high current rectifiers is presented.

Some of the topologies that are used in industry are given below.

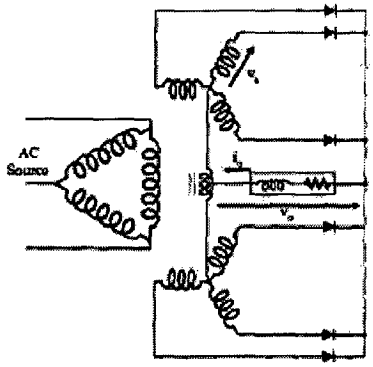

Figure-2.1: Delta –Star Topology

Delta-Star topology consists of delta-star transformer which rectifies the input voltage. The secondary side consists of two star connected windings the neutral of which in connected via an inter-phase reactor to prevent circulating currents between the two windings. The two star secondaries are paralleled to provide high output current. But he design of the transformer becomes complex and may lead to circulating currents.

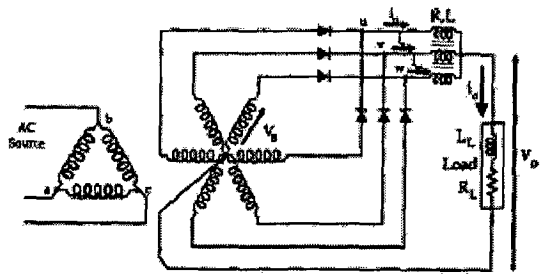

Figure-2.2 (a): 3-single phase center-tapped topology

Topology shown in figure-2.2 (a) can be considered as three single-phase center-tap rectifiers that are connected in parallel through a three phase output filter inductor. Each rectifier is supplied by one of the three separately center-tapped secondary windings of the transformer. Because of the 120° phase among the transformer secondary voltages, the full-wave output voltage of each rectifier will be displaced 60° among others. Theoretical output voltages of the rectifier are shown in figure-2.2 (b).

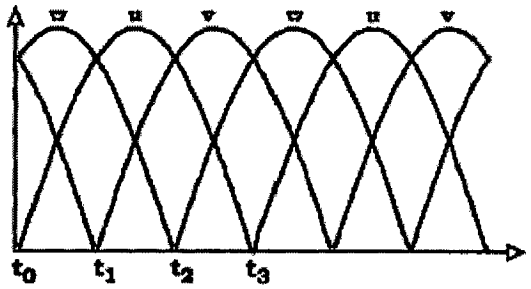

Figure-2.2 (b): Theoretical Output Voltages of rectifier shown in figure-2.2 (a)

The figure-2.2(b) shows that the output voltage has ripple six times the fundamental input frequency as in the case of conventional rectifier. The average value of the output voltage is given by

$$Vo = \frac{2\sqrt{2}}{\pi} Vs$$

Where Vs is the rms value of secondary phase-to-center-tap voltage of the transformer.

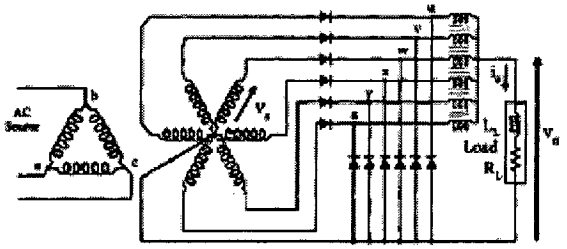

Figure-2.3: 6 Single Phase Half-Wave Rectifier Topology

Topology shown in figure-2.3 can be considered as six single-phase half-wave rectifiers that are connected in parallel through a 6-phase output inductor. Each single phase rectifier is supplied by each phase of the secondary winding of the three phase transformer that is connected as a three-phase-to-six-phase converter. The total output

voltage of the rectifier can be considered as superposition of the output voltage of six single phase half-wave rectifiers.

Another topology that has been proposed in [7] is based on the peculiar connection of transformers in which current sharing is ensured by the series connection of the primaries. The inter-phase transformers are eliminated, the current is forced to divide equally between various unmatched semiconductors and bus-bar symmetry is no longer critical. Furthermore, the main transformer being divided into several units, dry-type construction can be used. The design of the individual transformers is kept simple. The primary windings are connected in zigzag. There, voltage is high and the current level low, so that connections can be made with cables rather than wires. The secondaries are all identical double-star circuits. The increase of the pulse number is easily obtained by the addition of transformers. The power semiconductors are better utilized; current is shared between more devices. Therefore, smaller devices can be selected. Reliability is improved by the fact that, even if the semiconductors age differently, the operation of the system is not affected.

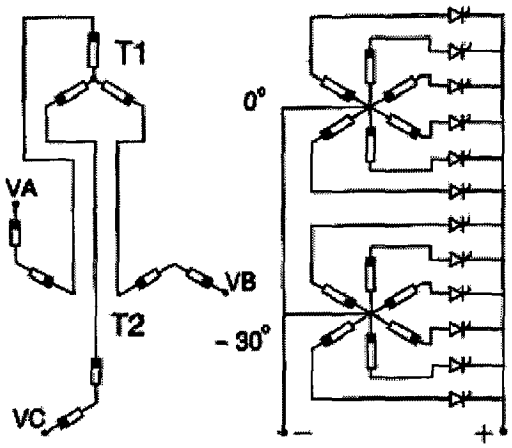

Figure-2.4: 12-Pulse converter with series primary winding

Figure-2.4 shows the 12 pulse converter with series winding which can be seen as the extension as an extension of the conventional 6-phase double star rectifier with a wye primary. The operation of the 6-phase double star arrangement depends on the connection of the primary windings. Of a delta connected transformer is used, the diodes or the thyristors conduct for 60°. However, with a wye connected primary, the conduction period increases to 120° and the power devices only carry half the dc current. The primary

wye connection plays the same role as the interphase transformer and forces two diodes to conduct simultaneously.

The 12-pulse converter of figure-2.4 is composed of two double-star converters connected directly in parallel on the dc side. Each converter is fed by its own transformer. The primary winding of transformer T1 is connected in wye while that of the transformer T2 is connected in zigzag. Moreover, the primary winding of both the transformer are connected in series. The zigzag connection provides the phase-shift needed to obtain a 12-pulse system. In this topology if one power device conducts, at least four other must also conduct to satisfy the ampere-turn equilibrium. In fact, in this circuit, five semiconductors are always in conduction and each of them conducts for 150°. Their average current is one twelfth of the dc current. Again the series connection of the primary windings forces the current to divide in many paths.

A DC high current low-voltage power generating system that is implemented by using a combination of a three phase alternator and a rectifier has been proposed in [2]. A special generator that produced almost trapezoidal voltage waveform has been used in this proposed system. The rectifier consists of three single-phase bridge rectifiers, each connected to a phase winding of the generator, as shown in figure-2.5.

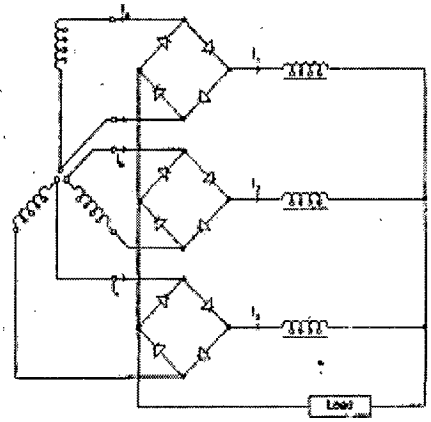

Figure-2.5: Three Phase Output of a generator connected to three bridgerectifiers

These three bridge rectifiers operate simultaneously so that, the current in each rectifier is one third of the total DC or the load current. The ideal configuration is, a square wave voltage connected to the rectifier in order to have the minimum ripple at the DC output current. The nearly square wave or the trapezoidal wave voltage is the most possible waveform generated in three phase generator, and if connected to the rectifier the

DC current produced will also have minimum ripple. In order to develop the square wave voltage in the winding, the configuration of the generator proposed in [2] is based on the fact that the gap flux over the pole shoe should be kept constant, the air gap is made constant so that the curve of the flux density induced in the air gap is square wave shaped.

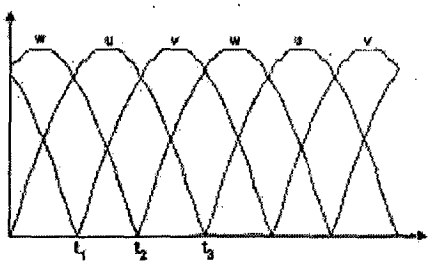

Figure-2.6: Output DC voltage & Current of conventional sinusoidal voltage wave form

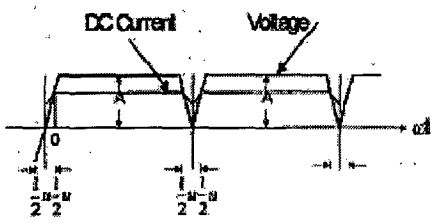

The almost square AC Input

Another topology that has been proposed in [1] is shown in figure-2.7. The DC chopper is operated at high frequency (about 5 kHz). The IGBT inverter is operated as a six- step inverter with the fundamental frequency of 5 kHz. By using this high frequency inverter the required transformer will be small. Because the inverter is operated as a six step inverter, the output voltage of the rectifiers will be similar to the output voltage of a three-phase chopper under 2/3 duty cycle.

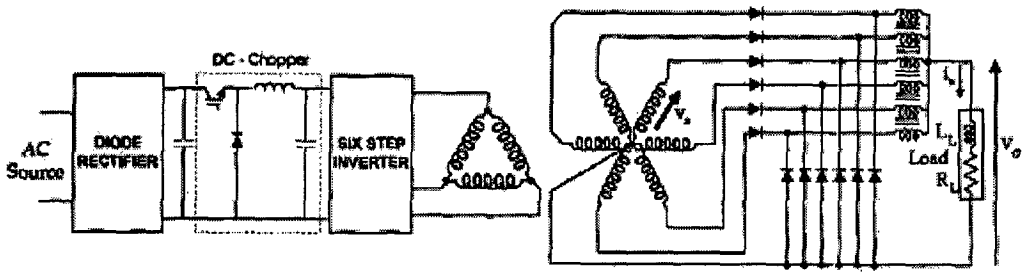

Figure-2.7: A power supply for the cathodic protection system

Another topology that has been used in CERN Switzerland [4] for supplying the superconducting LHC (Large Hadron Collider) particle accelerator which requires high currents (~12.5 kA) and relatively low voltages (~ 10 V) for its magnets has been shown in figure-2.8.

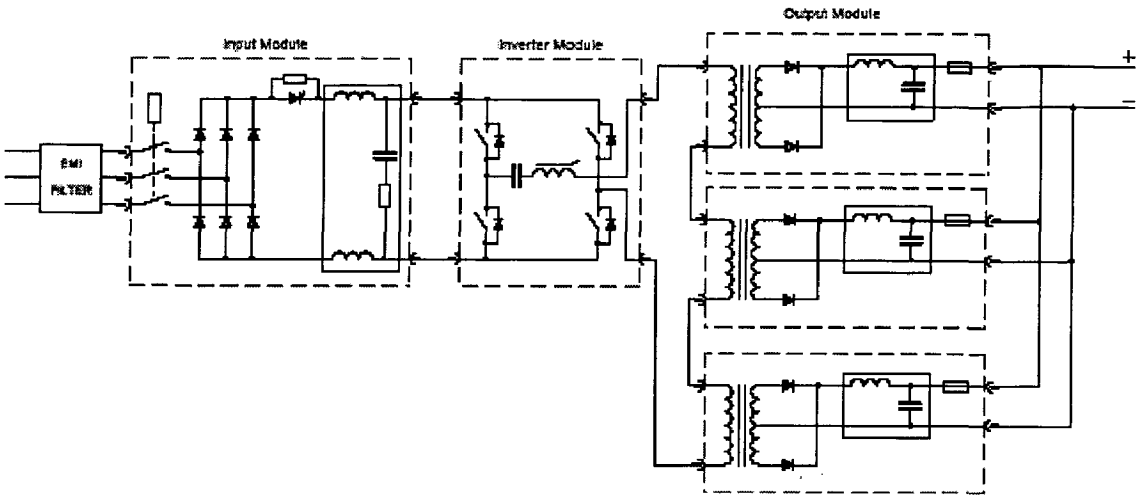

Figure-2.8: Topology used for supplying the LHC magnets at CERN

The chosen topology for the converter is splitin three modules figure-2.8:

- **Input Module** : A power contactor on the AC mains (400V, 50 Hz), a diode rectifier with damped LC filter (70 Hz)
- **Inverter Module**: Full Bridge Zero Voltage Zero Current Switching Phase Shift inverter (FB-ZVZCS-PS) operating at 25 kHz.
- **Output Module**: High frequency transformers, rectifier stage and output filter. To fulfill the weight constraint the module 3 is physically split into three modules of 1.1 kA.

Input Module: The 3-phase mains voltage is rectified and smoothed in the input module. An input contactor disconnects the complete sub-converter from the mains if there is no demand for power or in case of a severe fault. The input module is also equipped with a pre-charge circuit to limit the inrush current when the sub-converter is powered up.

Inverter Module: The filtered DC intermediate voltage from the input module feeds the inverter operating at 25 kHz. This stage employs a "phase shifting" switching mode inverter (ZVZCS-Zero Voltage Zero Current Switching). The control of the power semiconductors is done, instead of turning off the diagonally opposite switches in the bridge simultaneously as for a classical PWM, by introducing a phase-shift between the two legs of the bridge. This phase-shift determines the output power where as the

switching frequency is fixed. The needed energy for the soft commutation of the leading leg (ZVS) comes from the series inductance, the leakage inductance and the output filter inductance. This means that the energy stored is large enough to discharge the parallel switch capacitances (parasitic and snubber) and the parasitic capacitance of the transformer. By using a DC blocking capacitor and a saturable inductance the primary current is reset during the free-wheeling period, which provides the ZCS conditions for the lagging leg switches.

Output Module:

High Frequency Transformer and Schottky diodes:

To achieve the required output parameters (1100A, 16V) with one module, a special transformer with ferrite core UU93 and thin copper foil windings has been used. The secondary is separated into 4 sections each of them feeds a center-tapped rectifier with 2 schottky diode rectifier modules to handle the current with 20% safety margin. Considering to the skin and proximity effect, the foils are wound in such a special way, that the current in each section and also in the Schottky diodes is almost identical. The series/ parallel connection of the split module guarantees a good current sharing between them.

Passive Filter: To achieve the required output ripple of only 10mVpp at 3.25kA a triple stage filter was implemented. The filter stages consist of powder iron cores and electrolytic capacitors with very low ESR and high reliability.

Parallel Operation: The converter has been designed such that several sub-converters can work in parallel. The inverter topology means that the sub-converters are inherently voltage sources. Because of the required parallel connection, a fast current loop transforms the sub-converters into current source. Under normal conditions, all the sub-converters are working in parallel. If one or more of the sub-converters fail, the on-state sub-converters reference will increase, so that the current and voltage of the load do not change. The sub-converters are capable of being started independently and working alone.

In this chapter, an overview of the various low voltage high current rectifiers has been provided. Some of the topologies utilize special transformer connections while others work on switch mode power supply topologies.

CHAPTER-3

HIGH POWER FACTOR RECTIFIERS

The high power factor rectifiers can be categorized as single phase and three phases or based on the fact whether the inductor current is continuous or discontinuous. The control techniques also vary even if the topology may remain the same. In this chapter, a brief review of various control techniques and various 3-phase topologies of high power factor rectifiers has been presented.

3.1 CONTROL TECHNIQUES:

If the single-switch boost rectifier, which is the most widely used topology for power factor correction in single-phase applications, is analyzed then also many control schemes are possible [6]. Figure-3.1 shows the single-switch boost rectifier with a generic controller.

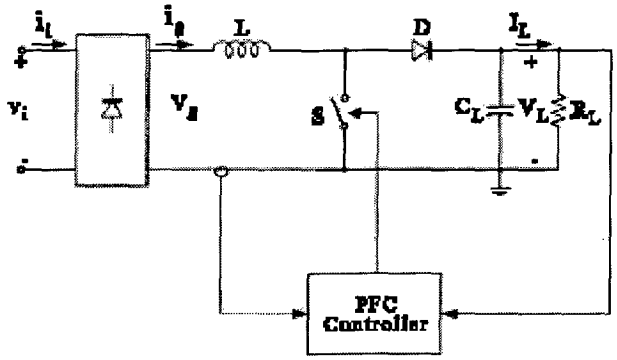

Figure-3.1: Principle scheme of a boost PFC

A diode rectifier brings the ac/dc conversion, while the controller operates the switch in such a way to properly shape the input current i_g according to its reference. The output capacitor absorbs the input power pulsation, allowing a small ripple of the output voltage V_L. The boost topology is very simple and allows low-distorted input current and almost unity power factor with different control techniques. Some of the widely used control techniques are:

Peak Current Control: The basic scheme of the peak current controller is shown in figure-3.2, along with input current waveform. As can be seen, the switch is turned on a constant frequency by a clock signal, and is turned off when the sum of the positive

ramp of the inductor current (i.e. the switch current) and an external ramp (compensating ramp) reaches the sinusoidal current reference.

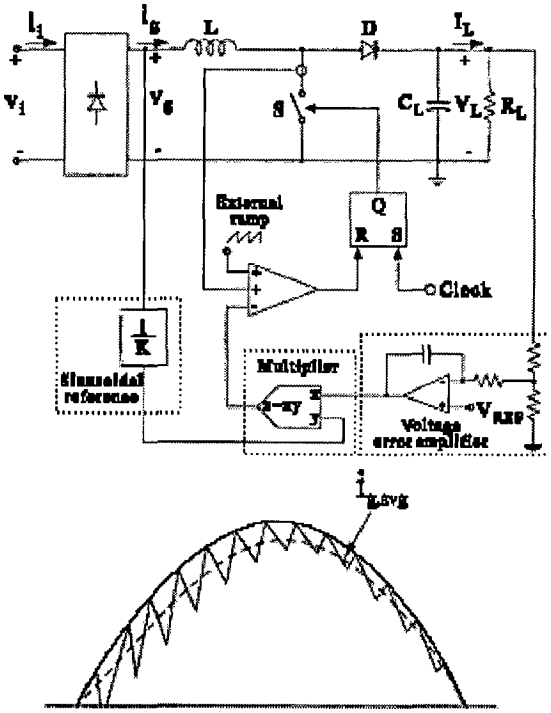

Figure-3.2: Peak Current Control Technique

The sinusoidal current reference is generated by multiplying the scaled replica of the rectified line voltage vg times the output of the voltage error amplifier, which sets the current reference amplitude. In this way the reference signal is naturally synchronized and always proportional to the line voltage, which is the condition to obtain unity power factor. As is evident from the figure-3.2 the converter operates in Continuous Inductor Current Mode (CICM); this means that the device current stresses as well as the input filter requirements are reduced. Moreover, with continuous input current the diodes of the bridge can be slow devices (operating at line frequency). On the other hand, the hard turn-off of the freewheeling diode increases losses and switching noise calling for a fast device. The advantages and disadvantages of the scheme are:

Advantages:

- constant switching frequency
- Only the switch current must be sensed and this can be accomplished by a current transformer, thus avoiding the losses due to sensing resistor.

- No need of current amplifier and its compensating network.
- Possibility of a true switch current limiting.

Disadvantages:

- Presence of sub-harmonic oscillations at duty cycles greater than 50%, so a compensation ramp is needed.
- Input current distortion which increases at high line voltages and light load and is worsened by the presence of the compensating ramp.
- Control more sensitive to commutation noises.

Average Current Control: Another method which allows a better input current waveform is the average current control shown in figure-3.3.

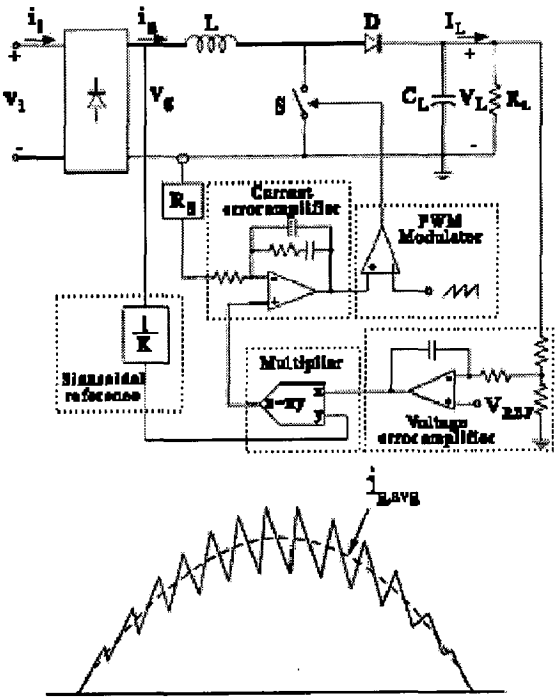

Figure-3.3: Average Current Mode Control

Here the inductor current is sensed and filtered by a current error amplifier whose output drives a PWM modulator. In this way the inner current loop tends to minimize the error between the average input current i_g and its reference. The latter is obtained in the same way as in the peak current control. The converter works in CICM so the same considerations done with regard to the peak current control can be applied.

Advantages:

- Constant switching frequency.

- No need of compensation ramp.
- Control is less sensitive to commutation noises due to the current filtering.
- Better input current waveform then for the peak current control since near the zero crossing of the line voltage the duty cycle is close to unity, so reducing the dead angle in the input current.

Disadvantages:

- Inductor Current must be sensed.
- A current amplifier is needed and its compensation network design must take into account the different converter operating points during the line cycle.

Hysteresis Current Control: Figure-3.4 shows this type of control in which two sinusoidal current references $I_{P,ref}$ and $I_{V,ref}$ are generated, one for the peak another for the valley of the inductor current.

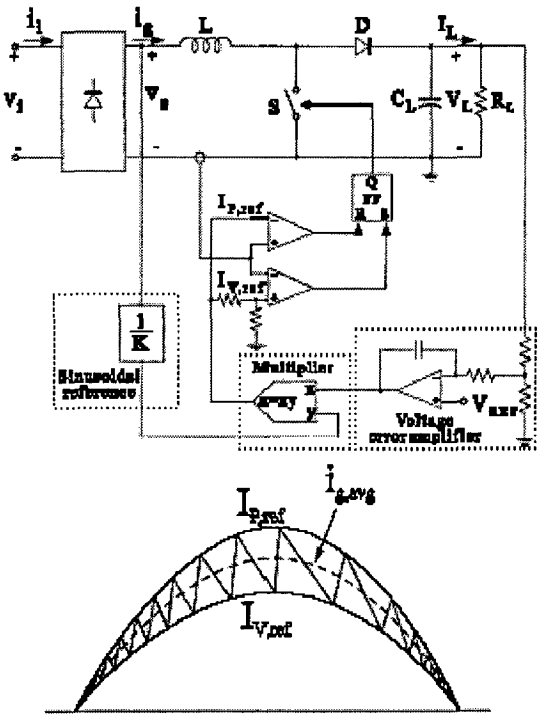

Figure-3.4: Hysteresis Control Scheme

According to this scheme the switch is turned on when the inductor current goes below the lower reference IV,ref and is turned off when the inductor goes above the upper reference IP,ref, giving rise to a variable frequency control. Also, with this technique the converter works in CICM.

Advantages:

- no need of compensation ramp
- Low distorted input current waveform.

Disadvantages:

- variable switching frequency
- Inductor current must be sensed.
- Control sensitive to commutation noises.

In order to avoid too high switching frequency, the switch can be opened near the zero-crossing of the line voltage so introducing dead times in the line current. **Borderline Control**: In this control approach the switch on-time is held constant during the line cycle and the switch is turned on when the inductor current falls to zero, so that the converter operates at the boundary between continuous and discontinuous inductor current mode. In this way, the free-wheeling diode is turned off shortly (no recovery losses) and the switch is turned on at zero current, so the commutation losses are reduced. On the other hand, the higher current peaks increase the device stresses and conduction losses, and may call for heavier input filters.

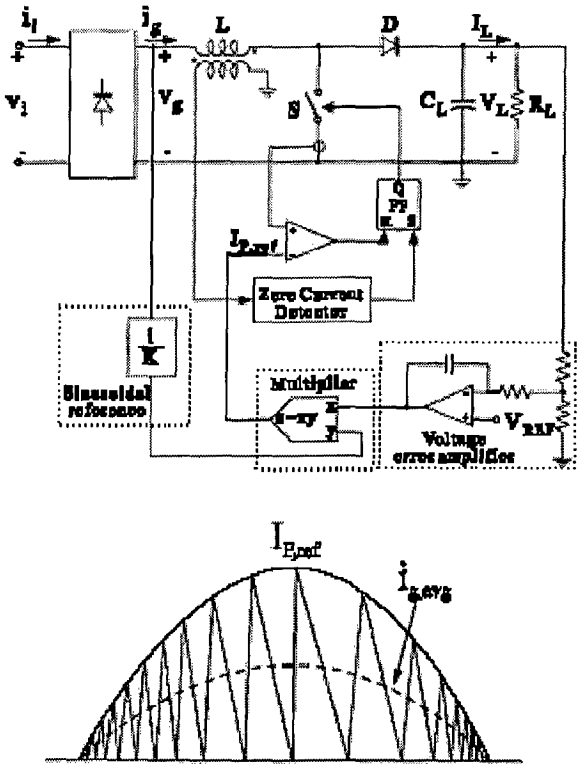

Figure-3.5: Borderline control approach

This type of control is special case of hsyteresis control where the lower reference $I_{V,ref}$ is zero everywhere. The instantaneous input current is constituted by a sequence of triangles the peaks of which are proportional to the line voltage. Thus the average input current becomes proportional to the line voltage without the duty cycle modulation during the line cycle. This characterizes this control as an "automatic current shaper" technique. The same control strategy can be generated without using a multiplier, by modulating the switch on-time duration according to the output signal of the voltage-error amplifier. In this case, switch current sensing can be eliminated.

Advantages:

- no need of a compensation ramp
- no need of a current error amplifier
- For controller using switch current sensing, switch current limitation can be introduced.

Disadvantages:

- variable switching frequency
- inductor voltage must be sensed in order to detect the zeroing of the inductor current
- For controllers in which the switch current is sensed, control is sensitive to commutation noises.

3.2: FORCE-COMMUTATED THREE-PHASE CONTROLLED RECTIFIERS

Three phase controlled rectifiers have a wide range of applications They are used for electrochemical process, many kinds of motor drives, traction equipment, controlled power supplies, and many other applications. They can be classified as either line commutated or force-commutated rectifiers. The force commutated rectifiers have got better performance than the line commutated rectifiers.

Force-commutated rectifiers are built with semiconductor devices with gate turn-off capability. The gate turn-off capability allows full control of the converter, because valves can be switched ON or OFF whenever required. This allows commutation of the valves hundred of times in one period which is not possible with line commutated

rectifiers where thyristors are switched ON or OFF only once a cycle. This feature has the following advantages:

a) The current or the voltage can be modulated (Pulse Width Modulation or PWM), generating less harmonic contamination;

b) Power factor can be controlled, it can be made leading also;

c) They can be built as voltage or current source rectifiers;

d) The reversal of power in thyristor rectifiers is by reversal of voltages at the DC link. Instead, the force commutated rectifiers can be implemented for both reversal of voltage and reversal of current.

A variety of 3-phase ac-dc PWM rectifiers are known; the most well-known topology is the three-phase ac-to-dc boost rectifier, illustrated in figure-3.6.This converter requires six current-bidirectional two quadrant switches. The inductors and the capacitors filter the high frequency switching harmonics, and have little influence on the low –frequency ac components of the waveforms.

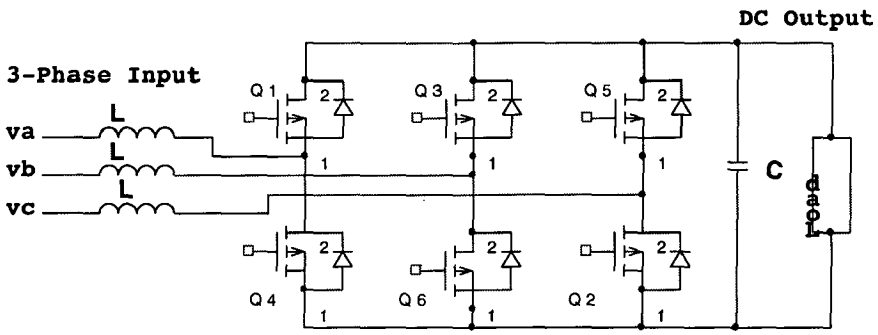

Figure-3.6: Boost type 3-phase AC-DC Rectifier

The switches of each phase are controlled to obtain input resistor emulation, either with a multiplying controller scheme employing average current control, or with some other approach. To obtain undistorted line current waveforms, the DC output voltage must be greater than or equal to the peak line-to-line ac input voltage. This converter topology resembles the well known voltage source inverter, except that the converter is operated as a rectifier, and the converter is controlled via high frequency pulse-width modulation. The ac input line currents are non-pulsating, and hence very little additional input EMI filtering is required. As in the case of single-phase boost rectifier, the rms switch current and also the conduction losses of the 3-phase boost rectifier are low

relative to other 3-phase ac-dc topologies such as those shown in figure-3.7. The converter is capable of bidirectional power flow.

A disadvantage is the requirement for six active devices; when compared with a dc-dc converter of similar rating the active semiconductor utilization is low. Also, since the rectifier has a boost characteristic, it is not suitable for direct replacement of traditional buck-type phase-controlled rectifiers.

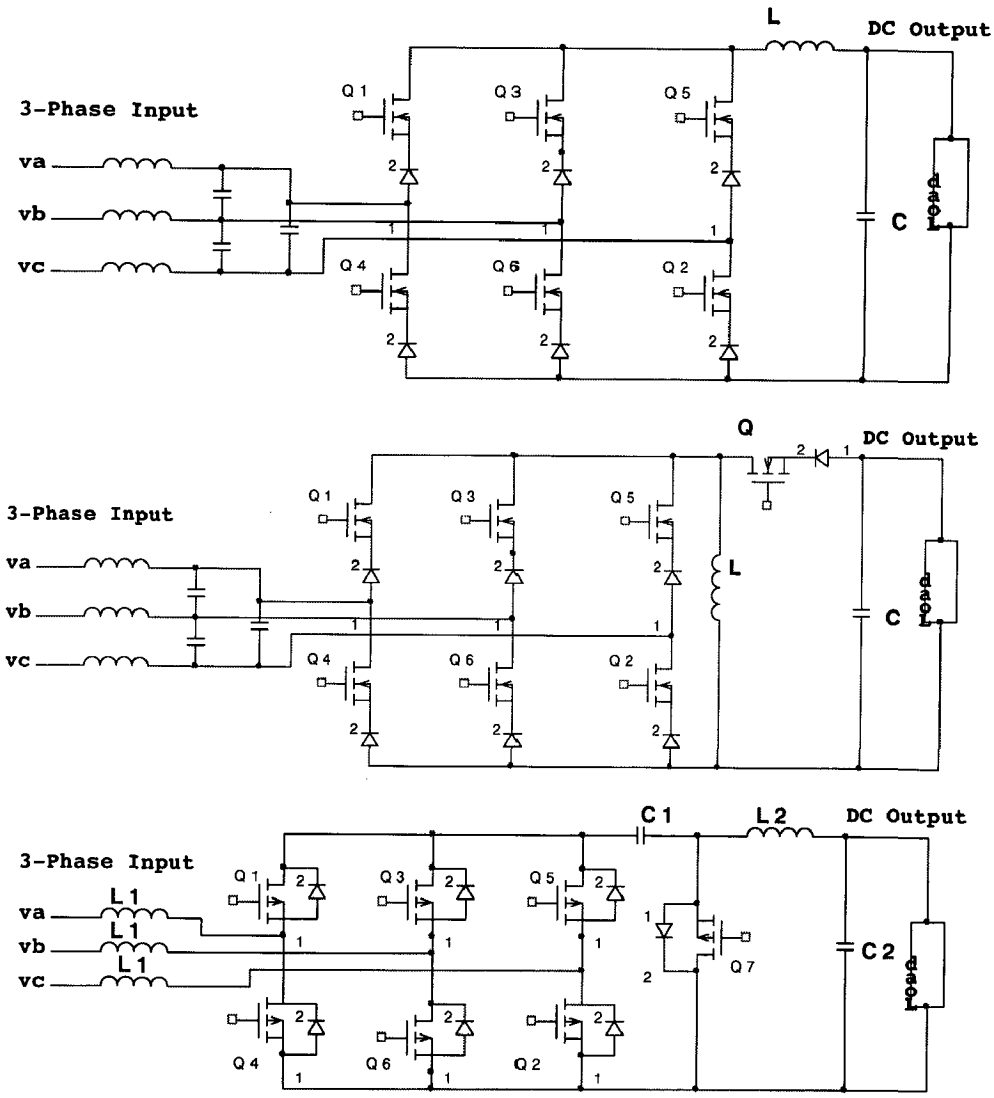

Figure-3.7: 3-phase ac-dc rectifiers based on: (a) buck dc-dc converter, (b) buck-boost dc-dc converter (c) Cuk dc-dc converter.

Three-phase ac-to-dc rectifiers having buck, buck-boost, or other characteristics are possible, but find much less use than the boost topology. An example is the 3-phase ac-dc buck rectifier shown in figure-3.7 (a). Unlike the single-phase case, in

three-phase applications the buck topology can supply constant power to a dc load, with negligible distortion of the ac line current waveforms. When the voltage of one of the phases is zero, the other two phases have nonzero voltage and can supply the dc load power. This converter produces a controlled dc output voltage that is less than the peak line-line ac input voltage. This converter resembles what is known as the current-source inverter, except that the converter is operated as a rectifier, and the converter is controlled via high-frequency pulse-width modulation.

Two-quadrant voltage-bidirectional switches are required in this converter. A disadvantage of the 3-phase buck rectifier is the higher conduction losses induced by the series connection of the devices. Also, the rms transistor currents are greater than that in the 3-phase boost rectifier; this therefore increases the conduction loss. The converter is capable of operation in the inverter mode by reversal of the polarity of the output voltage. A substantial input filter is usually required to smooth the pulsating ac line currents.

PWM 3-phase ac-dc rectifiers which resemble most other dc-dc converter topologies are also possible. Two examples are the 3-phase ac-dc rectifiers of figures-3.7(b) and 3.7(c), based on the dc-dc buck-boost and Cuk converters respectively. These converters can be viewed as being derived from parent dc-dc converters via a transformation in which the dc input and switch network are replaced by a three-phase input and six-switch bridge network. High-frequency isolation can also be incorporated into most of these converters.

The various forced commutated rectifiers discussed above operate in continuous conduction mode and require six or more active devices. Compared with the conventional low-power factor passive rectifier approaches, the increased active silicon area and reduced silicon utilization of the six-switch approach can be expensive. Low-harmonic 3-phase ac-dc rectification can be preformed using a conventional passive six-diode rectifier and a harmonic trap filter; hence fundamentally, no semiconductor devices other than the diodes are required. When control of the output voltage is required at least one active device is needed. If it is desired to avoid the use of low-frequency filter elements, then a source of high-frequency switching harmonics is needed, again necessitating inclusion of at least one active device. So, a single active device is the minimum needed to synthesize low-harmonic 3-phase rectifiers containing no low-

frequency reactive elements, having control of the output voltage, and having unidirectional power flow.

Several single-switch approaches to three-phase rectification are known, of these the single-switch boost rectifier, shown in figure-3.8(a), operating in discontinuous conduction mode (DCM) is the most popular one. Figure-3.8(b) shows the input current waveform of such a converter. The switch is here controlled in the same manner as in a dc-dc boost converter. The inductors L1, L2, and L3 are of equal small value, such that they operate in the discontinuous conduction mode in conjunction with diodes D1-D6. At the end of the switch conduction sub interval, the inductor currents reach peak values which are also proportional to the applied 3-phase line-to-neutral voltages. When the switch turns off, the diode D7 becomes forward-biased and the inductors release their stored energies to the DC output. Since the peak currents are proportional to the applied input line-to-neutral voltages, then the average values of the input currents are also proportional to the input line-to-neutral voltages. Thus, approximate three-phase input resistor emulation is obtained. The three phase DCM boost rectifier does generate a modest amount of low-frequency input current harmonics; the THD can be reduced by increasing the dc output voltage.

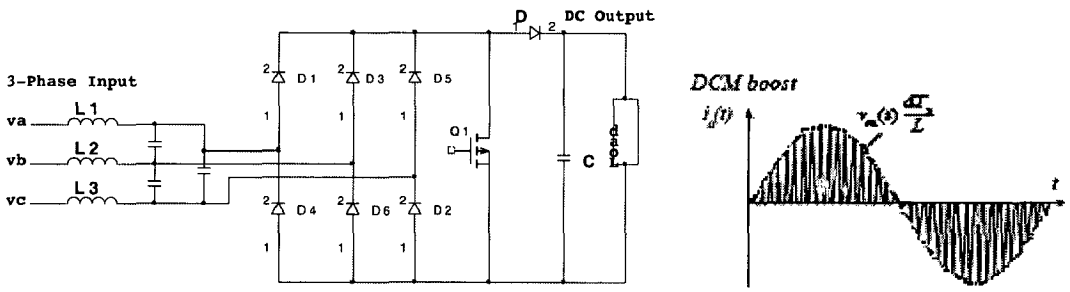

Figure-3.8: (a) Single-switch three phase DCM boost rectifier. (b)Input current waveform

The three-phase DCM boost rectifier has the advantage of very simple control. The switch can operate at constant switching frequency. Variation of duty cycle allows the control of the dc output power. Only a single active switch such as a MOSFET or IGBT is needed. A disadvantage is the need for an input filter to remove the high-frequency components of the pulsating input currents. As in all single-switch three-phase rectifiers, bidirectional power flow is not possible. It is this topology of single-switch boost rectifier that has been used in this dissertation because of the above mentioned advantages,

moreover, in the present case of DC Conduction Pump there is no possibility of bidirectional power flow.

A similar scheme, based on the DCM flyback converter is illustrated in figure-3.9. This converter is effectively three independent single-phase DCM flyback rectifiers, which share a single-switch. The peak transformer magnetizing currents follow the applied ac phase voltages. This causes the average input currents to directly follow the applied line-to-neutral voltages, without generation of the low-frequency current harmonics.

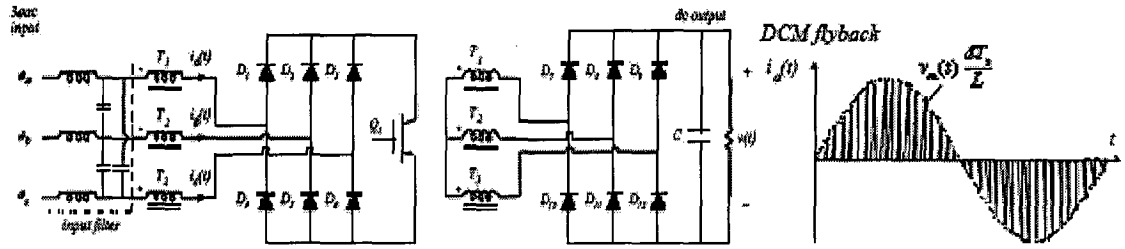

Figure-3.9: (a) single-switch three-phase DCM flyback rectifier (b) Input current waveform

The rectifier can both increase and decrease the voltage magnitude and is capable of inrush current limiting. In low-power applications this is simple way to obtain low-frequency three-phase rectifier which incorporates high-frequency isolation transformers. It has the disadvantage of requiring an input filter for removal of high-frequency components of the pulsating input current waveforms.

A buck-derived single-switch rectifier is shown in figure-3.10. This converter is based on the zero-current switching (ZCS) quasi-resonant dc-dc buck converter. A resonant inductor Lr is placed in each phase.

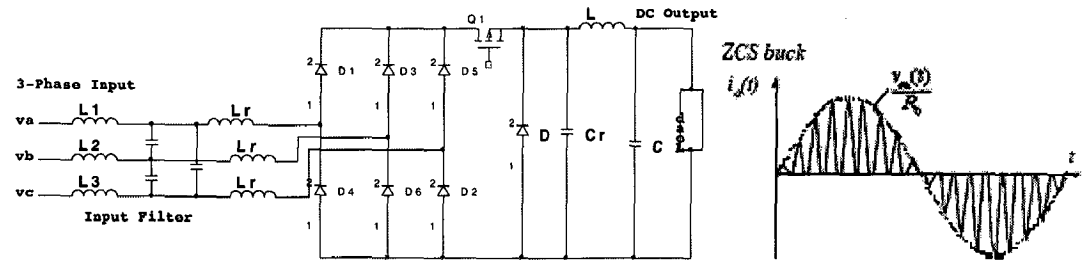

Figure-3.10: (a) Single-switch 3-phase ZCS quasi-resonant buck rectifier (b) input current

When the switch conducts, the resonant inductors Lr ring in conjunction with resonant capacitor Cr. The input currents are approximately sinusoidal pulses, having peak amplitude proportional to the applied input line to neutral voltages. At full load, a

THD of approximately 13-14% is observed; nearly all of the THD can be attributed to the fifth harmonic. The THD can be reduced to less than 10%, by use of any control scheme that leads to constant instantaneous power flow.

The switch operates with zero current switching. An IGBT, inverter-grade SCR, or other device can be used. The peak voltage stress on the switch is equal to the applied peak input line-to-line voltage, while the peak current is approximately twice the dc output current. The switch operates with approximately constant on-time, equal to the length of the resonant current pulse. The output power is controlled by variation of the switch off-time, and hence the converter operates with variable switching frequency. The rectifier requires an input filter to remove high-frequency components of pulsating input current waveforms.

In this chapter, the various control techniques as well as the various topologies for high power factor rectifiers have been presented. The most of the control techniques differ only in the way the input current is controlled either in CCM or DCM. Some techniques lead to constant switching frequency while others to variable switching frequency. The various 3-phase topologies utilize either six or more active power switching devices or have got a single active switch. Generally, the performance of six –active switches configurations is better than that of the single-switch topologies but with increased cost and complexity.

CHAPTER-4

PROPOSED TOPOLOGY

In this chapter, the proposed topology for the low voltage high current rectifier will be discussed. The reasons which lead to the selection of the proposed topology will also be enunciated. In chapter-2, various low voltage high current topologies were presented where as in chapter-3 various high power factor rectifier topologies were presented. The aim of this work is to have a low voltage high current rectifier with reduced harmonic distortion and improved power factor while having reduced weight and size.

The topologies shown in figures-2.1, 2.2(a), 2.3 and 2.4 do provide high current at low voltages but they require complex transformer arrangements which add to cost, weight and size of the overall system. Topologies of figures- 2.1, 2.2(a), and 2.3 also require interphase transformer which also adds to the weight and size of the system. The topology of figure-2.5 require a special type of generator which may not be suitable in many cases due to the additional space required by the generator, moreover it adds to the maintenance costs also.

The cathodic protection system of figure-2.7 has got control of the output voltage and current but is quite complicated and bulky since it has got a chopper, a six-step inverter and a rectifier along with a complex transformer. The number of active devices is quite high in this topology. The power supply for supplying the LHC magnets (figure-2.8) has got less weight and volume but it incorporates a passive filter at the input after the diode rectifier section which adds to the weight and size of the system. If this topology be modified so that the passive filter is removed without compromising with the power factor and harmonic distortion then it can serve as a suitable low voltage high current rectifier.

In chapter-3 various high power factor rectifiers along with various control techniques have been presented. The force commutated topologies have got excellent power factor and response but the number of active switches increases. Out of the various single-switch boost topologies the single-switch boost rectifier operating in discontinuous conduction mode (DCM) is quite a promising solution for less than 10kW applications and has got good response and power factor with just a single controllable switch.

4.1: Existing Topology

The existing topology of low voltage high current rectifier for supplying the D.C. Conduction Pump, at IGCAR Kalpakkam (T.N.), India is shown in figure-4.1.

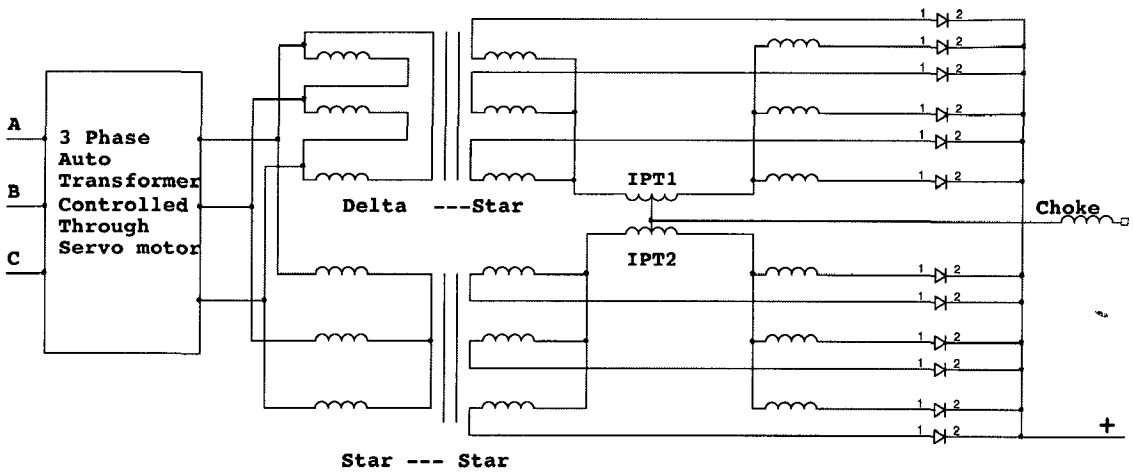

Figure-4.1: Existing Topology of Low Voltage High Current Rectifier

It consists of a diode bridge rectifier that is fed through star-star and delta-star transformers, the input to which is again controlled through a three phase transformer which is controlled by a servo-motor for closed loop operation. The disadvantage with such a system is that it becomes bulky (since the transformers are operated at power frequency) as well as the response becomes slow since it is controlled through a servo motor for closed loop operation. In order to overcome these difficulties the topology shown in figure-4.2 has been proposed.

4.2: Proposed Topology

The proposed topology shown in figure-4.2 consists of a front end boost rectifier operating in discontinuous inductor current mode (DICM) the output of which is fed to a single inverter which is operated at high frequency and is controlled by phase-shift control strategy which is quite a reliable and simple control strategy for obtaining ac output which is then rectified to yield controlled dc output. The high frequency transformer provides the step-down function and then the output is rectified to give the DC output. Since the entire control is electronic the response is quite fast and there is no problem of mechanical wear and tear. The transformer operates at high frequency so the size and weight of the transformer gets reduced.

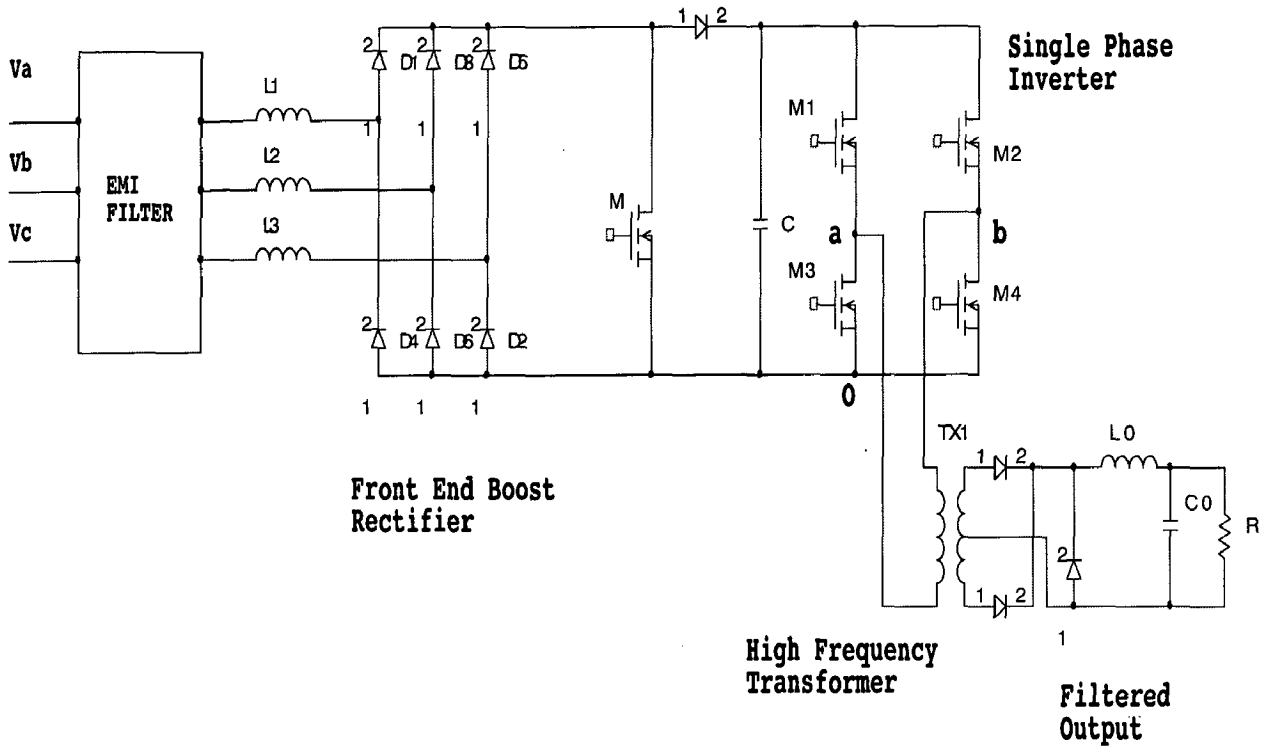

Figure-4.2: Proposed topology for Low Voltage High Current Rectifier

The topology of low voltage high current rectifier consists of:-

Front End Boost Rectifier: This is used for obtaining a DC voltage at a high power factor and low distortion factor from the mains power supply. An EMI Filter is used to filter the high frequency components of inductor current.

Single Phase Inverter: It is operated at high frequency and is controlled through phase shift control.

High Frequency Transformer: It is used to provide both isolation and required voltage level conversion. The secondary of the transformer is center-tapped.

Output Filter: It is used to filter the pulsed output and provide a regulated smooth DC voltage.

In this chapter, the topology for the low voltage high current rectifier has been proposed and the reasons for selecting the topology have also been mentioned. In the next chapters modeling of the system will be done and the performance of the given system will be investigated.

CHAPTER-5

Modeling of Low Voltage High Current Rectifier

In this chapter, the modeling of the proposed low voltage high current rectifier (LVHCR) will be presented. The modeling has been split into various parts where first the models of the different subsystems (DCM boost rectifier, phase-shift inverter control and output Buck rectifier) will be presented and then the overall integrated model of the LVHCR will be presented.

5.1 Modeling Single-Switch DCM Boost Rectifier

This section provides a simplified analysis and design for the single-switch DCM boost rectifier [8, 14]. Because of the symmetry of three-phase systems, the analysis of the operating stages can be limited to the interval 0< <. /6. For the purpose of mathematical representation of the DCM boost rectifier operation, the input voltages are assumed to be

$$v_a = V_{pk} \sin\theta \quad \text{... (5.1)}$$

$$v_b = V_{pk} \sin(\theta - \frac{2\pi}{3}) \quad \text{... (5.2)}$$

$$v_c = V_{pk} \sin(\theta + \frac{2\pi}{3}) \quad \text{... (5.3)}$$

Where V_{pk} is the peak input line-to-neutral voltage.

Four operating stages can be identified in a switching period of the single-switch DCM boost rectifier, as shown in Figure-5.1. In the same figure-5.1, k represents the k^{th} switching period within the line period Tr. In the first operating stage, the power switch is turned on to linearly charge the input inductors according to the phase voltage that is applied across each one. In the second operating stage, the power switch is turned off to reset the inductors. The inductor with the lowest peak current resets first. In the third operating stage, the two remaining inductor currents are reset to zero at the same rate. Once the reset interval has finished, the output load is supplied by the energy stored in the output filter capacitor until the next switching period restart. In the analysis that follows, the line-to-neutral input voltage v_a is taken as the reference voltage for the three-phase system established in (5.1-5.3).

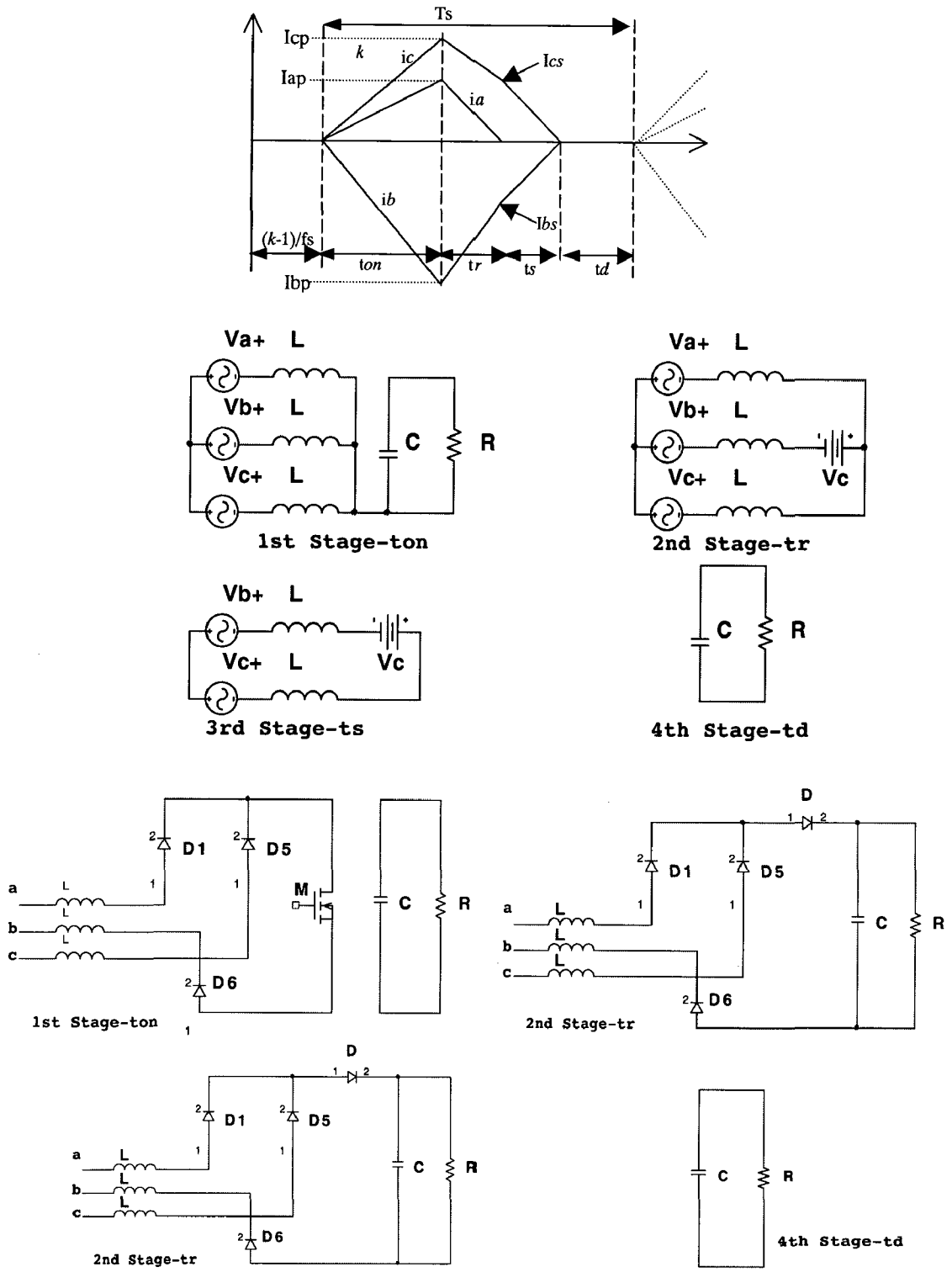

Figure-5.1: Current in the boost inductors and operating stages in the interval 0< <. /6 of the input AC voltages.

duration of the second operating stage, t_s is the time duration of the third operating stage, and T_s is the switching period.

The duration of the second stage is the time taken by the current through inductor L_a to be reset:

$$t_r = \frac{L(0 - I_{ap})}{v_{La}} \quad \text{... (5.10)}$$

The voltage v_{La} across the inductor connected to line *a* can be obtained from the equivalent network of the second operating stage, as shown in Figure-5.1. As a result, the second operating stage provides the following expressions:

$$\begin{aligned} v_a - v_{La} - V_o + v_{Lb} - v_b &= 0 \\ v_a - v_{La} + v_{Lc} - v_c &= 0 \\ v_{La} + v_{Lb} + v_{Lc} &= 0 \end{aligned} \quad \text{.... (5.11)}$$

Solving the above expressions for the voltage across the input inductors during the second stage results in the following:

$$v_{La} = v_a - \frac{V_o}{3} \quad \text{... (5.12)}$$

$$v_{Lb} = v_b + \frac{2V_o}{3} \quad \text{.... (5.13)}$$

$$v_{Lc} = v_c - \frac{V_o}{3} \quad \text{... (5.14)}$$

Substituting (5.4-5.6) and (5.12-5.14) into (5.10), results in the time duration of the second operating stage as a function of output and input voltages, duty cycle and switching frequency:

$$t_r = \frac{D}{f_s}\left[\frac{3v_a}{(V_o - 3v_a)}\right] \quad \text{... (5.15)}$$

During the second operating stage, the voltage across the input inductors connected to lines b and c can be obtained from (5.4-5.6) and (5.12-5.14):

$$v_{Lb} = \frac{L(I_{bs} - I_{bp})}{t_r} \quad \text{... (5.16)}$$

$$v_{Lc} = \frac{L\left(I_{cs} - I_{cp}\right)}{t_r} \qquad \text{... (5.17)}$$

Equations (5.4-5.6), (5.12-5.14) and (5.15) can be substituted in (5.16-5.17). The resulting set of equations can be solved for the current through lines *b* and *c* at the end of the second operating stage:

$$I_{bs} = \frac{D}{Lf_s}\left[\frac{(v_b + 2v_a)V_o}{V_o - 3v_a}\right] \qquad \text{... (5.18)}$$

$$I_{cs} = \frac{D}{Lf_s}\left[\frac{(v_c - v_a)V_o}{V_o - 3v_a}\right] \qquad \text{... (5.19)}$$

It is still necessary to determine the time duration of the third operating stage in order to calculate the average current through the power lines. From Figure-5.1, the equivalent network of the third operating stage provides the following expressions:

$$v_b - v_{Lb} + V_o + v_{Lc} - v_c = 0 \qquad \text{... (5.20)}$$

$$v_{Lb} + v_{Lc} = 0 \qquad \text{... (5.21)}$$

In order to determine the duration of this stage, it is necessary to write down the equation of the voltage applied across inductors L_b or L_c:

$$v_{Lb} = -v_{Lc} = \frac{L\left(0 - I_{bs}\right)}{t_s} \qquad \text{... (5.22)}$$

From (5.18-5.19), (5.20-5.21) and (5.22), one can obtain the expression of the time duration for the third operating stage as follows:

$$t_s = \frac{D}{f_s}\left[\frac{-2V_o\left(2v_a + v_b\right)}{\left(V_o - 3v_a\right)\left(V_o + v_a + 2v_b\right)}\right] \qquad \text{.... (5.23)}$$

From the previous analysis, the average currents through the power lines can be obtained by substituting (5.1-5.3), (5.4-5.6), (5.15), (5.18-5.19) and (5.23) into (5.7-5.9). The result is described as follows as a function of the phase angle. :

$$i_a = \frac{D^2 V_o V_{pk}}{2Lf_s}\left[\frac{\sin\theta}{V_o - 3V_{pk}\sin\theta}\right] \qquad \text{... (5.24)}$$

$$i_b = \frac{D^2 V_o V_{pk}}{2Lf_s}\left[\frac{2\sqrt{3}V_{pk}\sin(2\theta) - V_o\sin\theta - \sqrt{3}V_o\cos\theta}{\left(V_o - 3V_{pk}\sin\theta\right)\left(V_o - \sqrt{3}V_{pk}\cos\theta\right)}\right] \quad \text{... (5.25)}$$

$$i_c = \frac{D^2 V_o V_{pk}}{Lf_s}\left[\frac{-\sqrt{3}V_{pk}\sin(2\theta) - V_o\sin\theta + \sqrt{3}V_o\cos\theta}{\left(V_o - 3V_{pk}\sin\theta\right)\left(V_o - \sqrt{3}V_{pk}\cos\theta\right)}\right] \quad \text{... (5.26)}$$

Equations (5.24-5.26) are not normalized, and for this reason it restricts the value of the analysis. The normalized version of (5.24-5.26) is given in the following set of expressions:

$$i_{an} = \frac{D^2 M}{2}\left[\frac{\sin(\theta)}{(M - 3\sin(\theta))}\right] \quad \text{... (5.27)}$$

$$i_{bn} = \frac{D^2 M}{2}\left[\frac{\sqrt{3}\sin(2\theta) - M\sin(\theta + \Pi/3)}{(M - 3\sin(\theta))(M - \sqrt{3}\cos(\theta))}\right] \quad \text{... (5.28)}$$

$$i_{cn} = \frac{D^2 M}{2}\left[\frac{-\frac{\sqrt{3}}{2}\sin(2\theta) - M\sin(\theta - \Pi/3)}{(M - 3\sin(\theta))(M - \sqrt{3}\cos(\theta))}\right] \quad \text{... (5.29)}$$

where:

$$M = \frac{V_o}{V_{pk}}$$

$$\left\langle i_{an}\ i_{bn}\ i_{cn}\right\rangle = \frac{\left\langle i_a\ i_b\ i_c\right\rangle Lf_s}{V_{pk}} \quad \text{... (5.30)}$$

In the expression above, M is the voltage conversion ratio of the single-switch three-phase DCM boost rectifier, while i_{an}, i_{bn} and i_{cn} are the normalized instantaneous average currents through the power lines a, b and c, respectively.

The analysis performed in the first 30°interval of the input line voltages can be extended to the entire line period. Because of the symmetry of the three-phase system, it is enough to expand the analysis of the converter up to one quarter of the line period, as shown in Table [5-A]. By phase-shifting the expressions given in (5.27-5.29), one can extrapolate the average line currents to the entire line period.

Line	Current During Interval $0<\theta<\pi/6$	Current During Interval $\pi/6<\theta<\pi/3$	Current During Interval $\pi/3<\theta<\pi/2$
A	$i_{an}(\theta)$	$i_{cn}(\pi/3-\theta)$	$-i_{bn}(\theta-\pi/3)$
B	$i_{bn}(\theta)$	$i_{bn}(\pi/3-\theta)$	$-i_{cn}(\theta-\pi/3)$
C	$i_{cn}(\theta)$	$i_{an}(\pi/3-\theta)$	$-i_{an}(\theta-\pi/3)$

Table [5-A]: Extending the results given in (5.27-5.29) to one quarter of the line period.

Critical Conduction

The single-switch boost rectifier operates in discontinuous mode (DCM) so it is important to know the boundary between the continuous and discontinuous operating modes so that the converter is designed to operate in DCM under all possible operating conditions. In DCM operation, the currents in the boost inductors are zero before the power switch is turned on again. The converter will operate in DCM if the value of inductor is less than the critical inductance for all operating conditions. The maximum power delivered by the converter also decides the value of critical inductance.

For a DC/DC boost converter, the results shown in Appendix (A-1) can be directly used to calculate the boost inductor. In fact, if the boost inductor of the DC/DC converter is selected so that the critical power in Eqn. (A-3) is greater than the maximum delivered power, the DC/DC converter operates in DCM.

For a single-switch three-phase boost rectifier, the solution is not so straightforward [14]. That is because the duty cycle D, critical power, and delivered power are functions of the instant of the sinusoidal input voltages. In other words, over one line cycle, the critical power is time-variant. At some instants, the critical power is going to be minimum. Hence, if these instants can be found and the inductor is designed at these worse cases, then the converter will operate at DCM over the whole line cycle.

Under balanced three-phase input voltages, the equivalent input voltage of the circuit in Figure-5.2 has to be:

$$V_{in\_e} = max[|V_{ab}(\omega t)|, |V_{bc}(\omega t)|, |V_{ac}(\omega t)|] \quad \ldots (5.31)$$

which repeats every $60°$ and reaches maximum at $\omega t = n \times 60°$, $n = 0, 1, 2,...$, when the equivalent inductor is $L_e = 2L$. This is because at these moments one phase voltage is zero, and other two phase voltages applied to the input see two inductors in series. According to Eq. (A-3), once the input voltage reaches the maximum, the duty cycle D is minimum, and the critical power reaches the minimum. In other words, at these moments, the converter is going to operate in CCM the earliest as load is increased.

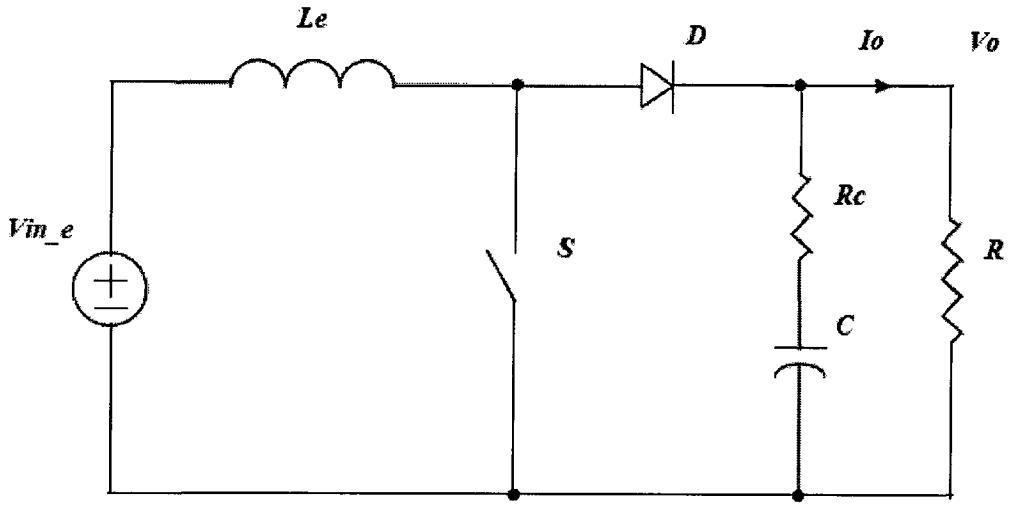

Figure-5.2: An equivalent circuit of the single-switch three-phase boost rectifier

For example, during $0° \leq \omega t \leq 60°$, $\omega t = 0°$ and $\omega t = 60°$ are the two moments at which the critical power reaches the minimum, and the converter is going to operate in CCM earlier than the other moments. So, as long as the inductors are selected to ensure the DCM operation at these two particular moments as load is maximum, the converter is going to operate in DCM in the whole load ranges and whole time periods. This is the inductor value selection guideline for the single-switch three-phase boost rectifier. Generally some margin of about 20-30% is also taken while deciding the value of boost inductance to take into account the input voltage variation andother variations.

5.2 Inverter Operation with Phase Shift Control

This section presents the modeling of single phase inverter with phase – shift control. The single phase inverter is controlled by means of phase shift control. At high-power levels, the full bridge phase-shifted dc-dc converter has been an attractive choice, since it provides high-power density with high efficiency and low electromagnetic interference. Besides, the constant frequency operation with linear output characteristics, it can also integrate the stray elements (junction capacitances and leakage inductance). The circuit operates at a fixed frequency and output regulation is achieved by pulse width modulation technique. Thus the control circuit is easier to design. The circuit diagram for the full-bridge phase-shifted PWM converter along with the waveforms is shown in figure - 5.3.

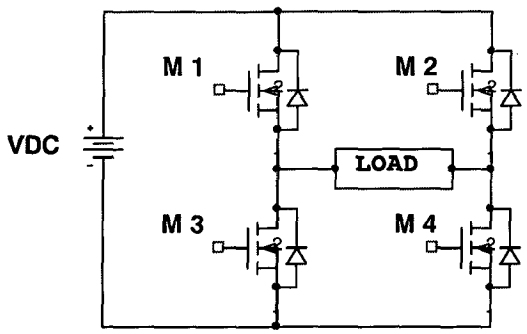

Single Phase Inverter

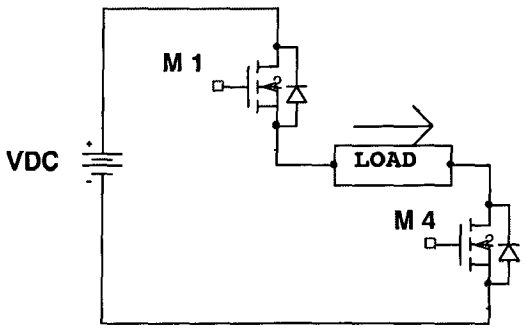

When M 1 & M 4 conducts Vo = VDC

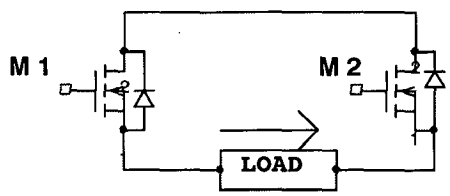

When M 1 & M 2 conducts Vo = 0

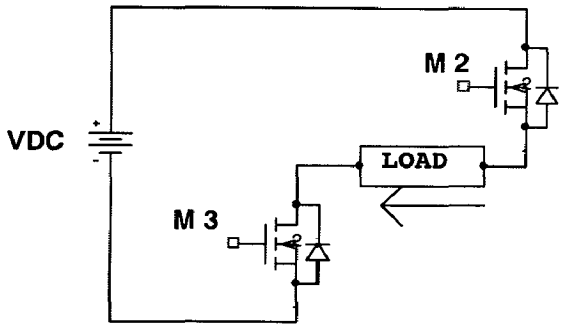

When M 2 & M 3 conducts Vo = -VDC

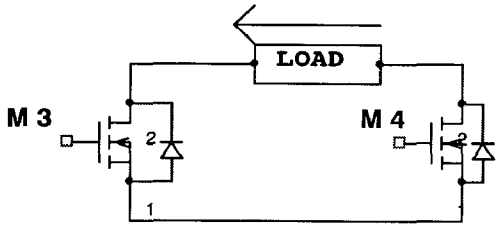

When M 3 & M 4 conducts Vo = 0

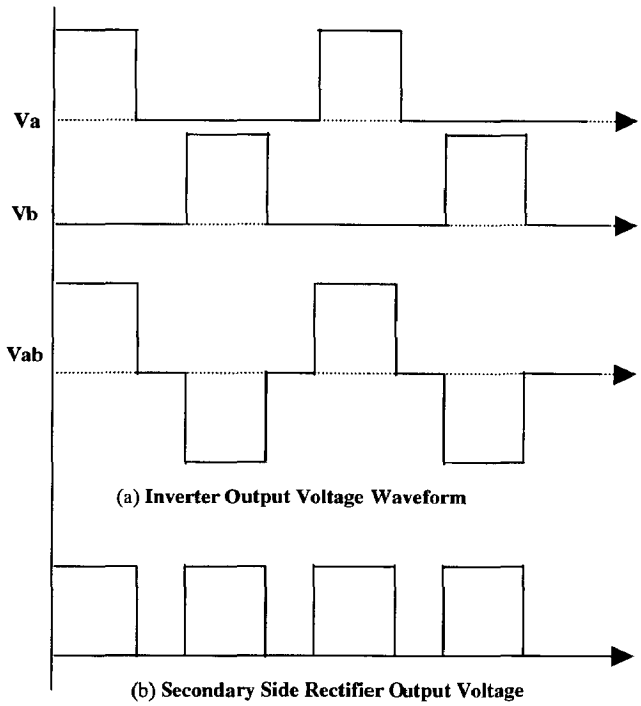

(a) Inverter Output Voltage Waveform

(b) Secondary Side Rectifier Output Voltage

Figure-5.3(contd.): Inverter operation through Phase-Shift Control

The gate pulses and the resulting voltage waveforms are as shownin figure 5.4.

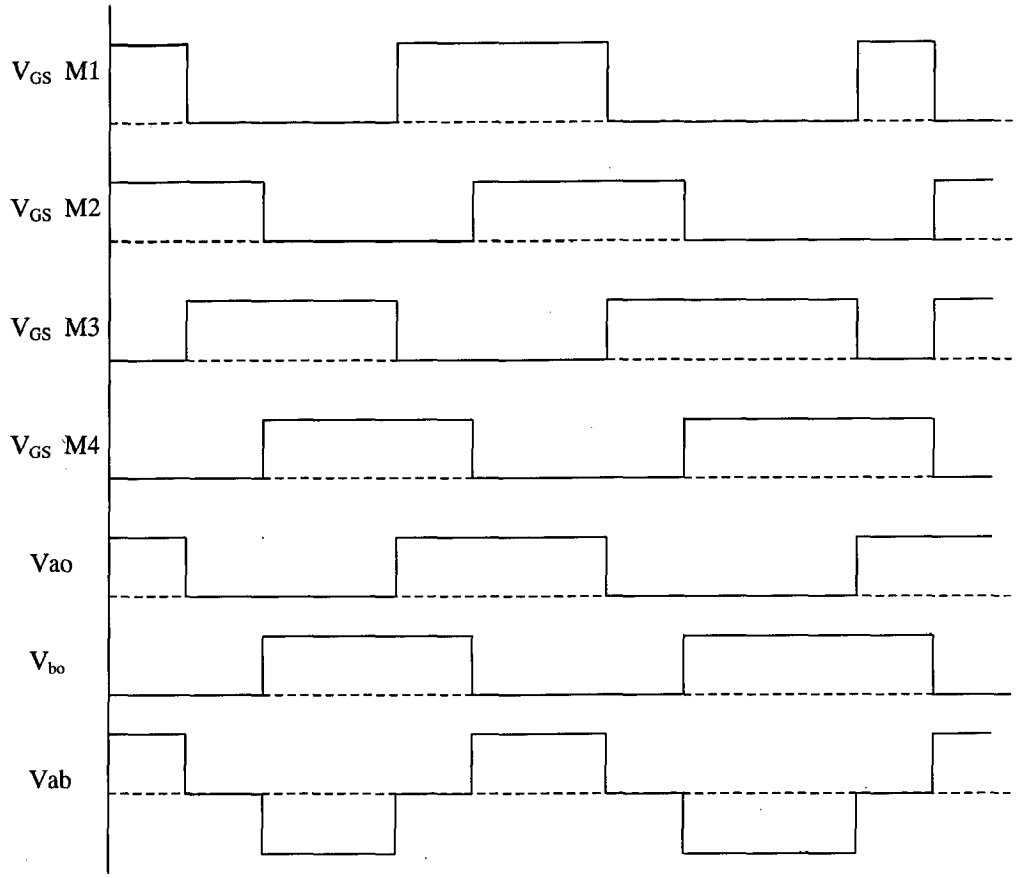

Figure 5.4: Phase-shift control of single phase Inverter

The secondary output is like the output of a buck converter which is controlled by varying the duty cycle. In our case we are controlling the duty cycle by varying the phase shift. As phase shift is varied from zero to 180° the pulse width or the duty ratio of the output pulses varies from unity to zero. Thus, by controlling the phase shift, the control of the output voltage is achieved. Since a high frequency transformer is there the voltages on the primary and the secondary side can be quite different thus making such a configuration suitable for low voltage high current type applications.

5.3 OUTPUT RECTIFIER SECTION

The output section of the proposed topology consists of a high frequency transformer the secondary of which is center-tapped and the output of which is rectified by the diodes to provide D.C. output. This output section behaves similar to a buck converter the duty cycle (D_{buck}) of which is controlled by controlling the phase shift of the single phase inverter and is given by

$$D_{buck} = (1 - \frac{\phi}{180}) \quad \text{... (5.32)}$$

Where, ϕ is the phase shift of the single-phase inverter and can vary from 0° to 180°.

The output voltage is given by

$$V_{out} = D_{buck} V_s \quad \text{... (5.33)}$$

Where, Vs is the voltage amplitude at the secondary side of the transformer.

The value of filter inductance and capacitance[15] is given by

$$L_f = \frac{D_{buck} V_s (1 - D_{buck})}{f_s \Delta I} \quad \text{... (5.34)}$$

$$C_f = \frac{V_s D_{buck} (1 - D_{buck})}{8 L_f f_s^2 \Delta v_c} \quad \text{... (5.35)}$$

Where, ΔI is the peak-to-peak inductor current ripple and ΔV_c is the capacitor voltage ripple.

In order to have better efficiency of conversion the diode used should either be Schottky diodes or synchronous rectification should be used so that the voltage drop across the output section is negligible. Proper consideration should be paid to this drop while designing the high frequency transformer. Moreover, paralleling of various devices can be done at high currents so that available device ratings can be suited for the purpose. Over-current protection can also be had by limiting the phase shift of the inverter and thus controlling the duty cycle of the buck converter.

5.4 OVERALL MODEL OF LOW VOLTAGE HIGH CURRENT RECTIFIER

Since all the system components have been modeled the overall system can also be modeled and an integrated model relating the input current drawn from the supply to the output current of the system or the duty cycle of the buck converter can be formed.

The output voltage of the boost rectifier (see Appendix-A-1) operating in the discontinuous conduction mode (DCM) is given by

$$V_o = 0.5V_{pk}\left[1+\sqrt{(1+\frac{2D^2R}{f_sL})}\right] \quad \text{... (5.36)}$$

It is evident from the above equation that the output voltage depends not only on the duty cycle of the boost rectifier (as in the case of continuous conduction mode (CCM)) but also on the load R on the D.C. side of the rectifier. This means that the output voltage will change with the change in the load on the D.C. side, making a closed-loop control of output boost voltage necessary. Thus if voltage conversion ratio M is maintained constant the duty cycle of the boost rectifier can be given by

$$D = \sqrt{(}\left[(2M-1)^2 - 1\right]\frac{f_sL}{2R}) \quad \text{... (5.37)}$$

Thus the duty cycle D has to be adjusted with change in load (R) on the DC side to have constant value of conversion ratio M. The load in the present case is the reflected resistance (R_{refl}) and is given by

$$R_{refl} = \frac{n^2R_{dc}}{D_{buck}{}^2} \quad \text{... (5.38)}$$

Where, n is the turns ratio of the high frequency transformer, R_{dc} is the resistance on the output side (or a resistance equivalent to the DC load in the case of pump or motor load) of the rectifier. D_{buck} the duty cycle of the buck converter is also related to the phase-shift. Thus, the overall expression for duty cycle of the boost rectifier can be given by

$$D = \frac{1}{n}(1-\frac{\phi}{180})\sqrt{(}\left[(2M-1)^2 - 1\right]\frac{f_sL}{2R_{dc}}) \quad \text{... (5.39)}$$

Once the expression for duty cycle has been evaluated the input current can also be computed by substituting the value of duty cycle D in the expressions for input current as developed in section-5.1 But in those equations the conversion ratio M has been

assumed constant which if replaced by the dynamic value of M yields much better modeling of the overall system. M is the ratio of the output DC link capacitor voltage to the peak input voltage (it may be either line-to-line voltage or the phase voltage depending on the type of equations used in modeling. In [8] the voltage equations are based on line-to-line voltage where as here they have been provided based on line-to-neutral voltage) but the peak voltage should be the maximum of the three phase voltages. This maximum value is not constant but keeps on varying with angle ωt so if this value is used to calculate the value of M and subsequently the input currents a much better model of the system results as is evident from the simulation results shown in chapter-6.

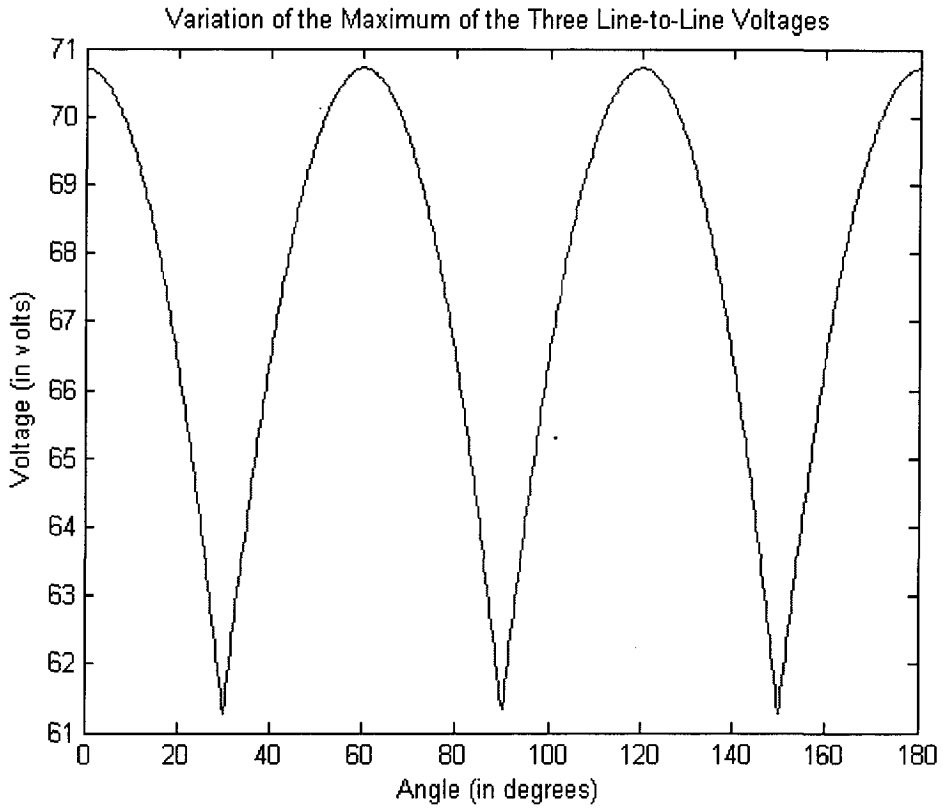

Figure 5.5: Variation of the Maximum of three Line-to-Line voltages with angle ωt

From figure-5.5 it is evident that the maximum input voltage to the DCM boost rectifier is not constant but varies with ωt. This variation should be taken into account while evaluating the value of M and also when modeling the converter.

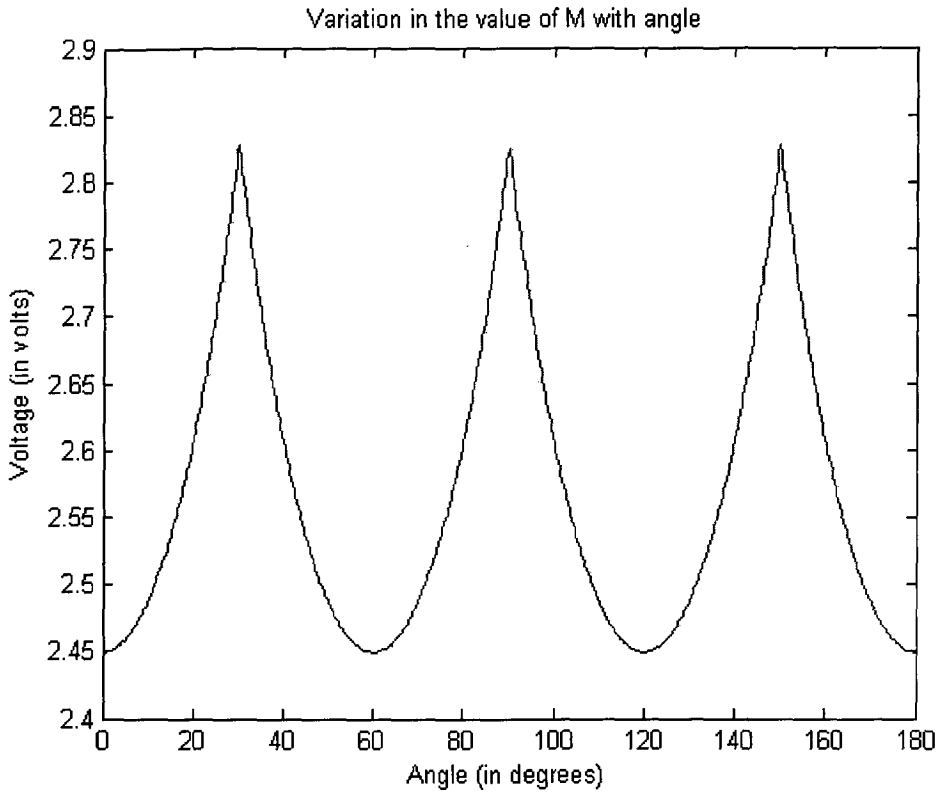

Figure 5.6: Variation of M with angle ωt

As is evident from the figure-5.6 the value of M is not constant but varies with angle ωt, the minimum value of M is given by Vboost / VL-L where Vboost is the DC link capacitor voltage and VL-L is the rms value of line-to-line voltage.

5.5: Selection of Minimum M value

Another point in the DCM boost rectifier is the minimum value of the conversion ratio M which greatly affects the performance of the converter and is governed many considerations some of them are:

a) **THD Requirements:** At higher values of M (>2) the THD is reduced quite significantly but this means that either the output voltage is quite high, which implies a greater voltage stress on the switches of the inverter and the DCM boost rectifier, or the input voltage is kept low but this would mean that the current drawn

from the input mains increases requiring devices with greater current carrying capability.

b) **Input Voltage Variation**: The input voltage variation has also to be taken into account; the value of M should be so selected that even at the maximum input voltage the value of M should not be below the specified or the desired conversion ratio value. Thus ensuring that even in the worst case of maximum line voltage the THD requirements are met.

5.6: Assumptions in the Analysis:

The following simplifying assumptions have been made in the analysis of the system [8]:

1) Purely sinusoidal, symmetric mains voltage system
2) The ripple of the voltages across the filtering capacitance is negligible (<10%)
3) Constant output voltage, ripple less than 5%.
4) Constant output current
5) The operating frequency is much greater than the line frequency (i.e. mains voltage approximately constant within a pulse period).
6) Ideal system components, especially neglection of losses switching times, etc.

In this chapter, the model of Low Voltage High Current Rectifier (LVHCR) has been developed relating the input current with the phase-shift of the single-phase inverter, the transformer turns-ratio and the output DC resistance. A modified approach to modeling the single-switch DCM boost rectifier has also been presented.

CHAPTER-6

SIMULATION RESULTS

The low voltage high current rectifier (LVHCR) consists of a front-end boost rectifier, a single-phase high frequency inverter and a buck-type output rectifier section. The single-switch boost rectifier operates in discontinuous-conduction mode (DCM). The single-phase high frequency inverter is controlled by means of phase-shift control. In order to theoretically investigate the performance of the proposed low voltage high current rectifier (LVHCR) the simulation of the proposed topology was done in MATLAB/ SIMULINK. The boost inductance was taken as 270uH for 2volts 20Amp set up as per the criterion given in section 5.1. The output DC resistance was set as 0.1 ohms so that at 2V 20Amp of current can flow. In the case of 3000Amp set-up, the output DC resistance was set as 0.00067 ohms.

6.1: Simulation Results of Experimental Prototype

Figures below show the simulation results for the experimental setup providing 20 Amps at 2 volts.

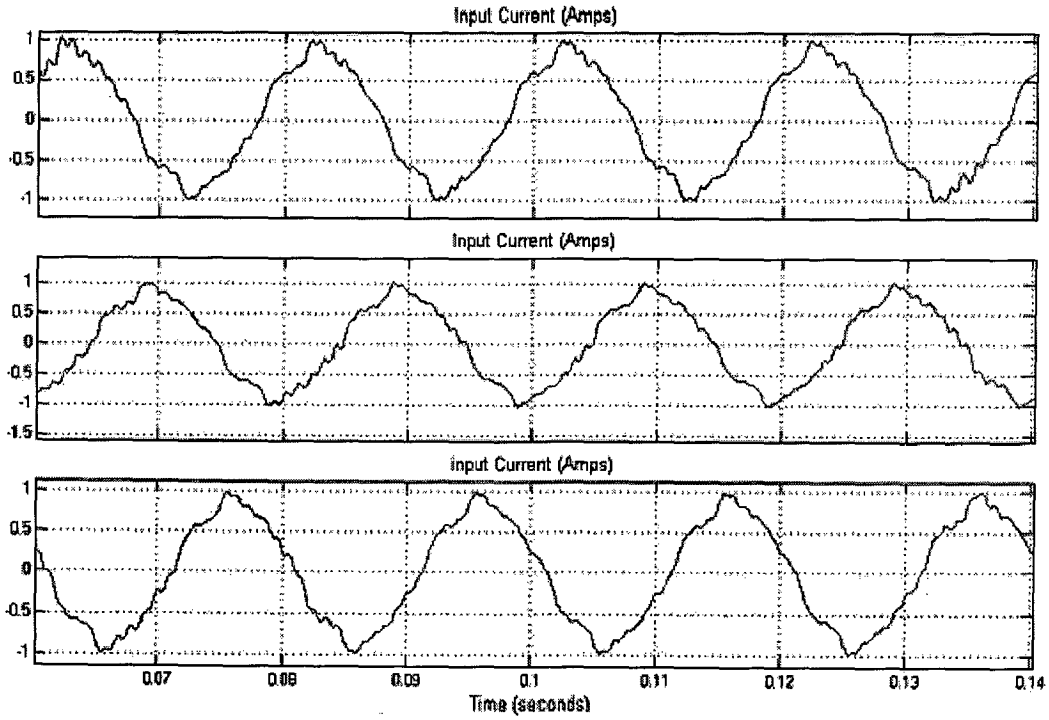

Figure-6.1(a): 3-phase input current drawn from the supply when I_{DC} = 20Amp

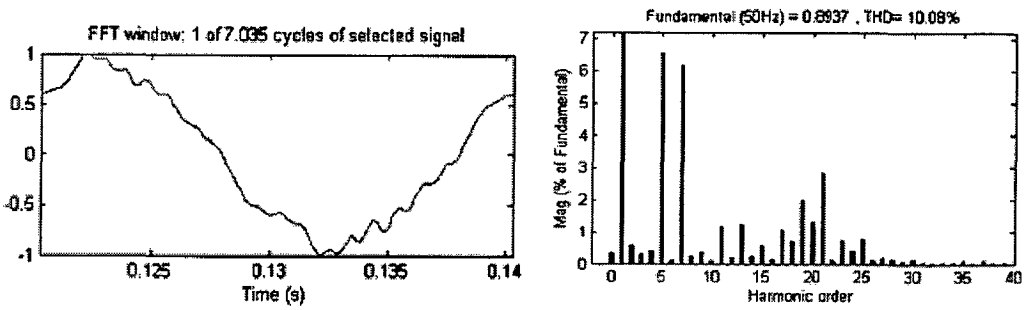

Figure: 6.1(b): Harmonic Spectrum of Input Current

Figure 6.1 (a) shows the waveforms of 3-phase input currents as drawn from the ac-mains. From the figure 6.1(a) it is evident that the currents drawn are quite close to sinusoidal thus yielding high power factor. The harmonic spectrum of the input current is shown in figure-6.1(b). The main contributors to the total harmonic distortion (THD) are the 5^{th} and the 7^{th} harmonics.

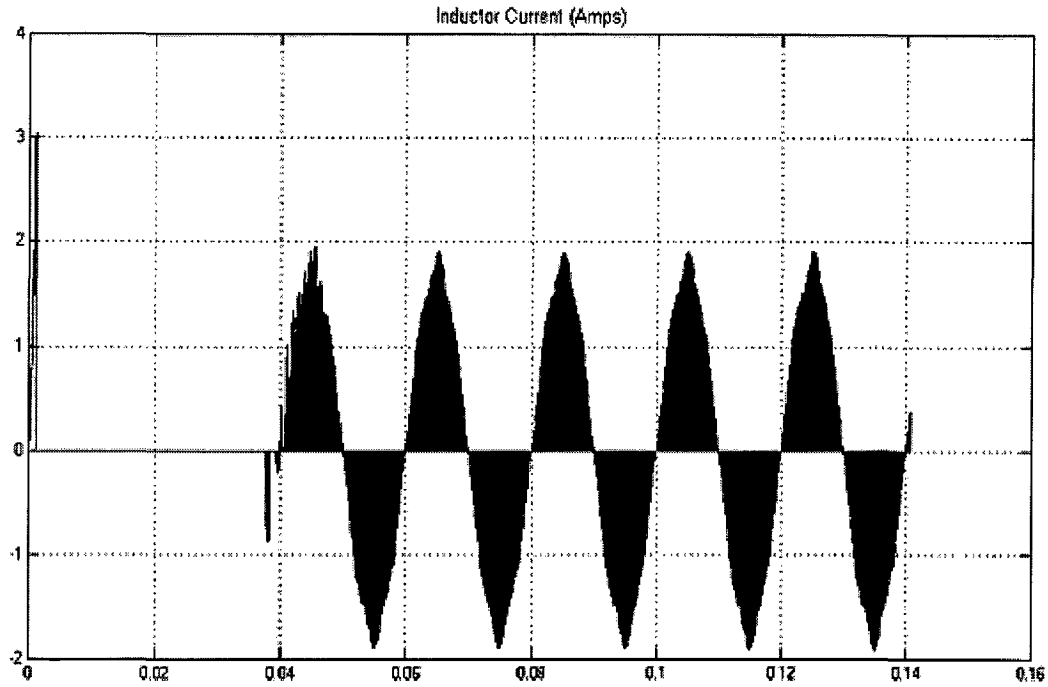

Figure 6.2(a): Inductor Current Waveform

Figure-6.2(a) shows the typical boost inductor current waveform. The boost rectifier operates in discontinuous conduction mode (DCM) andat a high frequency the expanded view of the inductor current is as shown in figure 6.2(b). The initial peak in the current waveforms is due to the charging current drawn by the DC link capacitor.

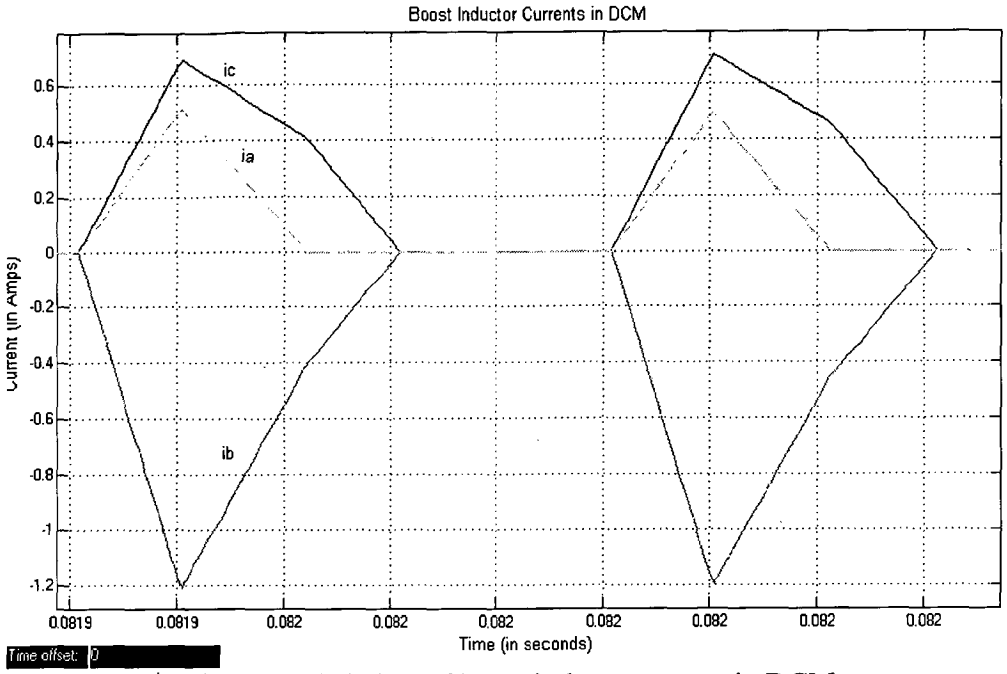

Figure-6.2(b): Expanded view of boost inductor current in DCM

As is evident from figure-6.2(b) the boost rectifier operates in discontinuous conduction mode (DCM) as all the phase currents become zero before the start of the next switching period.

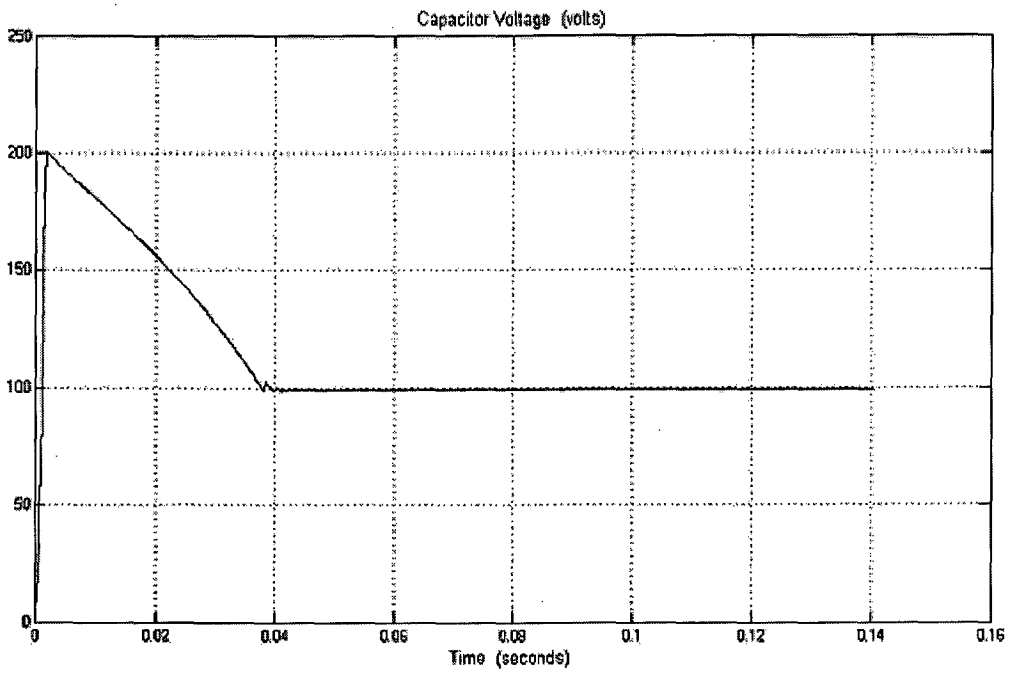

Figure-6.3: Voltage across the DC link Capacitor

6.2: Simulation of the 3000Amp power supply:

Output current

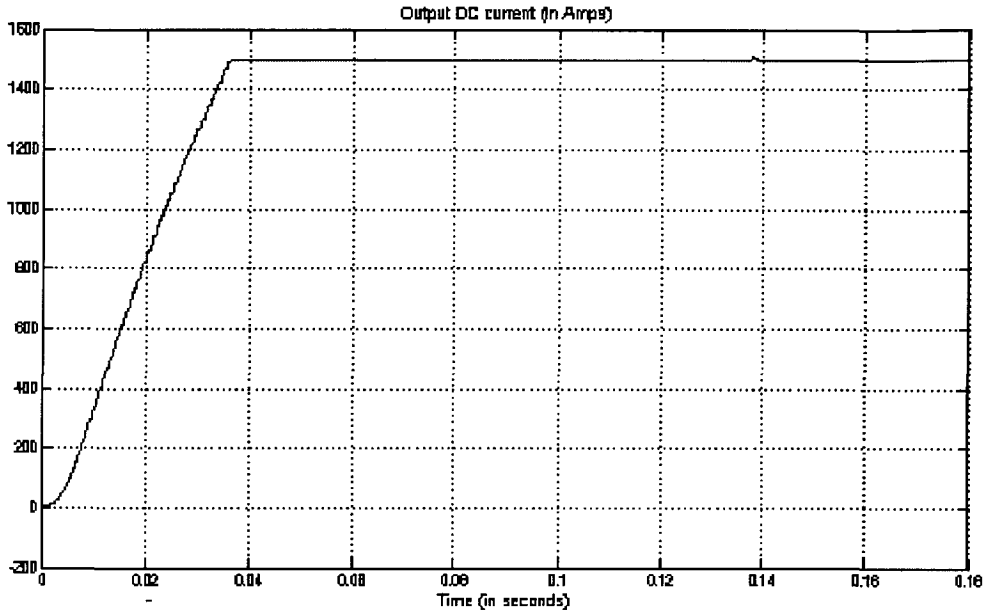

Figure-6.4(a): Output DC Current waveform

Input current

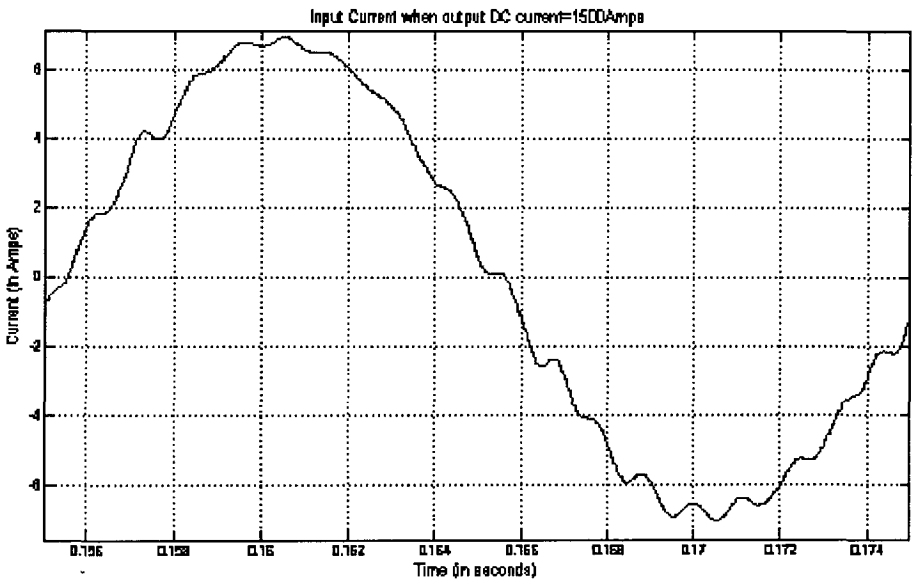

Figure-6.4(b): Input current waveform

From the figure 6.4(b) it is evident that the current drawn by the LVHCR is quite close to sinusoidal one. The pulsation in the waveforms is due to the 5^{th} and other higher frequency harmonics.

Output Current:

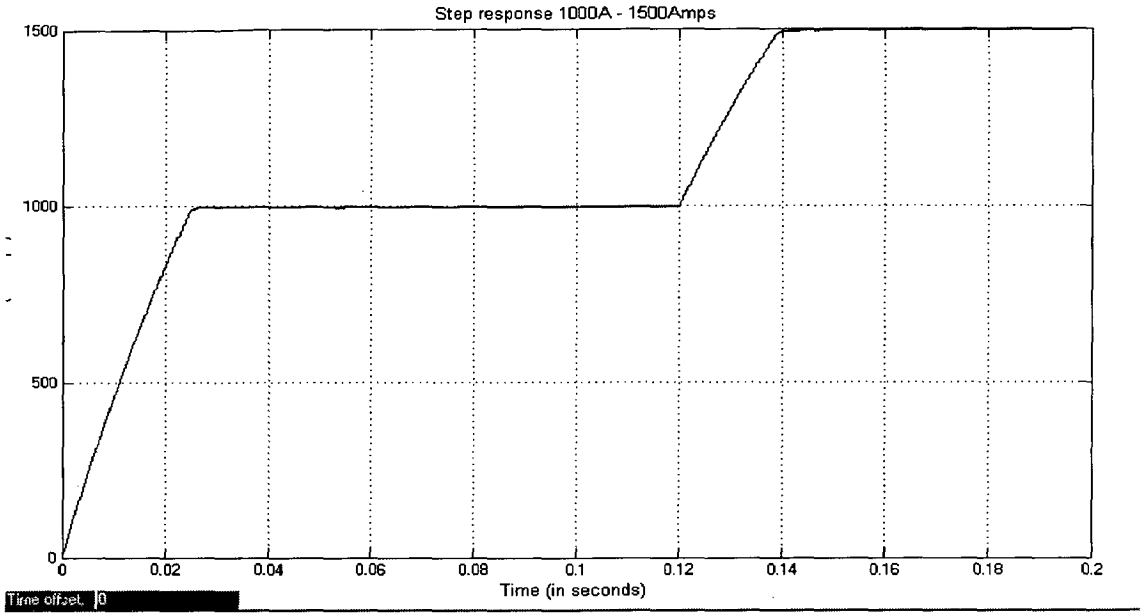

Figure-6.5: Step Response of Output Current

Output Current:

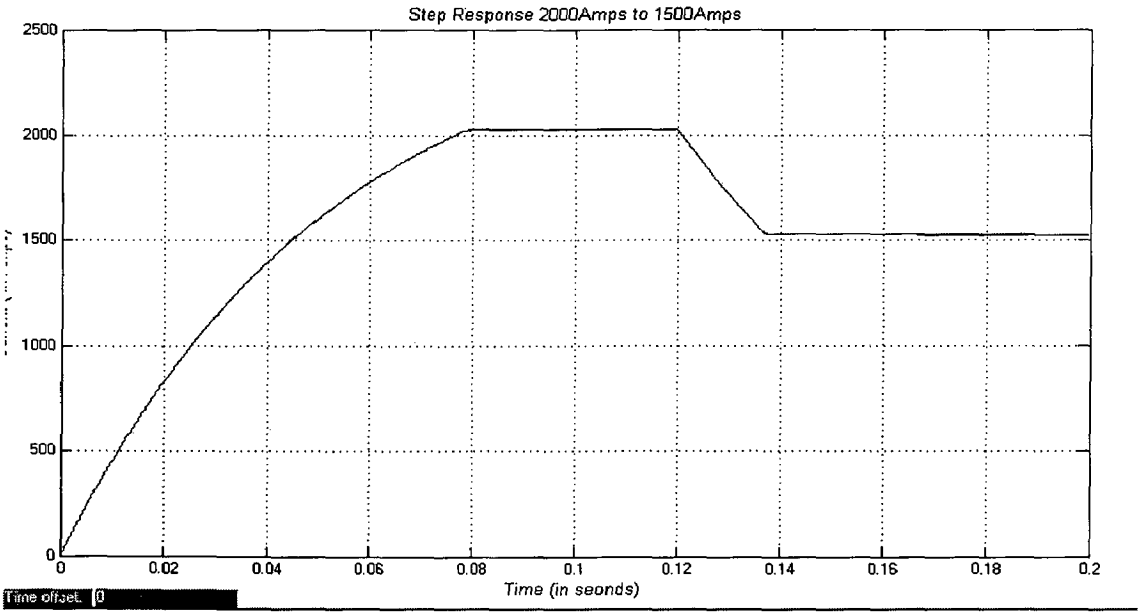

Figure-6.6: Step Response of Output Current

Figures-6.5 and 6.6 show the step response of the proposed low voltage high current rectifier. From the figures it is evident that the step response of the system is quite acceptable.

6.3: Calculated plots of Input Current from the Two Methods:

Method-1: M taken as constant
DC load current = 20Amps
Lb = 270uH f=10 kHz VL-L = 40volts Vboost = 80 volts
Input currents

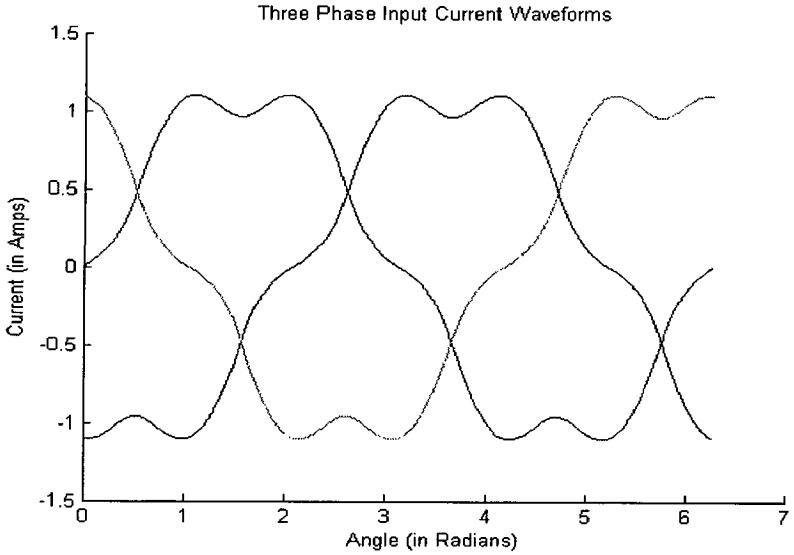

Figure-6.7(a): Three-Phase Input Currents

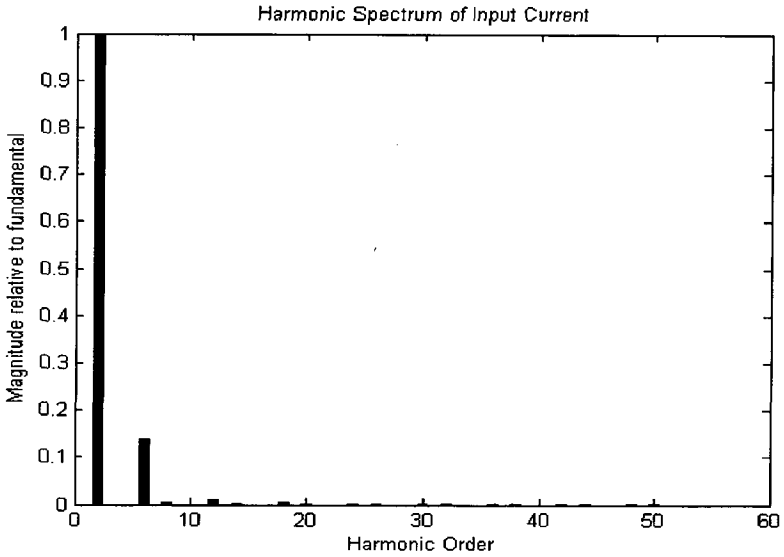

THD = 14.0457 %

Figure-6.7(b): Harmonic Spectrum of Input Current

The modeling done by taking M as constant results in current waveform having a dip at 90° due to the presence of 5^{th} harmonic as is evident from figures- 6.7(a) & 6.7(b).

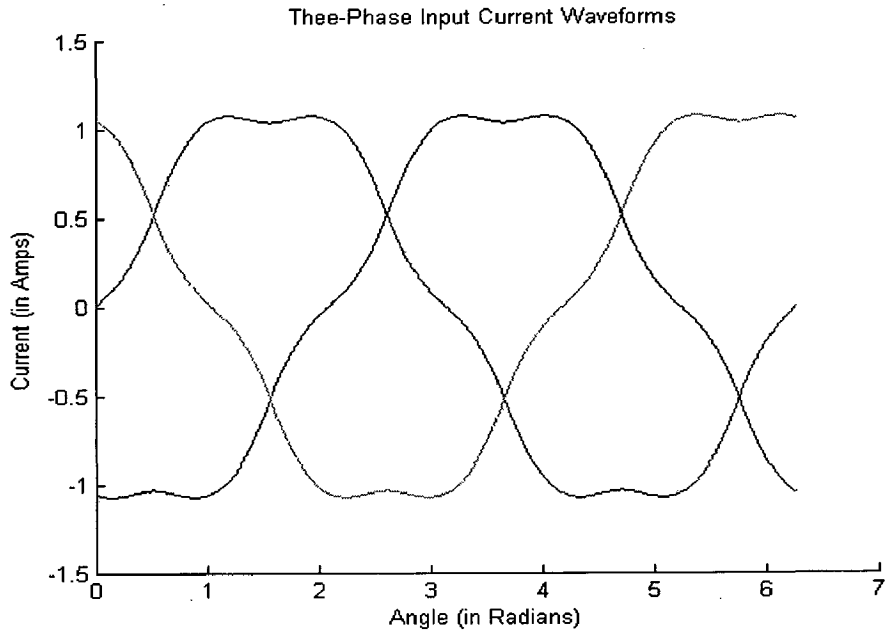

Figure 6.8: Input Current Waveform when Vboost / VL-L = 100/ 40
THD = 9.2177 %

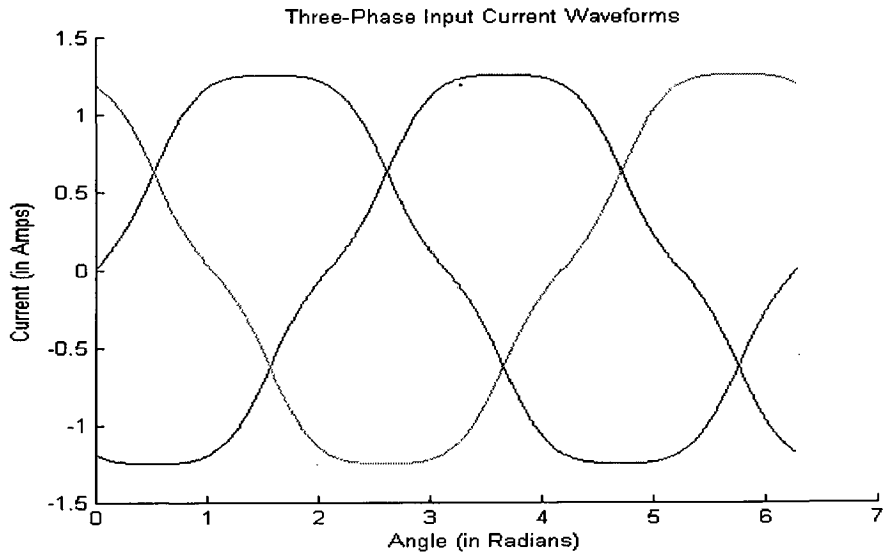

Figure 6.9: Input Current Waveform when Vboost/ VL-L = 100/ 30
THD = 5.9787 %

From figures-6.8 and 6.9 it is quite evident that as the ratio Vboost /VL-L increases the waveforms approach close to sinusoidal and the total harmonic distortion THD also gets reduced considerably.

Method-2: Dynamic value of M is taken

DC load current = 20Amps

Lb = 270uH f=10 kHz VL-L = 40volts Vboost = 80 volts

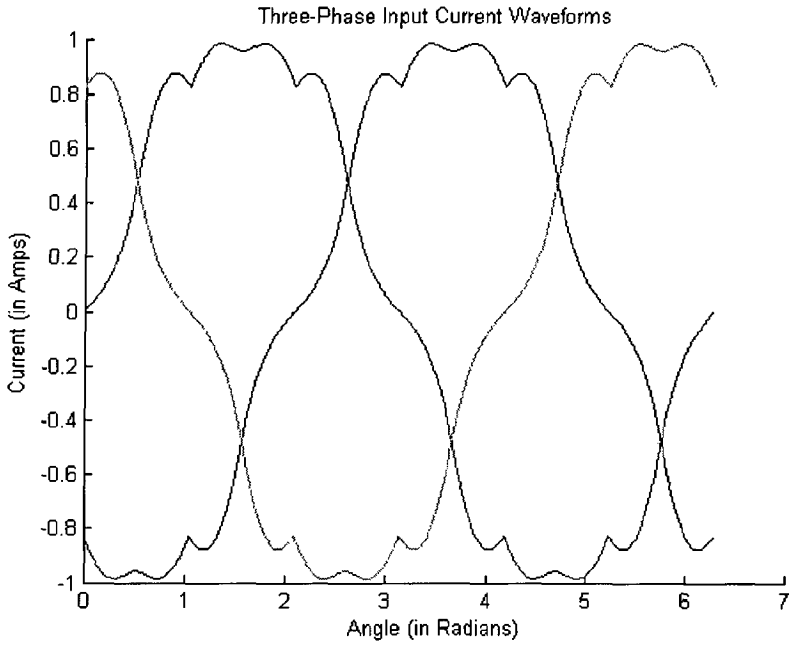

Figure-6.10(a): Three-phase Input Current waveforms

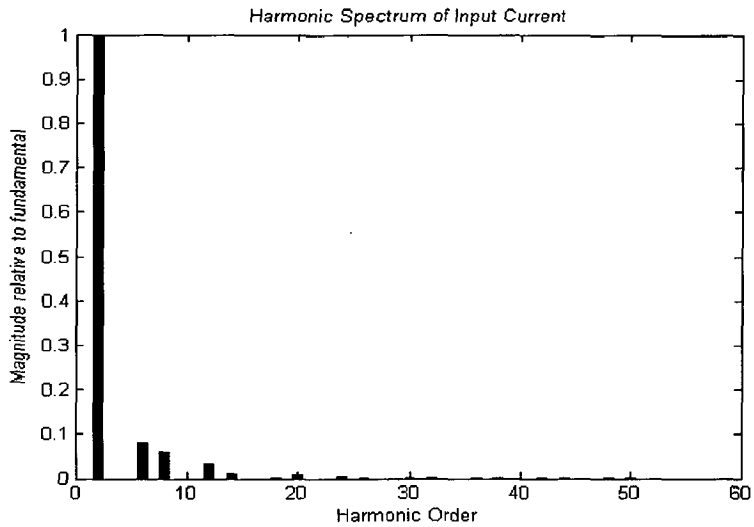

THD = 10.5968 %

Figure-6.10(b): Harmonic Spectrum of Input Current

The modeling of input current when dynamic value of M is taken results in waveforms which have much less dip at 90° (Figure-6.10 (a)). The harmonic spectrum of Figure-6.10(b) shows that 5th and 7th harmonics are the prominent ones.

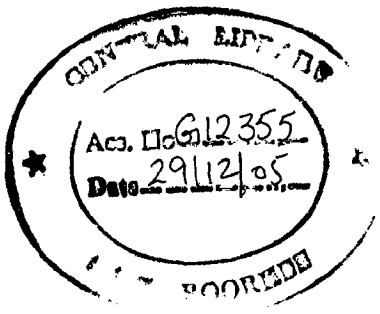

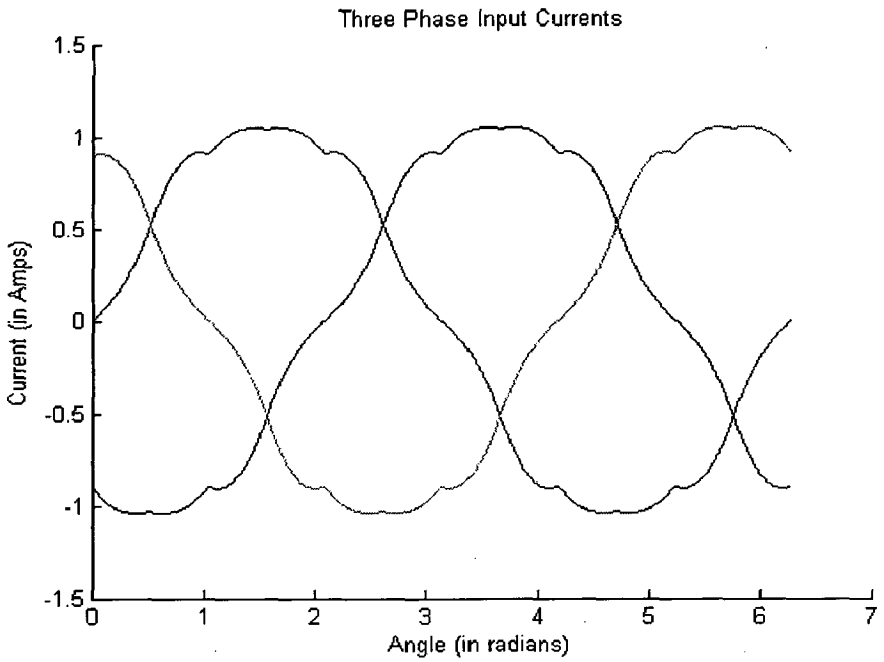

Figure 6.11: Input current waveforms when Vboost /VL-L =100 / 40
THD = 7.3469 %

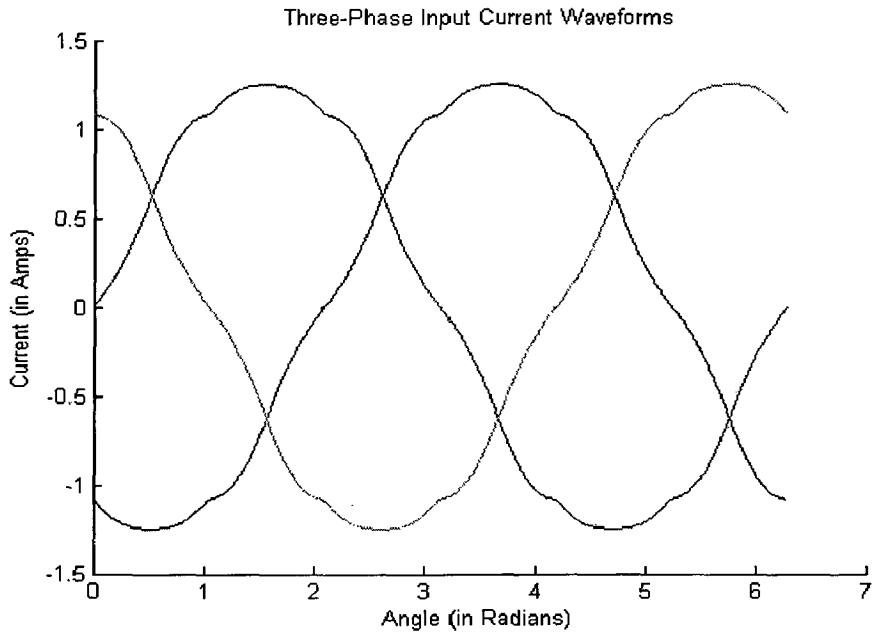

Figure 6.12: Input Current waveforms when Vboost / VL-L =100 / 30
THD = 4.9234 %

From figures-6.11 & 6.12 it is apparent that as the value of Vboost / VL-L increases the total harmonic distortion (THD) gets reduced and the waveforms approach close to sinusoidal ones. This is in agreement with the theory developed in chapter-5 since a higher value of conversion factor results in longer value of turn-on time ton thus the

duration for which the input currents are proportional to the input voltages (which are assumed to be sinusoidal) also increases. This results in a waveform more close to a sinusoidal one and with reduced total harmonic distortion (THD).

In this chapter the simulation results of the low voltage high current rectifier have been presented. From the results it is evident that the proposed configuration works satisfactorily as low voltage high current power source.Figure-6.2 shows the inductor current waveform in discontinuous conduction mode (DCM) of the proposed converter. From the equations developed in chapter-5, the plots of current waveforms have been obtained and the total harmonic distortion has also been calculated. It is evident from the waveforms shown in figure-6.7 and 6.10 that a much better modeling of input current with less harmonic distortion results if the dynamic value of conversion ratio M is taken, instead of taking a constant M value.

CHAPTER-7

HARDWARE DESIGN

This chapter describes the design of the hardware developed for the prototype low voltage high current rectifier (LVHCR) capable of supplying 20Amps of DC current at 2 volts of output voltage. The various design aspects of the LVHCR are discussed along with the design of control circuits for both the boost rectifier and the phase-shift control of single-phase inverter. The various issues related to the design and fabrication of high frequency transformer and filter inductor are also discussed.

Design of Single-Switch Boost Rectifier: The main point in the design of boost rectifier is the selection of the value of boost inductance. The boost inductance is selected based on the discussion in chapter-5. The value of boost inductance should be so selected that even at the maximum power output from the rectifier the converter operates in discontinuous conduction mode (DCM). The current rating of the input diode bridge is selected by calculating the peak value of inductor current drawn from the supply as given by equations (5.4, 5.5 and 5.6). The value of duty cycle is decided by the equation D = 1-(1/M). The value of M is decided keeping in mind the various considerations discussed inchapter-5.

Design of single-phase phase-shift Inverter: In the present case the maximum input line-to-line voltage is 50 volts rms and the maximum DC link capacitor voltage is 100 volts. The output voltage is 2 volts. After taking into account the drop in the diode rectifier section the turns-ratio of the high frequency transformer can also be calculated. The current rating of the switches of single-phase rectifier can be calculated by evaluating the current reflected on the primary side. The voltage rating of the switches is decided by the maximum voltage across the DC link capacitor.

The control circuits for both the Boost rectifier and for the phase-shift control have been developed. Since both boost rectifier and single-phase inverter operate at high frequency while designing the control circuits the components compatible with high frequency are selected. The design of high frequency transformer and the filter inductor has been done using ferrite-cores which are quite suitable for high frequency operation and results in low volume and weight of the products.

7.1: Boost Rectifier Control

The figure-7.1 shows the control circuitry for boost rectifier control.

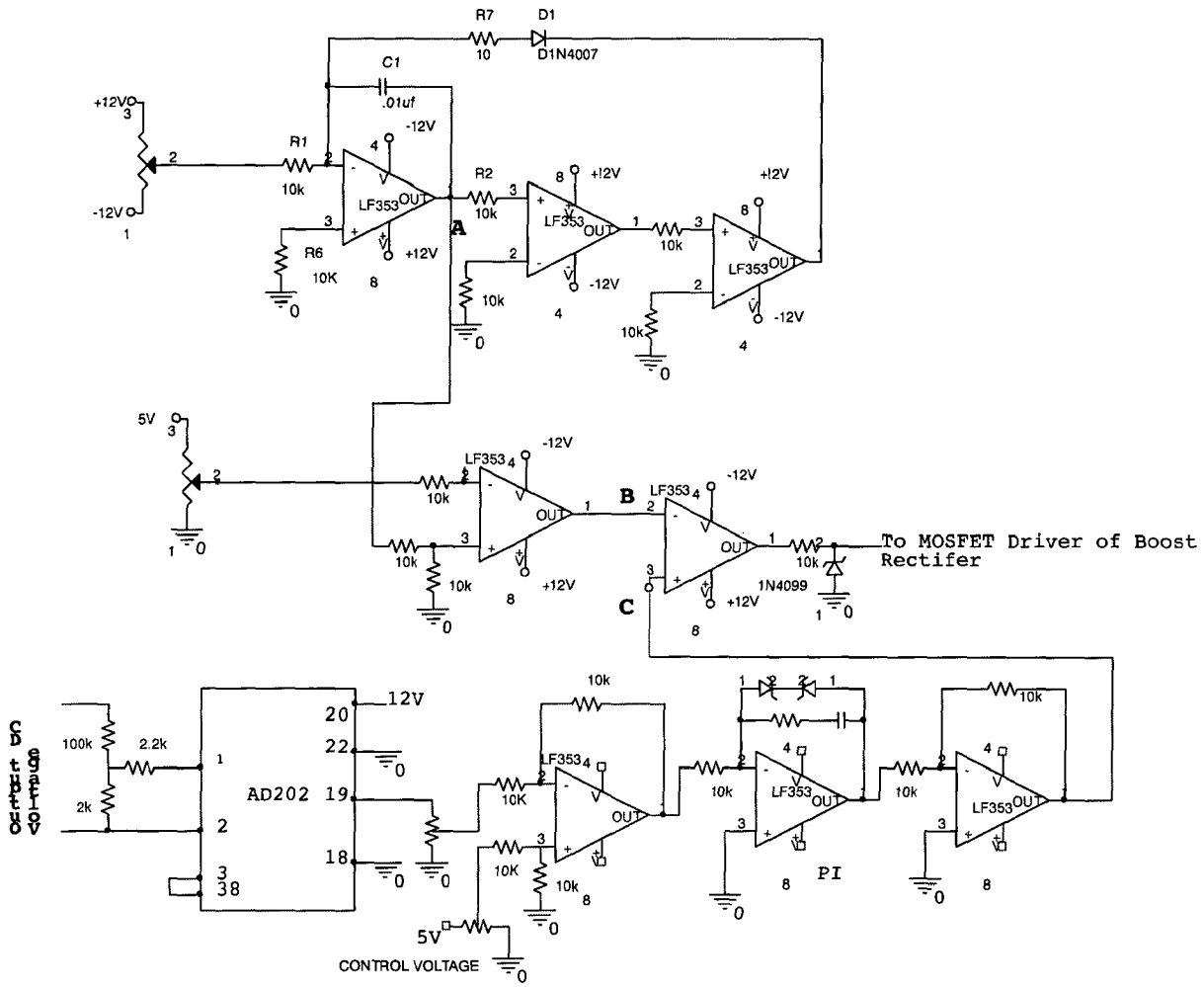

Figure-7.1: Boost Rectifier Control Circuit

At point **A** we have a sawtooth waveform of high frequency, this waveform is from zero voltage to some positive value but the output of the PI regulator at point C can be both positive and negative so to the waveform coming from **A** a dc voltage is subtracted so that a triangular waveform going both positive and negative is obtained at **B**. This waveform is then compared with the output of the PI regulator and accordingly the firing pulses for the MOSFET are generated. AD202 is used for sensing the output voltage of the boost rectifier and this sensed voltage is then compared with the reference voltage signal which is set to get the desired output voltage. The error between the reference and

the actual is then processed in a PI regulator. The output of this PI regulator is then inverted and then compared with the triangular waveform (at B) to yield firing pulses for the boost switch.

7.2: Philosophy of Phase Shift Control

The single phase inverter is to be operated at high frequency through phase shift control for which the circuit has been shown in figure-7.3. The philosophy of the circuit can be explained by means of figure-7.2 .First, a sawtooth wave (A) is generated by charging and discharging of capacitor through paths of different resistances. The output of the comparator consists of pulses going both positive and negative (B), the pulse going negative during the discharging period. This pulse is then clamped by a zener to 5 volts level (C) and then fed to a positive edge-triggered D-flip flop connected in divide by 2 configuration which converts this pulse waveform into a square waveform (D).

In order to generate another square waveform displaced from the firstone, the sawtooth waveform (A) is first made to go both positive and negative (E) because in the closed loop the output of the PI controller can go both positive and negative. This is done by subtracting a positive voltage. When the resultant waveform (E) is compared with the control voltage, again a pulsed waveform (F) swinging between positive and the negative supply is obtained. But this time the waveform is phase displaced with the waveform B and the phase shift is decided by the control voltage. The waveform (F) is then clamped (G) and then fed to a positive-edge triggered D-flip-flop which is as before arranged in divide by 2 configuration. This results in a square wave (H) which is phase shifted with respect to square wave D.

Thus a controllable phase shift as desired for the phase shift control of the single phase inverter is obtained.

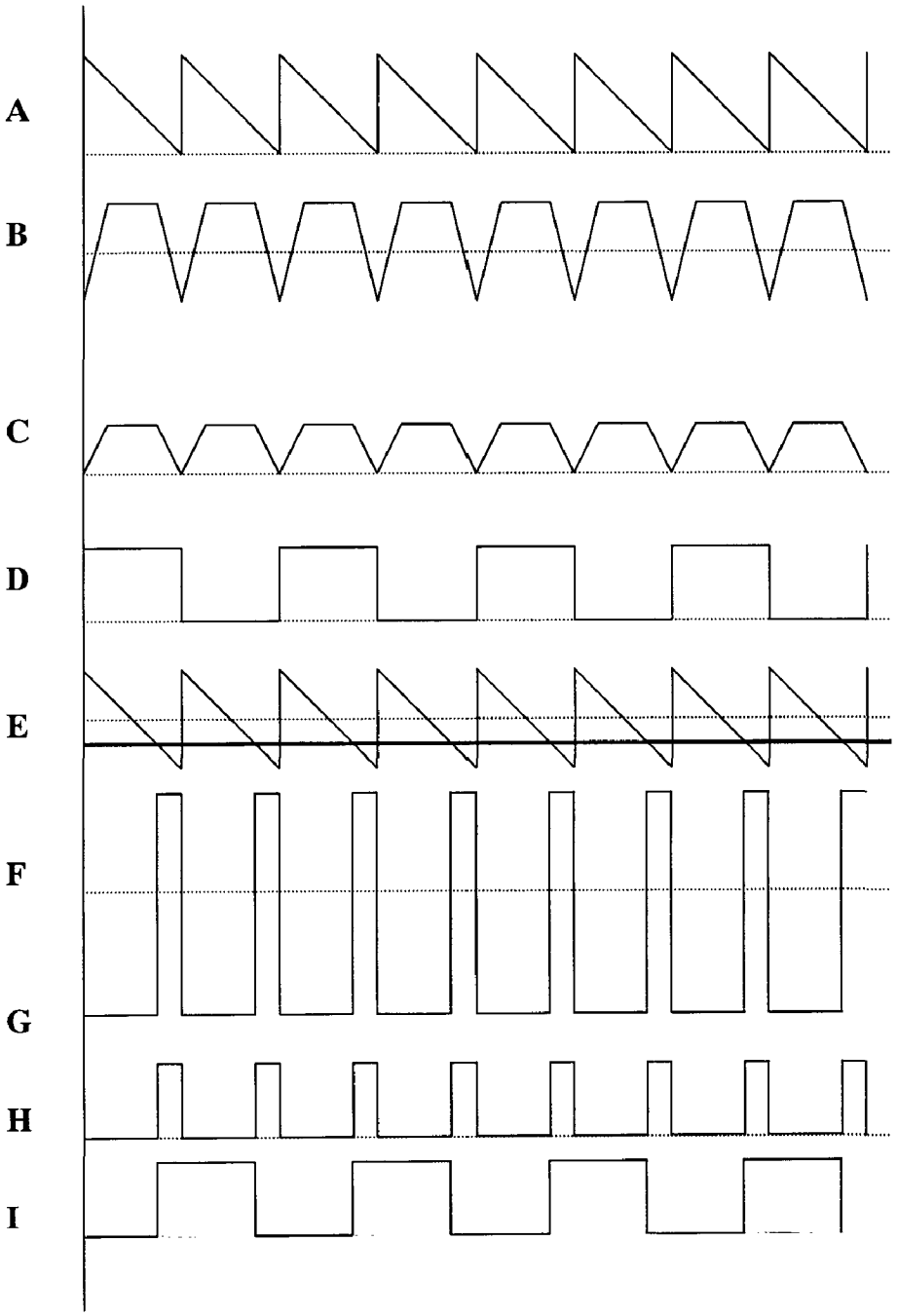

Figure 7.2: Generation of Phase Shifted Square Waves for Single Phase Inverter Control

PHASE-SHIFT Control Circuit

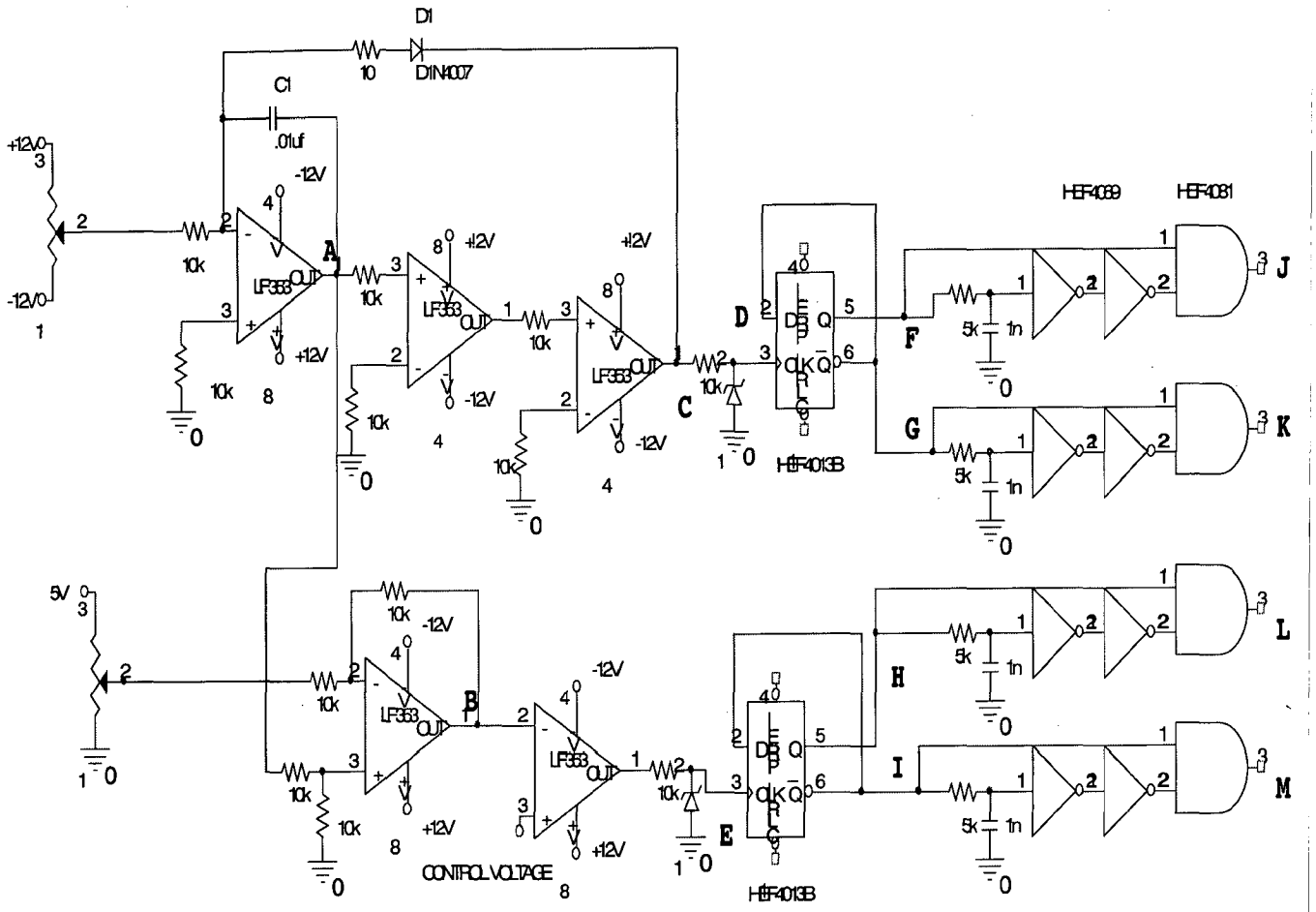

Figure-7.3: Full-Bridge Phase-Shift Control Circuit

The above circuit is for obtaining the four gate drive signals for the MOSFETs of the full-bridge inverter. At point **A** we have a sawtooth wave which is obtained as a result of the charging of the capacitor through the 1K ohm resistor and discharging through the 10ohm resistor. At point **C** we have a pulse waveform going from +12V to -12V which is then clamped to 5V and fed to a divide by 2 counter. At point **B** we have another triangular wave which goes both positive and negative and is compared with the control voltage (which in the case of closed loop operation is the output of a PI regulator). At point **E** we have another pulse waveform of the same frequency but phase displaced from that at **D** the displacement being decided by the control voltage. The waveforms at **F, G, H & I** are then passed through a delay network to introduce the delay between the turning off and on of the devices of the same leg of the inverter.

7.3: CURRENT SENSOR CIRCUIT:

The scheme to measure current is shown in figure-7.4. Hall Effect current sensor is used for current measurement. The main advantage of such transducer is that it is non-contact device with high resolution and very small size.

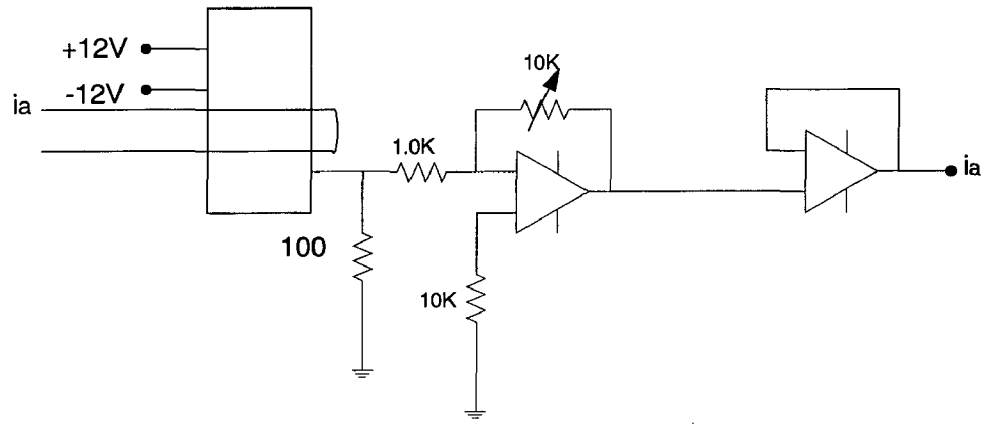

Figure-7.4: Current measurement circuit

The output of sensor is current which depends upon number of turns wound on sensor itself and current flowing in the primary circuit; the output current is given by

$$I_o = I_L * (N_p/N_s) \quad \ldots (7.1)$$

Where

N_p = Number of turns in the primary

N_s = Number of turns in the secondary

I_o= Output Current, I_L = Load Current

Secondary of sensor is wound for large number of turns, while primary is normally wound for one or two turns. The transformation ratio of the current sensor is1000:1

$$N_p = 2, N_s = 1000$$

$$I_o = 2 \times 10^{-3} I_L \quad \ldots (7.2)$$

The output of current sensor is converted into voltage signal by passing it across the 100. resistor. An inverting amplifier is used to amplify the voltage for scaling. A 10K. resistor is used in the negative feed back path of the OP-AMP for gain adjustment so as to obtain a voltage of 5 volt corresponding to 20 Amp (DC current).

7.4: POWER SUPPLIES

D.C regulated power supplies (±12 V, +12V and +5 V) are required for providing the biasing to various ICs, etc. the system development has in-built power supplies for this purpose. The circuit diagram for various dc regulated power supplies are shown in figure-7.5. As, shown the single phase AC voltage is stepped down and the rectified using diode bridge rectifier. A capacitor of 1000microfarad, 50V is connected at the output of the bridge rectifier for smoothing out the ripples in the rectified dc voltage of each supply. IC voltage regulated chips, 7812, 7912,7805 are used for obtaining the dc-regulated voltages. A capacitor of 0.1microfarad, 50 V is connected at the output of the IC voltage regulator of each supply for obtaining the constant, ripple-free dc voltage.

DC VOLTAGE	IC REGULATOR
+5V	7805 (TO-3)
+12V	7812 (TO-3)
±12V	7812 (220Type), 7912 (220Type)

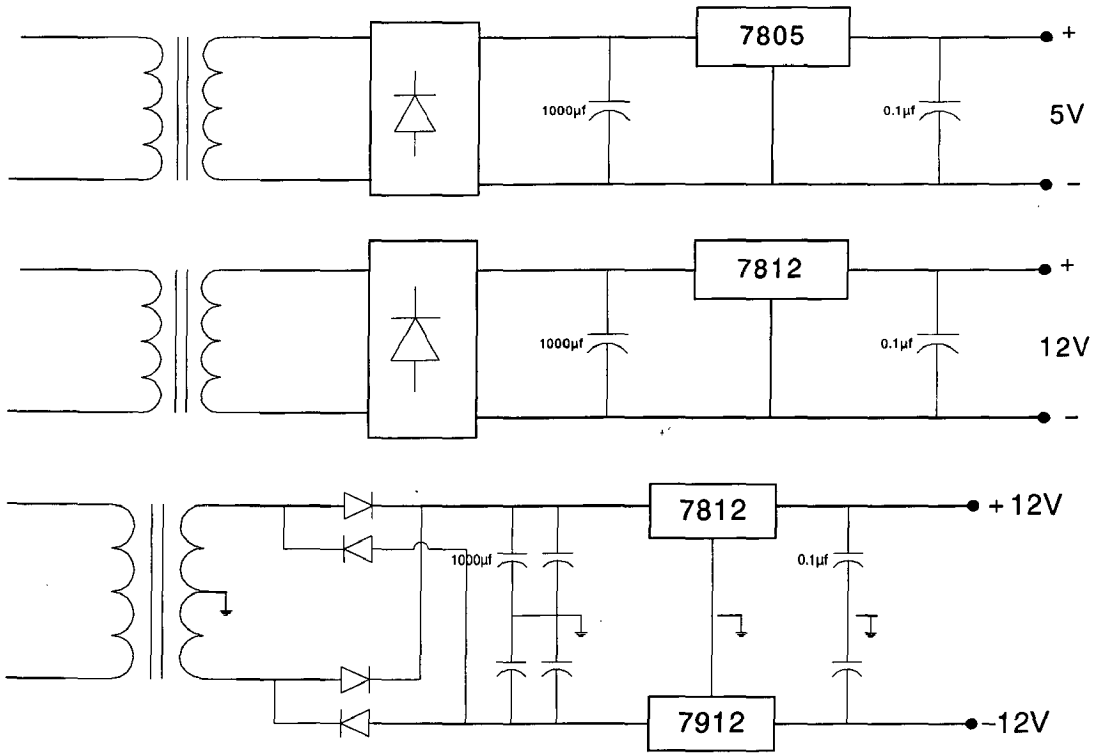

Figure-7.5: Power supplies (a) +5V supply (b) +12V supply (c) ±12V supply

7.5: Firing Pulse Amplification and Isolation Circuit

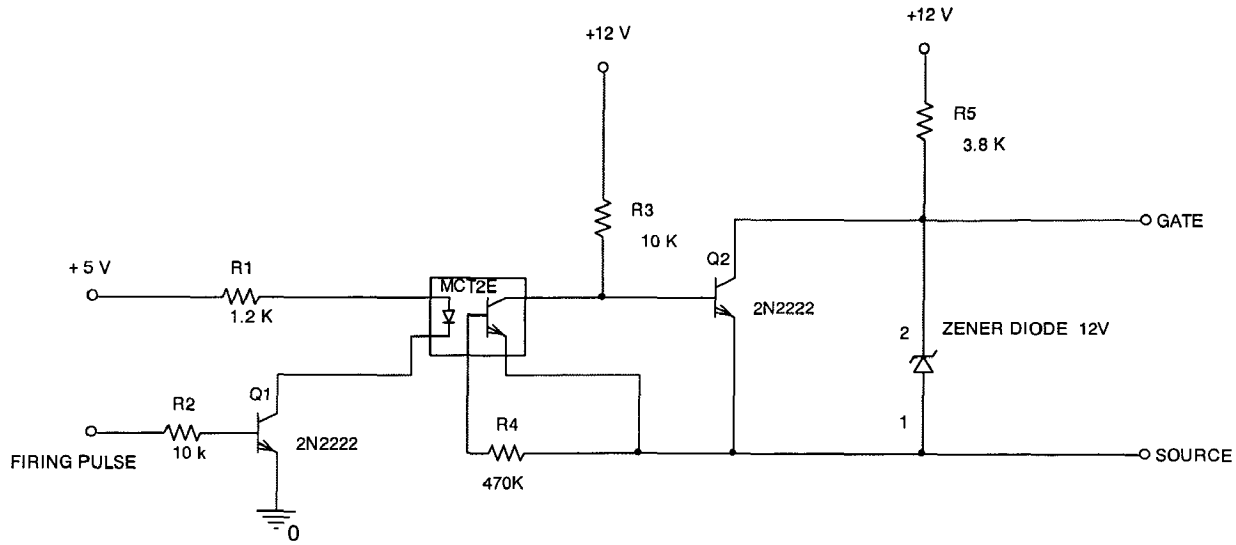

Figure-7.6: Pulse Amplification and Isolation Circuit for MOSFET

The pulse amplification and isolation circuit for MOSFET is shown in figure-7.6. The opto-coupler (MCT-2E or 4N35) provides the necessary isolation between the low voltage isolation circuit and high voltage power circuit .The pulse amplification is provided by the output amplifier transistor 2N222.

The 0-5V gating pulse from control circuit drives the base of 2N2222 switching transistor. When the input gating pulse is at +5V level, the transistor saturates, the LED conducts and the light emitted by it falls on the base of phototransistor, thus forming its base drive. The output transistor thus receive no base drive and, therefore remains in cut-off state and a +12 v pulse (amplified) appears across it's collector terminal (w.r.t.ground). When the input gating pulse reaches the ground level (0V), the input switching transistor goes into the cut-off state and LED remains off, thus emitting no light and therefore a photo transistor of the opto-coupler receives no base drive and, therefore remains in cut-off state .A sufficient base drive now applies across the base of the output amplifier transistor and it goes into the saturation state and hence the output falls to ground level. Therefore circuit provides proper amplification and isolation.

Further, since slightest spike above 20 Volts can damage the MOSFET, a 12 V Zener diode is connected across the output of isolation circuit .It clamps the triggering voltage at 12 V.

7.6: DESIGN OF FILTER INDUCTOR

Once the value of filter inductor is decided, the next step is to design it economically. The inductor can be designed by following the followingsteps [20]:-

1) Determination of coil current
2) Selection core material
3) Determination of optimum flux density and the magnetic field strength
4) Selection of wire size
5) Determination of optimum core volume
6) Selection of minimum size of core from manufacturer's catalogue
7) Determination of number of turns
8) Total power loss
9) Maximum temperature rise

Coil Current and Selection of Wire Size

The filter inductor in the switching buck regulator carries a dc current with a super imposed ripple current . I_L. From the calculation of inductance it is usually assumed that that the peak inductor current should not exceed 10 to 20% of the average load current. If the optimum peak current is assumed to be 15% of I_0, then the peak current becomes

$$I_p = 1.15\, I_0 \qquad \ldots (7.3)$$

The *rms* value of inductor current is very close to the average value. Therefore, for determination of coil gauge the average value may be considered. Double film insulated magnet copper wire is recommended. The size of the wire is limited by its current rating at the maximum allowable temperature. The usual current rating of copper wire as recommended in transformer does not apply to inductor. Instead it should be based on more practical consideration, i.e., maximum temperature rise. These ratings range typically from 3 to 6% of the wire fusing current. This rating applies at maximum operating temperature.

At 20.C the fusing current for the bare copper magnet wire of diameter d is found approximately by

$$I_{fuse} = 20{,}244\, d^{3/2} \qquad \ldots (7.4)$$

Where d is in inches.

Assuming 5% of the fusing current

$$I_0 = 0.05 * I_{fuse} \quad \text{... (7.5)}$$

The above assumption is approximately same as if the current density of the wire is chosen between 500 and 250 circular mil/Amp. Generally the current density of 300 is recommended for such design. Therefore, the size for I_0 is

Cross Section Area of wire $A_{copper} = 300 * I_0$ circular mil ... (7.6)

The gauge of the wire can be selected from a magnet wire chart (see Appendix-A-2).

Selection of core

In order to choose the right core material it is necessary to have the knowledge of the following:

a) Maximum operating frequency

b) Maximum temperature of operation

c) Required core properties

d) Core geometry and appropriate air gap

e) Coil space including bobbin

f) Cost

For switching regulators the major variables for consideration for selection of core materials is the operating frequency, permeability and cost. Among laminated silicon steel, nickel-iron strip, molypermalloy, iron powder and high permeability ferrites, high permeability ferrites and powder cores are generally used in switching regulators. Molypermalloy and powder cores are used without air gaps because an effective air-gap is introduced during there manufacture. Ferrite cores are used with gaps. Some cores have built in air gaps and in others gap is provided according to design requirements.

Advantages of Ferrites

Ferrites have a significant advantage over other types of magnetic materials, viz., high electrical resistivity and resultant low current eddy current losses over wide frequency range. Additional characteristic such as high permeability and time/temperature characteristic have extended ferrite uses into quality filer circuits, high frequency transformers, wide-band transformers, adjustable inductors, delay lines and other high frequency electronic circuits. It is comparatively cheaper than other magnetic

materials. For most favorable combination of low cost, high Q, high stability and lowest volume, ferrites are the best core material choice for frequency from10 KHz to 5MHz.

Ferrite is a very suitable material particularly for high frequency(5 KHz to 500 KHz) inverter power supplies. Ferrite may be used in saturating mode for low power (<50W) and low frequency (<10 KHz). They are used in flyback transformers which offer low core cost at high voltage capability.

There are various types of core geometries including Pot cores, double slab cores, E cores, EC and ETD cores, EP cores, RM cores and toroids. Some of them are briefly described below.

Pot cores

Pot cores when assembled, nearly surround the wound bobbin, this is helpful in shielding the coil from pick-up of EMI from outside sources. It is more expensive compared to other shapes of comparable size. Pot cores are not readily available at higher powers.

E cores

E cores are less expensive than pot cores and have the advantages of simple bobbin winding plus easy assembly, E cores do not, however, offer self shielding. E cores can be mounted in different directions. E cores are popular due to their low cost, ease of assembly and winding and ready availability of a variety of a hard wear.

PQ cores

PQ cores are designed specially for switch mode power supply. The design provides an optimized ratio to winding area and surface area. As a result both maximum inductance and winding area are possible with the minimum core size. The core thus provides maximum power output with a minimum assembly weight and volume, in addition to taking up a minimum amount of area on the printed circuit board.

Toroids

They are the cheapest of all comparable core shapes. No bobbin is required; accessory and assembly cost is nil. Toroids can be provided with air gaps for dc bias applications. Shielding is relatively good.

If we concentrate on ferrite materials only for the inductor design, it is necessary to assume the maximum operating flux density B_t at the maximum temperature.

Since the saturation flux density of ferrite materials varies from 4600 to 5000G the maximum operating flux density should be considered about 2000G, so that it does not saturate even at the maximum peak current through the coil.

The peak coil current is generally restricted to 10 to 20% of dc load current and therefore the operating bias flux density does not exceed 50% of the saturation level at maximum temperature.

Manufacturers' data sheets contain some useful quantities as Wa, Ac and "Inductance Factor" (A_L) which are helpful in inductor design. A_L is defined as the self-inductance of one turn coil of specified dimension and shape when placed on a core in a given position. Often the product WaAc is given for each core and serves as a criterion for selecting the core (see *Appendix-A-2*).

The criterion for the selection of the core is related to the cross-section of core Ac and the winding area, Wa. This gives an indication of the size of the core. It is known that the inductance L can be expressed as

$$L=NAc(.\ B/.\ I)*10^{-8} \quad \text{Henry} \qquad \ldots.\ (7.7)$$

From which

$$Ac = (LI_{max}/NB_{max})*10^{8}\ cm^2 \qquad \ldots\ (7.8)$$

The core winding area Wa is the available area for the coil and the bobbin. The actual window area of the core for winding turns is affected by the following:

Window area occupied by the bobbin

1) Window area of bobbin which may be safely bound
2) Area occupied by the insulation

Thus the fraction of the actual window area of the core which will be occupied by copper may be calculated from the window utilization factor K, where K is

$$K=K_1*K_2*K_3 \qquad \ldots\ (7.9)$$

$$K_1 = \frac{\textit{Bare}\ \text{conductor area}}{\text{conductor area, including insulation}}$$

$$K_2 = \frac{\text{wound area}}{\text{usable window area}}$$

$$K_3 = \frac{\text{usable window area}}{\text{actual window area}}$$

For a circular cross-section wire wound on a flat form, the ratio of wire area to the area required for the turns can never be greater than 0.91. In practice the maximum value depends on the tightness of the winding, variations in insulations thickness and wire layers. A typical value of K_2 for copper wire with heavy synthetic film insulation is 0.7. The value of K_1 depends on the gauge of the conductor.

If the bobbin window area is available, K3 may be ignored and the usable window area should be the available window area of the bobbin. If the area of the insulated is taken then K1 may be ignored and the value of K should be modified accordingly.

$$NA_{bare\ wire} = K\ Wa \qquad \ldots (7.10)$$

$$Wa = N\ A_{bare\ wire}/K \qquad \ldots (7.11)$$

Multiplying Ac with Wa , we get

$$WaAc = (LI_{max}A_{bare\ wire}/K\ B_{max})*10^8\ cm^4 \qquad \ldots (7.12)$$

The term WaAc is quite important. From the manufacturers' data sheet the right size of the core can be selected from the above data. To help in the selection of the core the square root of the WaAc product should be taken and this value should be taken as rough indication for Ac. The nearest standard core of this size should be considered. Once Ac is determined Wa is also known. The number of turns N can then be calculated as

$$N = \frac{L\,I_{max}*10^8}{B_{max}*Ac} \qquad \ldots (7.13)$$

7.7: TRANSFORMER DESIGN

Functions of a Transformer

The function of a transformer in a switch-mode power supply is to transfer power efficiently and instantaneously from an external electrical source to an external load. In doing so the transformer also provides important additional capabilities:

1) The primary to secondary turn ratio can be established to efficiently accommodate widely different input/output voltage levels.
2) Multiple secondaries with different number of turns can be used to achieve multiple outputs at different output levels.
3) Separate primary and secondary winding facilitate high voltage input/output isolation, especially important for safety in off-line applications.

The present practice is to select the operating frequency above 20 KHz in a switching regulator for an output power above 50W. In this frequency range the obvious core selection opts for ferrite cores. In a PWM switching converter using the push-pull, half-bridge or a full-bridge configuration the duty ratio of unity is considered for transformer design. The core flux density is normally chosen at 2000G, and accordingly the core geometry and number of turns are calculated. The type of ferrite core is selected from the loss consideration at the operating frequency and the associated permeability.

The transformer voltage equation is

$$E_P = 4*f*B_{max}*Ac*Np*10^{-8} \text{ , Volts} \qquad \text{... (7.14)}$$

Where, Ep = voltage applied at transformer primary

f = frequency

Np = number of turns in the primary

B_{max} = peak flux density G

Ac = core cross sectional area

In push-pull configuration Ep = (V_1-1) volts in each half of the primary winding; 1volt being the $V_{CE\,(Sat)}$ drop and Np is the number of turns in each half of the primary. For a half bridge circuit the applied voltage at the primary is (V_1-1) and for full bridge the applied voltage is (V_1-2).

The winding factor K is

$$K = \frac{NAw}{Wa} \qquad \text{... (7.15)}$$

where, Aw = Actual wire area ,cm2

Wa=Core window area in toroids,cm2, bobbin window area in other cores,cm2

N=Total number of turns

Thus,

$$N = \frac{KWa}{Aw} \qquad \text{... (7.16)}$$

Multiplying both sides by Ac,

$$NAc = \frac{KWaAc}{Aw} = \frac{Ep*10^8}{4fB_{max}} \quad \text{... (7.17)}$$

Combining the above equations

$$WaAc = \frac{EpAw*10^8}{4KfB_{max}} \quad \text{... (7.18)}$$

Let J=current density=$\frac{I}{Aw}$ A/cm2

$$\eta = \frac{P_0}{P_1} = efficiency \quad \text{... (7.19)}$$

In push-pull inverter, the maximum duty ratio is 50%, therefore, current flowing in the primary coil is = D* I1 whereas in half- bridge and full-bridge the duty ratio D =1 or I = I_1.

The total product of WaAc is

$$WaAc = WaAc_{(primary)} + WaAc_{(secondary)} \quad \text{... (7.20)}$$

Which can also be expressed as

$$WaAc = \frac{P_0*10^8}{4fKJB_{max}}(1+1/\eta) \quad \text{... (7.21)}$$

The total power

$$P_T = P_0 + P_0/\eta \quad \text{... (7.22)}$$

Therefore,

$$WaAc_{(total)} = \frac{P_T*10^8}{4fKJB_{max}} \quad \text{... (7.23)}$$

The above equation is quite valuable in the initial selection of a transformer for a given power level. It is seen that the power handling capability is proportional to the product of the core and the window area of the core. It is also proportional to core flux density, copper current density and frequency.

Once *WaAc* is obtained the type of core is selected from the vendor's catalogue and *Wa* and *Ac* are obtained separately. For a push-pull configuration,

$$Np = \frac{(V_1 - 1)*10^8}{4fKB_{max}Ac} \quad \text{... (7.24)}$$

The primary will have a centre-tap coil with *Np* on each side. The secondary turns are given by

$$Ns = \frac{(V_1 + 1)}{(V_1 - 1)} Np \qquad \text{... (7.25)}$$

The secondary will have centre tap with*Ns* on each side.

For a full bridge configuration, the primary winding will be a single winding and the number of turns will be given by

$$Np = \frac{(V_1 - 2) * 10^8}{4 f B_{max} Ac} \qquad \text{... (7.26)}$$

The secondary turns are given by

$$Ns = \frac{(V_0 + 1)}{(V_1 - 2)} Np \qquad \text{... (7.27)}$$

Hardware design has been discussed in this chapter. The criteria for designing the DCM boost-rectifier and the single-phase high frequency inverter have been discussed. The current sensing circuit, the pulse amplification and isolation circuit and the power supplies circuits have also been presented. The design of the high frequency transformer and the inductor has also been described.

CHAPTER-8

EXPERIMENTAL RESULTS

In order to investigate the performance of the proposed low voltage high current rectifier a prototype delivering 20Amps of DC current at 2 volts was fabricated (shown in figures-8.1 & 8.2). This chapter presents the experimental results as obtained from the prototype. Both the control circuit and power circuit waveforms have been presented under various conditions.

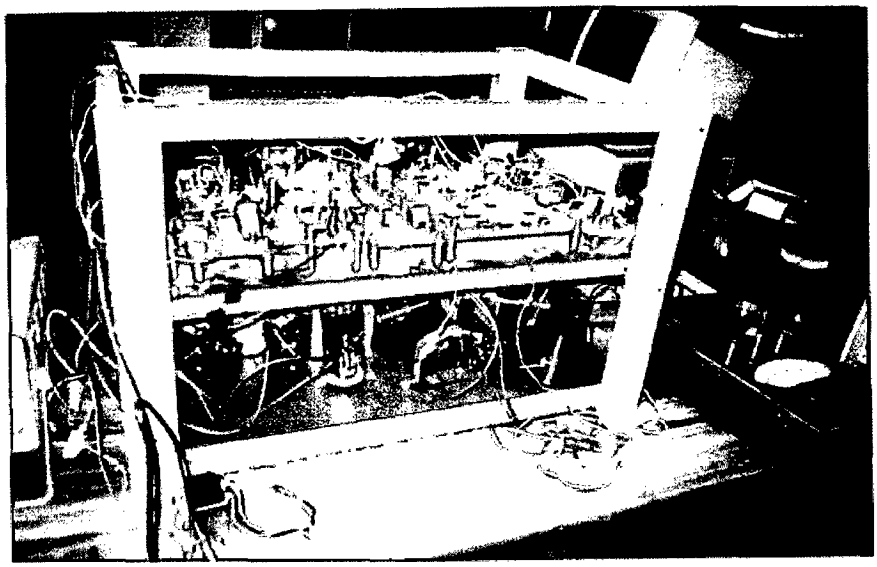

Figure-8.1: Experimental 2V 20Amp set-up

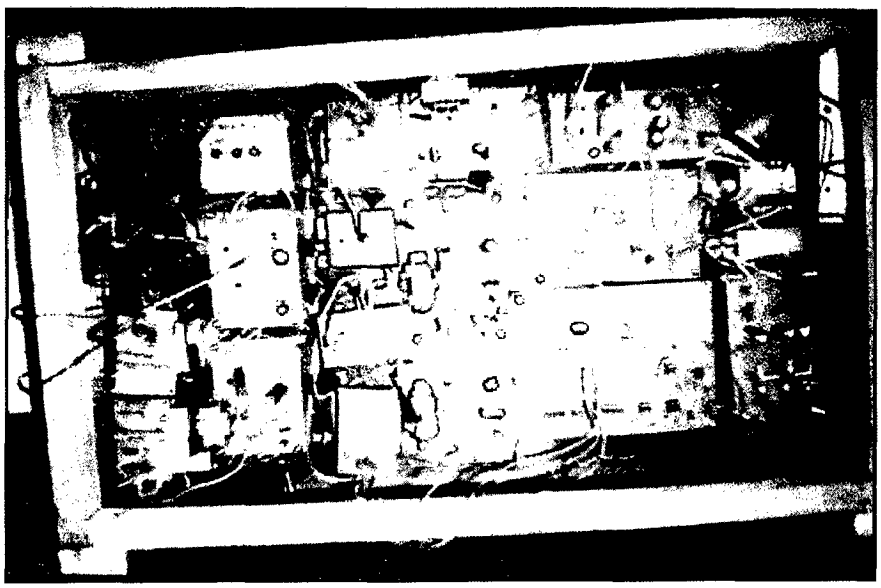

Figure-8.2: Control Circuits (Top View)

Control Circuit Waveforms

The control circuit for the generation of high frequency phase-shifted square wave pulses has been shown in figure-7.3. Figure-8.3 below shows the waveforms of the control circuit at various points. Figure-8.3(a) shows the sawtooth wave generated at point A. The waveform is having a notch at the rising edge due to the finite discharging time taken by the capacitor through the 10 ohm resistor. Ideally the capacitor should discharge through a circuit of negligible resistance instantaneously which is not the case here and hence it results in a notch. But since the circuit consists of positive-edge triggered D-flip-flop this notch does not cause any problem in the working of the circuit.

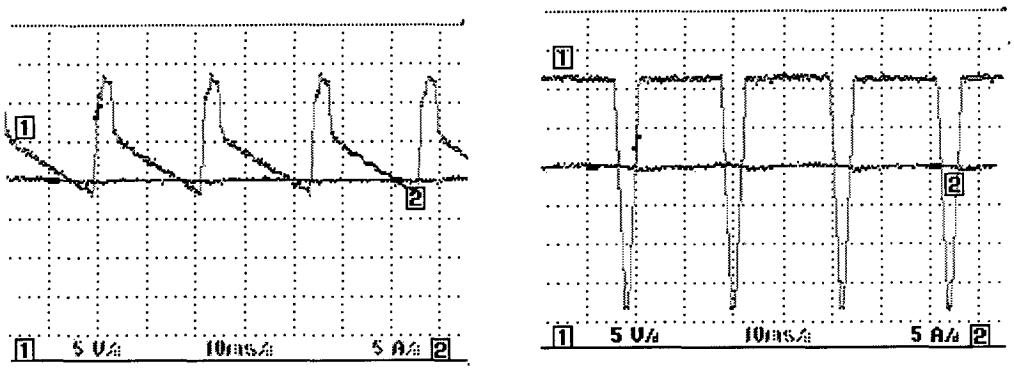

Figure-8.3(a) Sawtooth Waveform Generation (A) (b) Waveform at point C (in fig-7.3)

If the waveform shown in figure-8.3(b) is clamped so that the negative portion is trimmed off and the magnitude is limited to 5V, the resulting signal can easily be used for logic level signal generation. The resulting waveform is shown in figure 8.3(c).

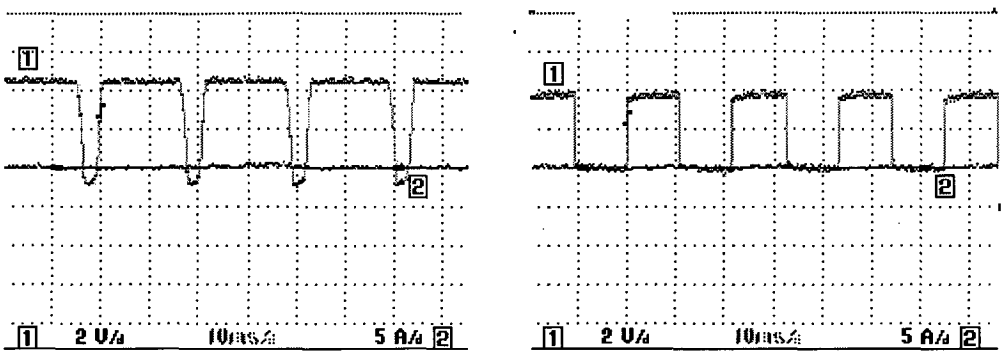

Figure 8.3 (c) Clamped waveform at point D (d) Square wave at point E

Figure-8.3: Phase-shift Inverter Control Circuit Waveform

The small negative voltage in the clamped signals shown in figure-8.3(c) is due to the drop in the zener diode used for clamping. But this is not a problem since the logic level circuits consider such signals as zero voltage level signals. When such a signal is fed to a positive-edge triggered D-flip-flop configured in divide-by-2 configuration a square wave as shown in figure-8.3(d) is produced.

Power Circuit Waveforms:

The power circuit was tested under different load conditions and at different operating frequencies. Various combinations of input and DC link voltages were taken so as to obtain the different value of conversion ratio M.

The boost inductance was taken as 270uH and different values of operating frequencies were tried to investigate the effect frequency variation upon the performance of the single-switch boost rectifier. The single-phase inverter was operated at a constant frequency of 10 KHz.

In the first case, when the boost operating frequency is 20 kHz output DC current is 6.0Amp & the input line-to-line voltage is 30 volts, the voltage across the DC link capacitor was adjusted to 80 volts so that the minimum value of conversion ratio is 3.265. The input current waveform (shown in figure-8.4) is close to a sinusoidal waveform with THD=14.2%. In the second case, the input voltage is 35volts rms and the DC link capacitor voltage is adjusted to 72 volts yielding a minimum M value of 2.519. The waveforms shown in figure-8.5 show that the THD increases to 20% which is in accordance with the theory since minimum M value has decreased. In figure-8.6, the minimum value of M is 2.85 which results in reduced harmonic distortion of 17%. In figure 8.7 the minimum value of M is 2.449 which again leads to increased THD of 23.1%.

From figures-8.8-8.13 the minimum value of M is kept constant at 2.45 and only the output DC current is varied. In all these figures the input current waveform remains more or less same in shape with only change in magnitude and the total harmonic distortion is almost stable around 18% which is in close agreement with the theory discussed in chapter-5 and the model developed by taking the dynamic value of conversion ratio, which gives a THD of 10.5% under the assumption of ideal conditions the model

also predicts that the shape of the waveform of input current will remain same with only change in magnitude with change in output load current.

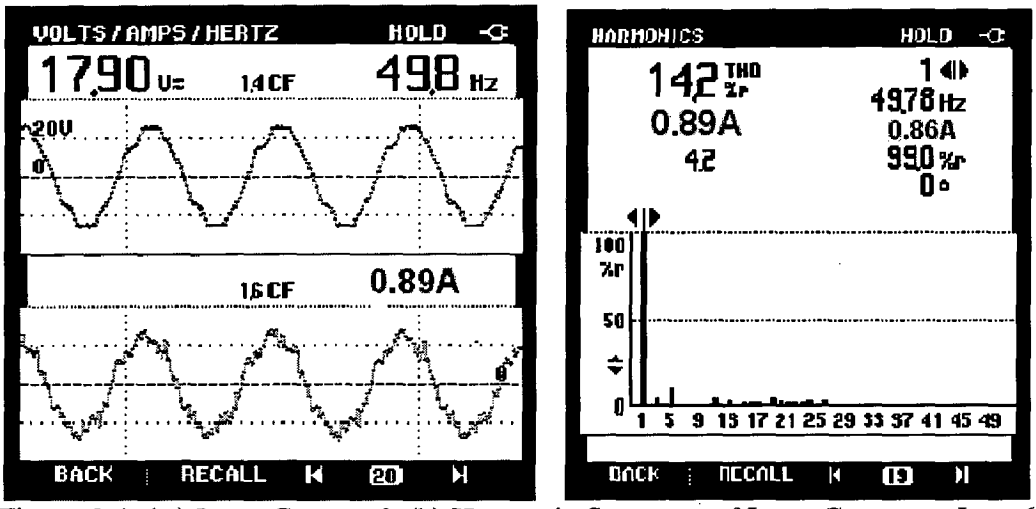

Figure-8.4 :(a) Input Current & (b) Harmonic Spectrum of Input Current at I_{DC} = 6.0Amp & Boost operating frequency = 20 kHz Vboost / VL-L= 80/30

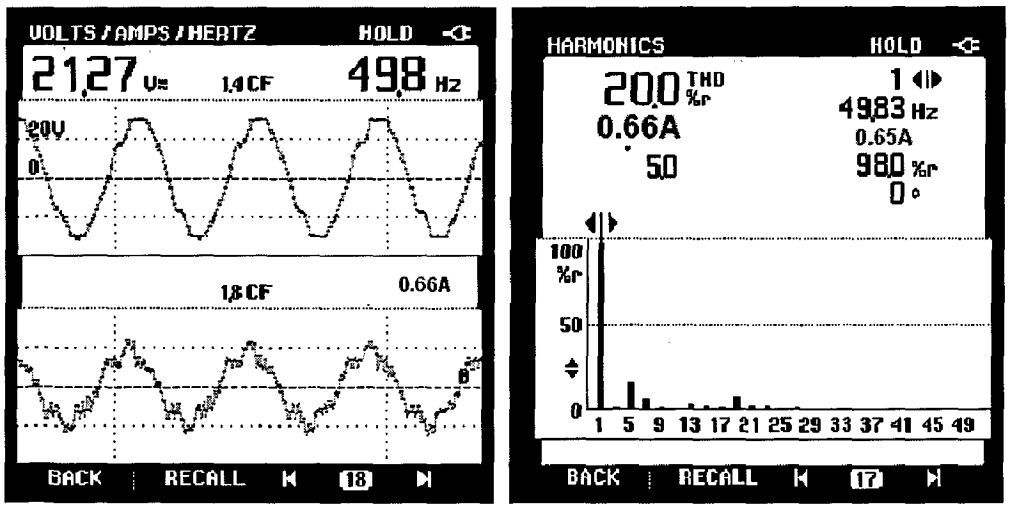

Figure-8.5: (a) Input Current (b) Input current Harmonic Spectrum; Idc=4.80Amp V_{L-L}=35V, V_{boost}= 72V, f_{boost} = 20 kHz

From the figures 8.4 & 8.5 it is clear that the total harmonic distortion (THD) increases as the value of V_{boost}/V_{L-L} decreases. Some distortion is also evident in the input phase voltage which also adds to the distortion of input current.

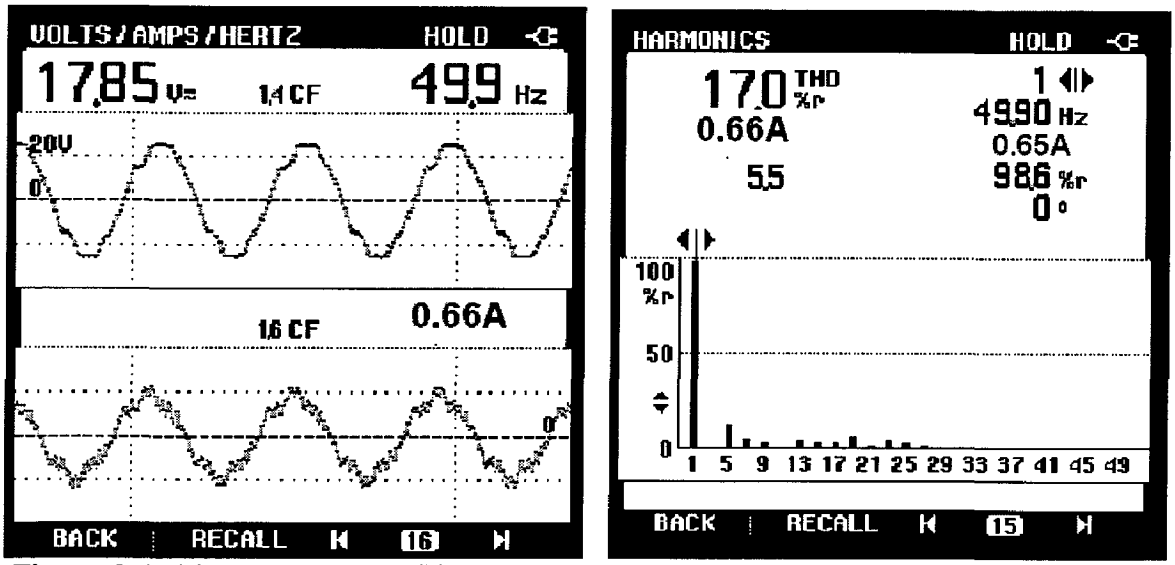

Figure-8.6: (a) Input Current (b) Input current Harmonic Spectrum; I_{dc}=4.40Amp $V_{L\text{-}L}$=30V, V_{boost}= 70V, f_{boost} = 20 kHz

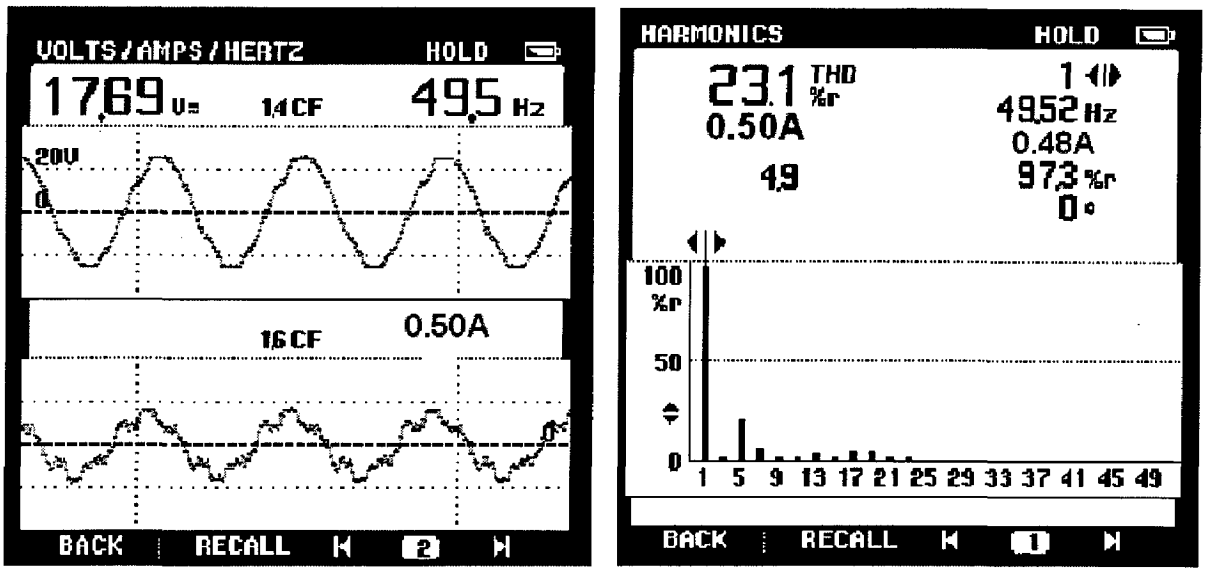

Figure-8.7: (a) Input Current (b) Input current Harmonic Spectrum; I_{dc}=3.20Amp $V_{L\text{-}L}$=30V, V_{boost}= 60V, f_{boost} = 15 kHz

Current waveforms shown in figure-8.6(a) & 8.7(b) do not have a dip in the middle at $\omega t = 90°$ which verifies the model developed by taking the dynamic value of M wherein no sharp dip at $\omega t=90°$ takes place (see figures-6.7 & 6.10).

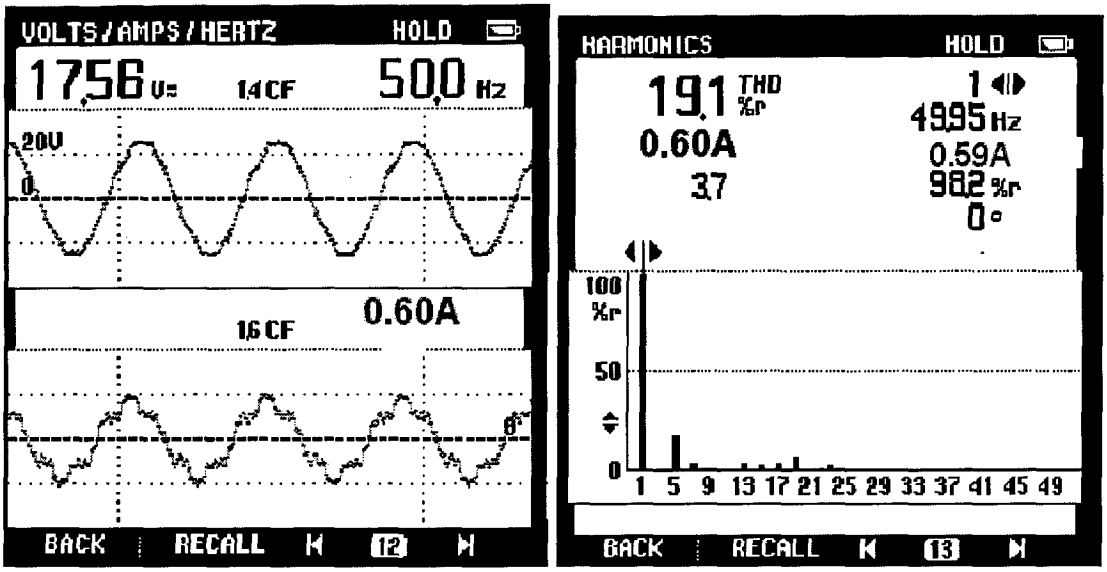

Figure-8.8: (a) Input Current (b) Input current Harmonic Spectrum; I_{dc}=4.80Amp
V_{L-L}=30V, V_{boost}= 60V, f_{boost} = 10 kHz

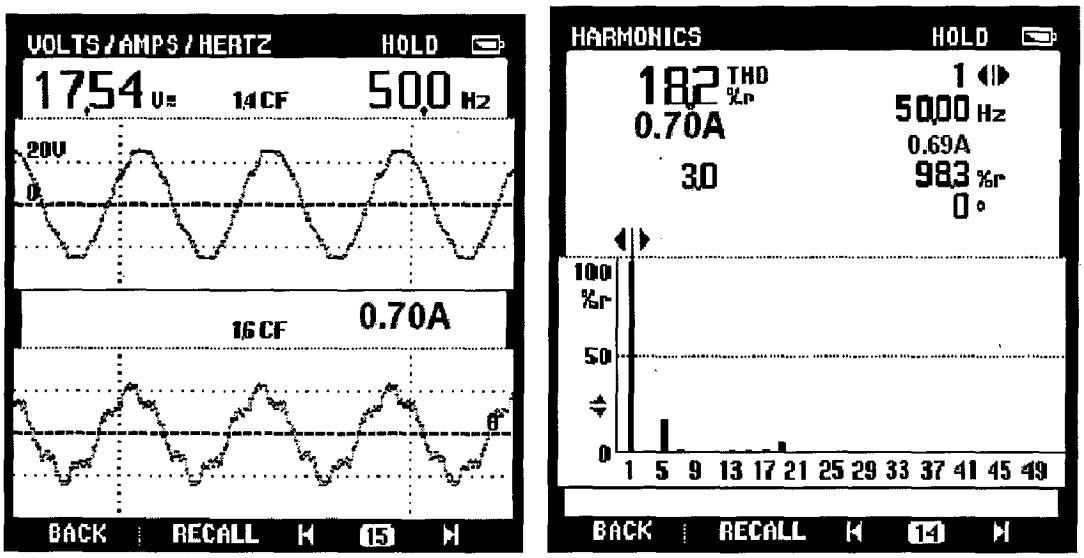

Figure-8.9: (a) Input Current (b) Input current Harmonic Spectrum; Idc=6.40Amp
V_{L-L}=30V, V_{boost}= 60V, f_{boost} = 10 kHz

The shape of the input current waveforms shown in figures 8.8 & 8.9 is more or less same. The total harmonic distortion is also nearly constant. The theory developed in chapter-5 also predicts that as the load on the output side changes the duty-cycle of the boost rectifier changes which brings a change in magnitude only, as long as the minimum value of M is not changed.

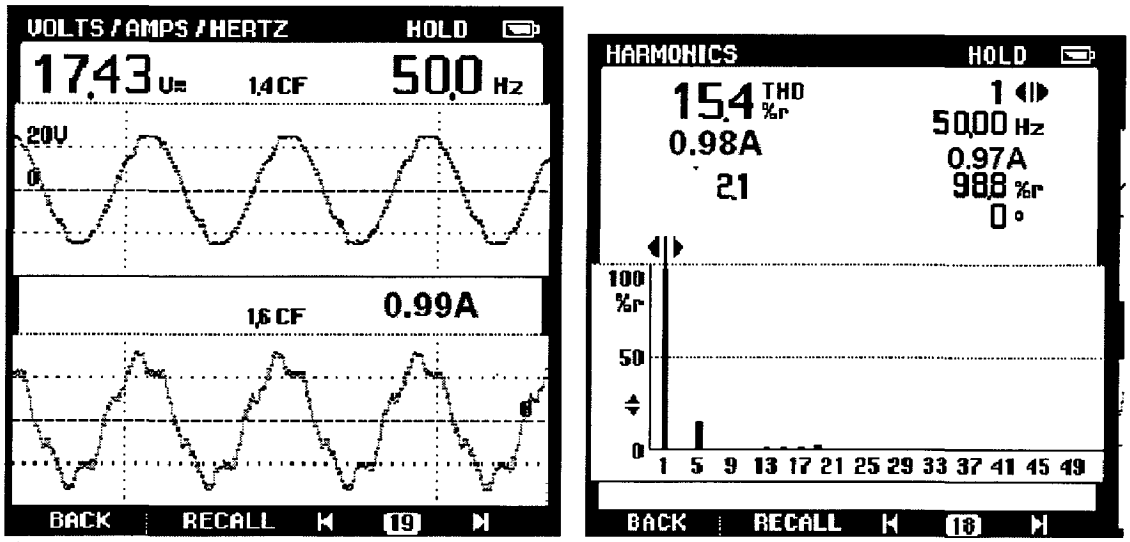

Figure-8.10: (a) Input Current (b) Input current Harmonic Spectrum; I_{dc}=9.40Amp
V_{L-L}=30V, V_{boost}= 60V, f_{boost} = 10 kHz

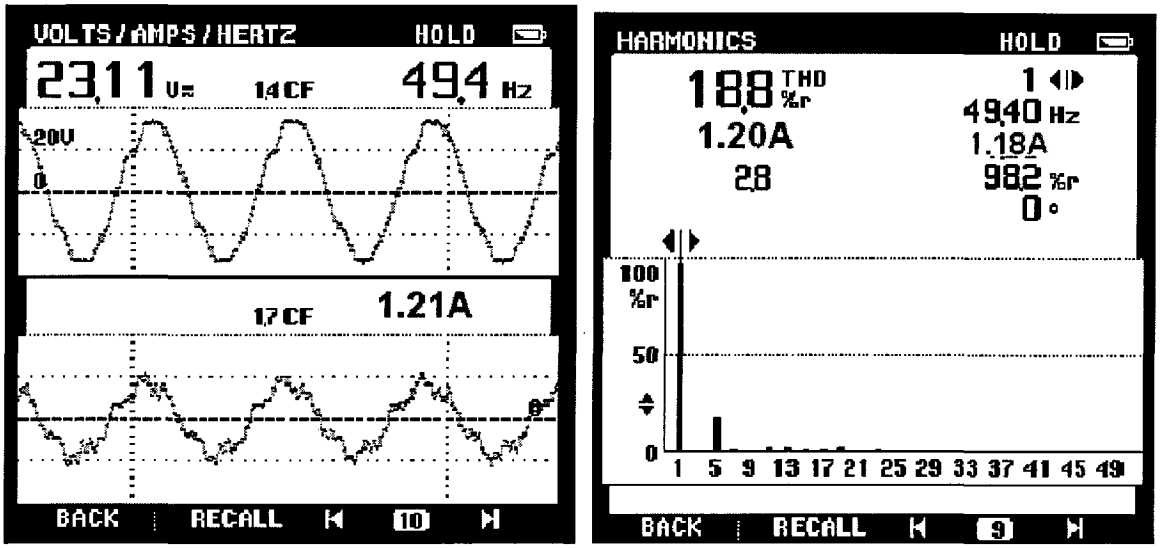

Figure-8.11: (a) Input Current (b) Input current Harmonic Spectrum; I_{dc} = 11.20Amp
V_{L-L}=40V, V_{boost}= 80V, f_{boost} = 10 kHz

The current waveform is having some high frequency components superimposed upon it. This is due to some inadequacy in the high frequency input filter. At high currents the THD is somewhat reduced due to the predominance of the fundamental frequency current over these small high frequency currents.

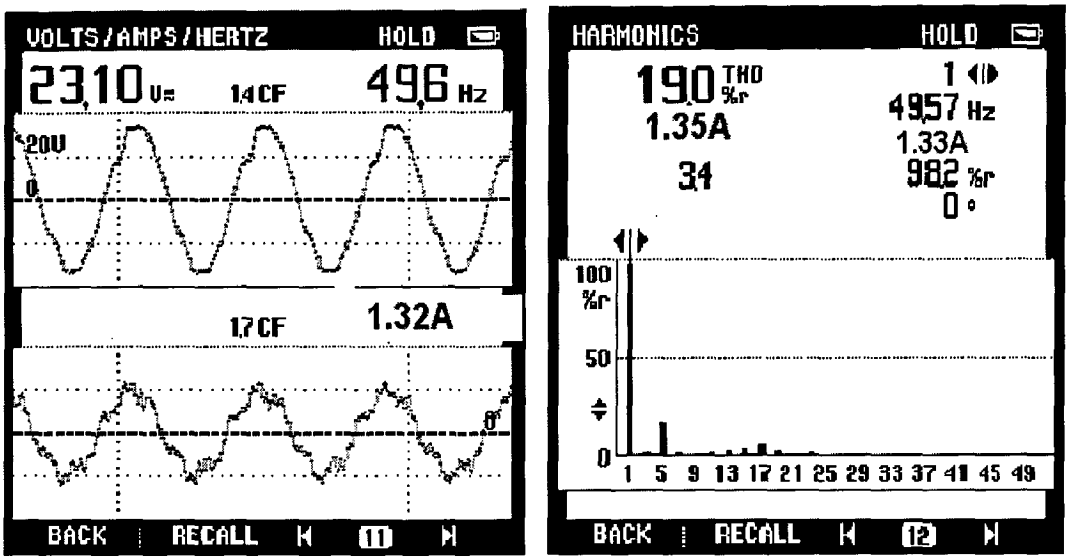

Figure-8.12: (a) Input Current (b) Input current Harmonic Spectrum; I_{dc} = 16.60Amp V_{L-L}=40V, V_{boost}= 80V, f_{boost} = 10 kHz

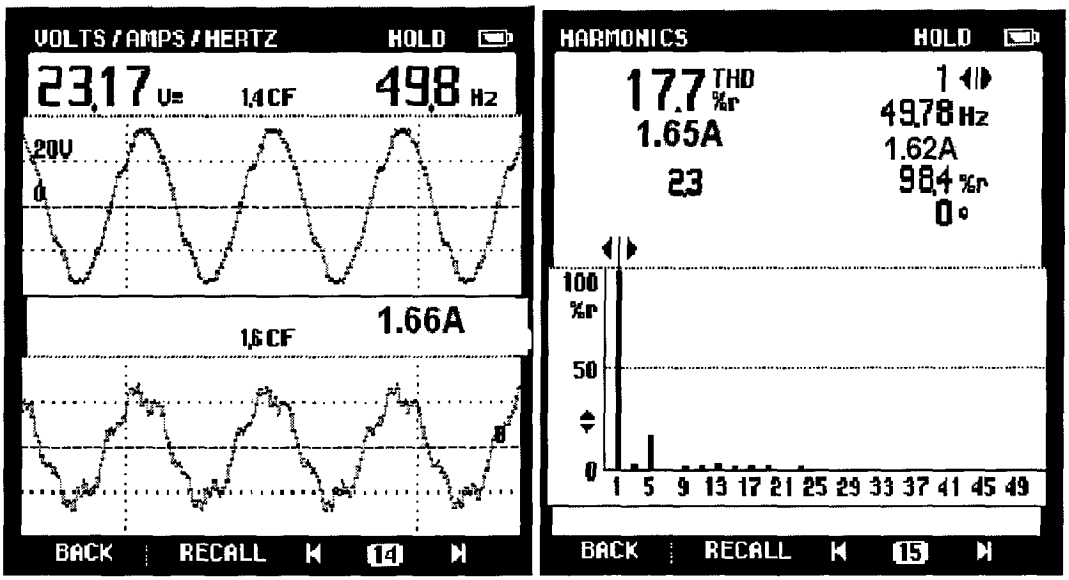

Figure-8.13: (a) Input Current (b) Input current Harmonic Spectrum; I_{dc} = 20.0Amp V_{L-L}=40V, V_{boost}= 80V, f_{boost} = 10 kHz

The magnitude of input current changes with variation in the output DC current, keeping the wave-shape more or less same but the change in magnitude is not as shown in simulation results since the efficiency of the practical set-up is less due to the drop in the output rectifier diodes, switching and other losses.

From the experimental results it is evident that the setup works well as a constant current source providing high currents at low voltages with comparatively reduced harmonic distortion. Some other points evident from the results are:

a) As the value of conversion ratio M increases the total harmonic distortion decreases.
b) As the output current changes the input current waveform remains the same only its magnitude changes, which is confirmation with the model developed and the simulation results obtained.
c) If the power drawn is more than the critical power the conduction tends to be continuous and the total harmonic distortion increases.

The boost rectifier has been operated in DCM at various frequencies, from 8 kHz to 50 kHz, and it has been found that above 50 kHz the switching losses in the devices increase resulting in increased chances of switch failure at higher frequency. So if higher frequency operation is desired then suitable techniques for reduced losses like ZVS and ZCS should be used. The one imperative for higher switching frequency is that the value and thus the size of the inductor as well as that of the transformer get reduced.

CHAPTER-9

Conclusion

Low voltage high current rectifiers are used in many industrial applications. Traditionally, these rectifiers have been manufactured using simple three phase diode bridge rectifiers fed through auto-transformer and transformer combination where the auto-transformer controls the input fed to the three phase transformer (and thus the output is also controlled) and the three phase transformer provides the required voltage level conversion. Another technique that has been used is through the controlled rectifiers where generally SCRs are used to provide controlled rectification. The disadvantage with these types of systems is that they are quite bulky and big in size. The power factor and the response of the system are also poor. Moreover, sometimes they require construction of complex power transformers which adds to the cost and complexity of the system. So, a topology which can overcome these limitations and can offer advantage in terms of size and weight is required.

Many solutions are being tried in the industry involving more of power electronics and with emphasis on size and weight reduction. Some of these topologies have been discussed in this work and there performance has also been discussed. In this work a switch-mode type of topology for low voltage high current rectifier has been presented which overcomes some of the disadvantages of the existing topologies.

The switch mode power supply consists of a front end boost rectifier, a high frequency single phase inverter linked through a high frequency transformer to the output rectifier and filter. The single switch front end boost rectifier, operating in discontinuous conduction mode (DCM), is used to improve the power factor and to reduce the total harmonic distortion of the input current drawn from the three phase input power supply. The single phase high frequency inverter is controlled by phase-shift control to provide a train of pulses to the output filter which acts as buck converter. The high frequency operation of the system results in reduced size and weight of the transformer and thus that of the overall system.

The simulation of both the boost rectifier and the overall bw voltage high current rectifier has been carried out and the response of the system is quite satisfactory. The control circuits for the phase shift control of inverter and for the boost rectifier have been developed and tested. The waveforms of the control circuit obtained experimentally have also been shown. The power circuit waveforms have also been shown and modeling of the system has also been presented.

Techniques like synchronous rectification and zero voltage switching (ZVS) and zero current switching (ZCS) can be employed to further improve the efficiency and performance of the system and to achieve operating frequencies greater than 20 kHz.

Thus, the proposed topology is suitable for low voltage high current rectifier as it has got high power factor, reduced harmonic distortion, fast response, reduced weight and is compact in size.

References

1. Pekik Argo Dahono, " A Family of Low-Voltage High-Current Rectifiers" presented at the 35th IAS Annual Meeting and World Conference on Industrial Applications of Electrical Energy, Rome 2000, pp 2526-2530
2. Qamaaruzzaman, Agus Purwadi, and Pekik Argo Dahono ," A DC High-Current Low-Voltage Power Generating System", 2002 IEEE proceedings
3. H.E. Jorgenson,DANFYSIK, Jyllinge, Denmark , F. Bordry, A. Dupaquier, G, Fernqvist, "High Current, Low Voltage Power Converter [20KA,6V] LHC converter Prototype", CERN, Geneva Switzerland, 1998.
4. G.K. Dubey, S.R. Doralda, A. Joshi, R.M.K. Sinha, "Thyristorised Power Controllers", New Age International Publishers,2003
5. Daniel Tollik, Andrzej Pietkiewicz, "Comparative Analysis of 1-Phase Active Power Factor Correction Topologies", Ascom Hasler Ltd, Energy Systems, Switzerland
6. L. Rossentto, G. Spiazzi, P. Tenti, "Control Techniques for Power Factor Correction Converters", University of Padova, Padova ,Italy.
7. Guy Oliver, Georges-Emile April, Eloi Ngandui, and Carlos Guimaraes, "Novel Transformer Connection to Improve Current Sharing in High-Current DC Rectifiers", IEEE Transactions on Industry Applications, Vol. 31, No.1, January/February 1995.
8. Johann W. Kolar, Hans ERTL, Franz C. Zach, "Space Vector-Based Analytical Analysis of The Input-Current Distortion of A Three Phase Discontinuous-Mode Boost Rectifier System", in Conf. Rec. 24th IEEE Power Electron. Special. Conf., Seatlle, WA, June 20-24, 1993, pp 696-703.
9. Marcelo Brunoro, Jose Luiz F. Viera, "A High-Performance ZVS Full-Bridge DC-DC 0-50-V/0-10-A Power Supply with Phase-Shift Control", IEEE Transactions on Power Electronics, Vol.14, No.3, May 1999.
10. Vytenis Leonavicius, Maeve Duffy Ulrich Boeke Sean Cian O Mathuna, "Comaprison of Realization Techniques for PFC Inductor Operating in

Discontinuous Conduction Mode", IEEE Trans. On Power Electronics, Vol. 19, No.2, March 2004

11. Jinrong Qian, Fred C.Y. Lee, "A High-Efficiency Single-Stage Single-Switch High-Power-Factor AC/DC Converter with Universal Input", IEEE Trans. On Power Electronics, Vol. 13, No. 4, July 1998.
12. Falcondes Jose Mendes de Seixas and Ivo Barbi, "A 12-kW Three-Phase Low THD Rectifier With High-Frequency Isolation and Regulated DC Output" , IEEE Trans. On Power Electronics, Vol. 19, No.2, March 2004
13. Vlatko Vlatkovie, Dusan Borojevie, and Fred C. Lee, "Input Filter Design for Power Factor Correction Circuits", IEEE Trans. On Power Electronics, Vol.11, No.1, January 1996
14. Peter Mantovanelli Barbosa, "Three-Phase Power-Factor Correction Circuits for Low-Cost Distributed Power Systems", PhD. Thesis Virginia Polytechnic Institute and State University, July 31, 2002.
15. Simon S. Ang, "Power-Switching Converters", Marcel Dekker, Inc, 1995
16. Philip T. Krein , "Elements of Power Electronics" , Oxford University Press, 2003
17. Muhammad H. Rashid, "Power Electronics. Circuits, Devices, and Applications", Prentice Hall of India, second edition, 2000.
18. M.D.Singh, K.B.Khanchandani, "Power Electronics", Tata McGraw-Hill Publishing Company Limited, 2000.
19. Mohan, Undeland, Robbins, "Power Electronics, converters, Applications and Design", 3rd edition, John Wiley & Sons ,2003
20. P.C.Sen, "Modern Power Electronics", S.Chand & Comapany, 2004.

APPENDIX- A-1

A Simple Method of Steady-State Analysis of PWM Converters

The steady-state analysis of PWM converters is the basis of the analysis and design. Here, a simple method for steady-state analysis is introduced based on a DC/DC boost converter as shown in Fig. A-1. Generally, this method can be extended to other type converters, including DC/AC and AC/DC converters.

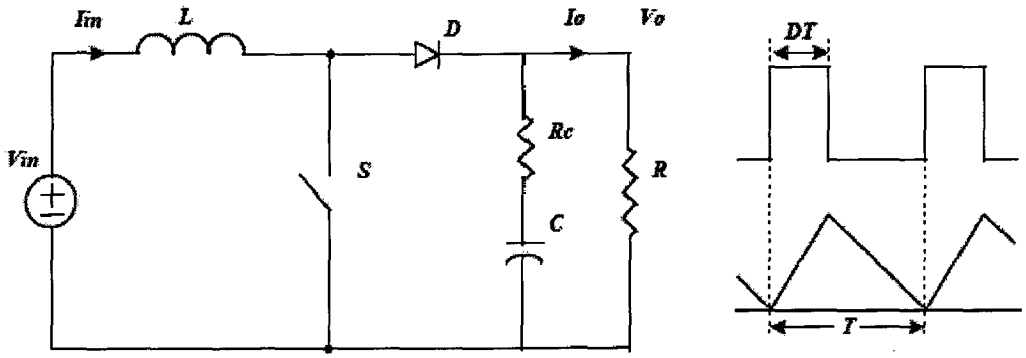

Figure A-1: DC/DC boost converter and its inductor current waveform

At first, some nomenclatures are defined: the *critical power* P_c *is* load power when the converter operates in conduction boundary between CCM and DCM; the *delivered power* P is power delivered by the converter from source to load; and d is the duty cycle in both CCM and DCM. Therefore, the critical power can be derived according to its inductor current waveform. At the boundary operation, the average inductor current is given by:

$$I_{in} = \frac{i_p}{2} = \frac{V_{in}}{2L} DT \qquad \text{... (A-1)}$$

where i_p is peak inductor current, D duty cycle in CCM, f switching frequency and $T=1/f$. Since it is still in CCM, the voltages and currents in input and output are related by

$$V_{in} = (1-D)V_o \qquad I_{in} = \frac{I_o}{1-D} \qquad \text{... (A-2)}$$

Substituting Eq. (A-2) into (A-1), the load current can be found. Thus, the critical power is obtained

$$P_c = V_o I_o = \frac{Vo^2}{2Lf} D(1-D)^2 \qquad \text{.... (A-3)}$$

Comparing the delivered power $P = V_o^2/R$ to the critical power in Eqn. (A-3), the steady-state can be obtained. On the one hand, if P is larger than P_c, the converter operates in CCM. The duty cycle is load independent and given by

$$d=D \qquad \text{... (A-4)}$$

On the other hand, if P is less than P_c, the converter operates in DCM, and the duty cycle is load-dependent. For constant output voltage, the voltage gain in DCM (referred to Table A-1) should be regulated to be equal to that in CCM, i.e.:

$$\frac{V_o}{V_{in}} = \frac{1+\sqrt{1+2d^2R/Lf}}{2} = \frac{1}{1-D} \qquad \text{... (A-5)}$$

Figuring out d and simplifying the expression by using P and P_c, the duty cycle can be represented as

$$d = \sqrt{\frac{P}{P_c}}D \qquad \text{.... (A-6)}$$

So, from heavy load to no load, the steady-state is given by Eqn. (A-4) or (A-6). Summarizing the above discuss yields a method for steady-state analysis of a DC/DC boost converter:

For a designed PWM converter, if the delivered power P is larger than Pc, then the converter operates in CCM and the duty cycle is given by Eqn. (A-4). Otherwise, the converter operates in DCM and the duty cycle is given by Eqn. (A-6).

It can be proved that the above method still holds for buck-type and flyback-type converters. The difference is that the critical power in Eqn. (A-3) should be replaced by those listed in Table A-1.

In AC/DC PFC converters or DC/AC inverters, the above method still can be used, even though the duty cycle D, critical power, and delivered power are functions of the instant of the sinusoidal input voltages. This is because, at a fixed ωt, these variables can be considered as constant and the method can be applied just as on a DC/DC converter. The most important thing is to find out proper representations of these variables.

	Boost-Type	*Buck-Type*	*Flyback-Type*
Critical Power	$\frac{V_o^2}{2Lf}D(1-D)^2$	$\frac{V_o^2}{2Lf}(1-D)$	$\frac{V_o^2}{2Lf}(1-D)^2$
Voltage Gain (CCM)	$\frac{1}{1-D}$	D	$\frac{D}{1-D}$
Voltage Gain (DCM)	$\frac{1+\sqrt{1+2d^2R/Lf}}{2}$	$\frac{2}{1+\sqrt{1+8Lf/d^2R}}$	$\sqrt{\frac{R}{2Lf}}d$

Table A-1: Critical power and voltage gains for general type PWM converters

APPENDIX-A-2

Table-A-2(a): E Cores with dimensions, magnetic properties and power handling capacities

SL No.			Cross section Magnetic			Window Area		Bobbin	W_AA_C
	Magnetic Core Number	Dimensions (cm) A/B/C	Area (cm^2) Ac C X F	Length (cm) *le*	Vol (cm^3) Ve	(cm^2) D X E	Weight (gram)	Window Area (cm^2)	(cm^4)
1	1810	1.93/1.62 /0.953	0.953x 0.476	4.01	1.82	1.18 x 0.711	8.5	0.344	0.156
2	2520	2.515/1.9 60/1.27	1.27 x 0.61	4.08	3.76	12.5 x 0.622	19	0.51	0.4
3	3007	3.01/3.00 /0.706	0.706x 0.697	6.56	3.94	1.941 x 0.646	20	0.833	0.5
4	3520	3.49/4.12 /0.953	0.953x 0.953	9.43	8.54	3.12 x 0.795	42	1.85	1.68
5	4011	4.001/3.3 98/1.069	1.069x 1.069	7.67	9.78	2.0 x 0.866	49	1.10	1.39
6	4020	4.28/4.22 /1.54	1.54 x 1.18	9.84	18.0	2.90 x 0.954	87	1.94	3.55
7	4022	4.28/4.22 /2.0	2.0 x 1.18	9.84	23.3	2.98 x 0.954	114	1.94	4.59
8	6016	6.0/4.46/ 1.56	1.56x 1.56	11.0	27.2	2.76 x1.45	135	2.89	7.18
9	5528	5.49/5.52 /2.06	2.06 x 1.68	12.3	43.1	3.708 x1.07	212	2.83	9.91
10	5530	5.49/5.52 /2.46	2.46 x 1.68	12.3	57.4	3.708 x1.07	255	2.83	11.8
11	7228	7.24/5.58 /1.9	1.9 x1.9	13.7	50.3	3.556 x1.69	264	4.02	14.8
12	8020	8.0/7.62/ 1.98	1.98 x1.98	18.5	72.1	5.64 x1.98	357	7.91	30.8

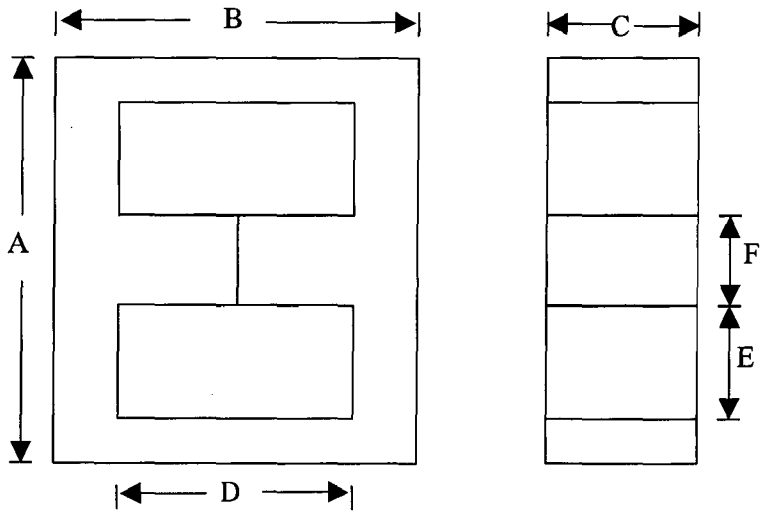

Table-A-2(b): Copper Wire Data

COPPER WIRE DATA								
	BARE WIRE						Enamel Covered	
	DIA		AREA		COPPER WIRE		DIA MILS	TURNS /INCH TIGHT
SWG	IN INCHES	IN M.MET	SQU. INCH	SQU. M.MET	Resistance μΩ/ins	Weight Lbs/10^3ins		
8	0.160	4.1	0.02011	12.97	33.20	6.45	164	6.10
9	0.144	3.65	0.01628	10.5	40.90	5.23	148	6.76
10	0.128	3.25	0.012868	8.30	51.8	4.13	133	7.5
11	0.116	2.94	0.010563	6.8	63.80	3.40	120	8.33
12	0.104	2.64	0.00849	5.48	78.50	2.73	108	9.3
13	0.092	2.33	0.0068	4.28	100.30	2.14	96.0	10.42
14	0.080	2.03	0.0050	3.24	133.00	1.62	83.5	12.0
15	0.072	1.83	0.0040	2.62	184.00	1.31	75.3	13.0
16	0.064	1.625	0.0032	2.075	207.00	1.03	67.1	14.9
17	0.056	1.42	0.0024	1.589	284.00	0.73	58.9	17.0
18	0.048	1.22	0.0018	1.1675	368.00	0.58	50.7	19.7
19	0.040	1.016	0.0018	0.81	531.00	0.408	42.5	23.9
20	0.036	0.91	0.00101	0.656	665.000	0.377	38.5	26.0
21	0.032	0.81	0.00080	0.5189	829.00	0.256	34.4	29.7
22	0.028	0.71	0.00061	0.397	1063.00	0.198	32.2	33.7
23	0.024	0.609	0.00046	0.29	1474.00	0.145	26.1	38.3
24	0.022	0.56	0.00038	0.2453	1750.00	0.122	24.0	41.7
25	0.020	0.508	0.00031	0.20	2120.00	0.101	21.9	45.7
26	0.018	0.457	0.00025	0.16	2620.00	0.082	19.8	50.5
27	0.0164	0.416	0.00021	0.136	3160.00	0.068	18.4	55.2
28	0.0148	0.376	0.00017	0.11	3880.00	0.0553	18.1	61.0
29	0.0136	0.346	0.000145	0.093	4590.00	0.0467	15.1	66.2
30	0.0124	0.315	0.00012	0.0779	5520.00	0.0338	13.8	72.5
31	0.0116	0.294	0.0001	0.068	6310.00	0.031	12.8	77.5
32	0.0108	0.274	0.000091	0.059	7290.00	0.0294	12.1	82.6
33	0.01	0.254	0.000073	0.0506	8490.00	0.0252	11.2	89.3
34	0.0092	0.233	0.000066	0.043	10030.00	0.0214	10.3	97.1
35	0.0084	0.213	0.000055	0.0357	12030.00	0.0178	9.3	105.3
36	0.0076	0.193	0.000045	0.0292	14700.00	0.0146	8.6	116.3
37	0.0068	0.172	0.000036	0.023	18400.00	0.0117	7.8	128.2
38	0.0060	0.152	0.000028	0.0182	23600.00	0.0091	6.9	144.9
39	0.0052	0.132	0.000021	0.0137	31400.00	0.0058	6.1	163.9
40	0.0048	0.121	0.000018	0.0116	36800.00	0.0053	5.6	178.6